12-17-2015

Studies on Boronic Acid-modified Nucleotides for Diagnostic Applications and Development of Fluorescent Chemoprobes for Molecules of Biological Importance

Ke Wang

STUDIES ON BORONIC ACID-MODIFIED NUCLEOTIDES FOR DIAGNOSTIC APPLICATIONS AND DEVELOPMENT OF FLUORESCENT CHEMOPROBES FOR MOLECULES OF BIOLOGICAL IMPORTANCE

by

KE WANG

Under the Direction of Binghe Wang, PhD

ABSTRACT

Post-synthesis DNA modification is a very useful method for DNA functionalization. This is achieved by using a modified NTP, which has a handle for further modifications, replacing the corresponding natural NTP in polymerase-catalyzed DNA synthesis. Subsequently, the handle can be used for further functionalization, preferably through a very fast reaction. Herein we describe polymerase-mediated incorporation of *trans*-cyclooctene modified thymidine triphosphate (TCO-TTP). Subsequently, the *trans*-cyclooctene group was reacted with a tetrazine tethered to other functional groups through a very fast click reaction. The utility of this DNA functionalization method was demonstrated with the incorporation of a boronic acid group and a fluorophore. The same approach was also successfully used in modifying a known aptamer for

fluorescent labeling applications. Boronic acid modified DNA molecules were further applied in aptamer selection for cancer cell recognition.

The second project was focused on developing fluorescent probes/sensors for biothiols. Because of the biological relevance of thiols and sulfides such as cysteine, homocysteine and hydrogen sulfide, their detection has attracted a great deal of research interest. Fluorescent probes are emerging as a new strategy for thiol and hydrogen sulfide analysis due to their high sensitivity, low cost, and ability to detect and image thiols in biological samples. A sulfonyl azide-based fluorescent probe has been developed for the quantitative detection of H_2S in aqueous media such as phosphate buffer and bovine serum. In addition, another novel fluorescent probe has been developed for the detection of homocysteine. The fluorescence response is selective for homocysteine over other biologically abundant thiols such as cysteine and glutathione. In addition, a linear calibration curve was also be obtained for quantitative analysis in phosphate buffer and plasma. These selective fluorescent probes could be very useful tool for biothiol tests.

INDEX WORDS: Post-synthesis modification, Bioorthogonal reaction, Oligonucleotides,
Gasotransmitter, Biothiol detection, Redox reaction

STUDIES ON BORONIC ACID-MODIFIED NUCLEOTIDES FOR DIAGNOSTIC APPLICATIONS AND DEVELOPMENT OF FLUORESCENT CHEMOPROBES FOR MOLECULES OF BIOLOGICAL IMPORTANCE

by

KE WANG

A Dissertation Submitted in Partial Fulfillment of the Requirements for the Degree of

Doctor of Philosophy

in the College of Arts and Sciences

Georgia State University

2015

STUDIES ON BORONIC ACID-MODIFIED NUCLEOTIDES FOR DIAGNOSTIC APPLICATIONS AND DEVELOPMENT OF FLUORESCENT CHEMOPROBES FOR MOLECULES OF BIOLOGICAL IMPORTANCE

by

KE WANG

Committee Chair: Binghe Wang

Committee: Peng George Wang

Aimin Liu

Electronic Version Approved:

Office of Graduate Studies

College of Arts and Sciences

Georgia State University

December 2015

DEDICATION

This dissertation is dedicated to my parents (Hongwei Wang and Hua Liu), who had instilled in me the strength of character that navigates me through each challenge. Without your unconditional love, encouragement and support, I would not be where I am today.

I also want to dedicate this dissertation to my grandparents (Jianxin Liu and Meiying Yang). Thank you for your love, inspiration and all the wonderful memories. Wish you could see my accomplishments and may you rest in peace.

ACKNOWLEDGEMENTS

I would like to express my deep gratitude to my advisor Dr. Binghe Wang, for his advice, patience, encouragement and support throughout the whole work. He is not only a supervisor for my research work, but also a mentor for my life, who benefits me a lot in personality development.

I would like to extend a special thank you to Dr. Peng George Wang and Dr. Aimin Liu for their time and patience in helping me throughout my PhD program. In addition to the professional knowledge I gained from their courses, their enthusiasm and passion in research has inspired me.

Besides, I would like to sincerely thank my colleagues, who have helped me a lot in past five years. I would especially thank Dr. Weixuan Chen, Dr. Chaofeng Dai and Dr. Hanjing Peng for their hand-on teaching and training of my professional skills. I would also thank Dr. Nanting Ni, Dr. Kaili Ji and Dr. Danzhu Wang for their help on biochemistry-related work. Technical support from Dr. Siming Wang and Dr. Lifang Wang should be also acknowledged. In addition, I would like to express my appreciation to Alexander Draganov, Dr. Krishna Damera, Dr. Xingyue Ji, Yueqin Zheng, Jalisa Holmes, Wenyi Wang, Mengyuan Zhu, Joy Yancey, Bingchen Yu, Zhixiang Pan, Vayou Chittavong and other group members for their help and discussion. Financial support from Molecular Basis of Disease program is gratefully acknowledged. Finally, my special thanks go to my boyfriend, Jixin Liu, for his generous love, care, encouragement and support through the whole process.

TABLE OF CONTENTS

LIST OF TABLES

LIST OF FIGURES

LIST OF SCHEMES

1 DEVELOPMENT OF BORONIC ACID-MODIFIED NUCLEOSIDE TRIPHOSPHATE FOR DIAGNOSTIC APPLICATIONS

1.1 Introduction

1.1.1 DNA modification methods

Beyond its natural functions as genetic codes, the utility of DNA in sensing,[1-2] new structural scaffolds,[3] therapeutics,[4-6] and *in vitro* aptamer selections[7-9] have been well-established. As such, modified DNA molecules are often used because of the possibility of endowing additional structural and spectroscopic properties, which allow for enhanced functions and detection.[10-11] Thus DNA modification has been a very active field of research; and several excellent results on DNA modification methods and applications by were reviewed.[12-14]

As a historical background, using modified nucleosides for biological incorporation and their various applications are far from a new thing, although recent interest levels are very high. Tritiated ([^{3}H]) thymidine autoradiography was firstly introduced in the late 1950's and served as a powerful technique for studying cell proliferation *in situ* for decades.[15-19] Later, less time-consuming strategies that do not rely on radioactive materials were developed to study cell proliferation and neurogenesis.[19] For example, many halogenated thymidine analogs such as BrdU, CldU, or IdU (Figure **1.1**) [19-20] were developed as alternative labeling methods. BrdU is currently the most commonly used metabolic label and has been widely used in areas such as cell proliferation and neurogenesis.[19, 21-22] In such an application, an antibody against BrdU is used to detect incorporation levels. However, harsh chemical denaturation conditions needed for processing the cellular DNA and poor tissue penetration of the BrdU antibody limit the utility of BrdU.[23] Especially important is the fact that these methods do not allow for studying live cells. In order to overcome limitations of existing methods, new chemistry is being developed. Such

new chemical strategies are bio-orthogonal, have a diverse set of structural properties for various applications, and allow for exploration of DNA in their native environments.[24-32] Often these newer approaches involve the use of click chemistry.[33-34]

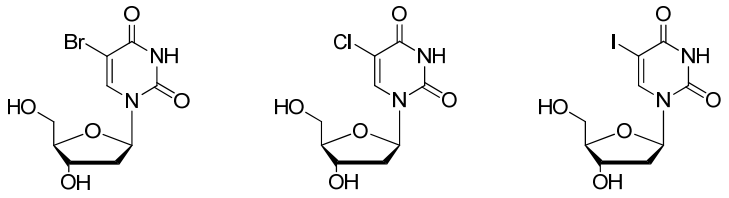

Figure 1.1 Structures of BrdU, CldU and IdU

In 2006, Seela[35] and Carell[36] firstly reported modifications of deoxynucleotides through copper(I)-catalyzed azide-alkyne cycloaddition (CuAAC) reaction developed by Sharpless[37] and Maldel.[38] In the earlier cases, only a small modification such as an azide or a terminal alkyne is initially introduced, to make sure the structure and function of the biomolecules remain virtually unchanged.[24-25] Later on, copper-free click chemistry was widely used in chemical biology applications,[39-41] in order to avoid issues related to copper.[42] Especially in DNA modification, several pieces of recent work including crossing-linking,[43-44] biomolecules labeling,[45-49] and cellular imaging[50] have been published in this area. Different types of "clickable" analogues have been used for visualizing DNA synthesis through secondary functionalization via click chemistry. In such an approach, a synthetic label containing a bio-orthogonal functional group is metabolically incorporated into the cellular target and subsequently probed using a chemoselective reaction.

Among all the nucleoside/tide modifications, which still allow for enzymatic recognition, modified thymidine analogs are probably the most commonly used. It has long been known that modification at the C5-position of deoxyuridine can be tolerated by various polymerases.[51-52] In

addition to examples of modified nucleosides being incorporated into DNA in live cells; there have also been interests in developing modified nucleosides/tides for direct incorporation into DNA in enzymatic reactions. In such an approach the triphosphorylated nucleosides are needed for polymerase-mediated DNA synthesis. The modified residues have to be recognized by polymerase and also be stable under primer extension and PCR conditions. An often-used strategy is to first modify the nucleoside with a handle that (1) is tolerated by DNA polymerases and (2) can be used to introduce additional functional groups after DNA synthesis.[14, 53-54]

There are several publications reported strain-promoted alkyne–azide cycloaddition (SPAAC) reaction being applied in nucleic acids labeling[55-56] and DNA ligation.[57] The Brown group reported ligation work[57] and DNA cross-linking using dibenzocyclooctyne (DIBO) and bicyclo [6.1.0] non-4-yne (BCN) modified phosphoramidite for chemical synthesis of modified DNA.[58] Recently, the same group reported successful enzymatic incorporation and labeling using DIBO and BCN modified triphosphates through primer extension (Figure **1.2**).[59]

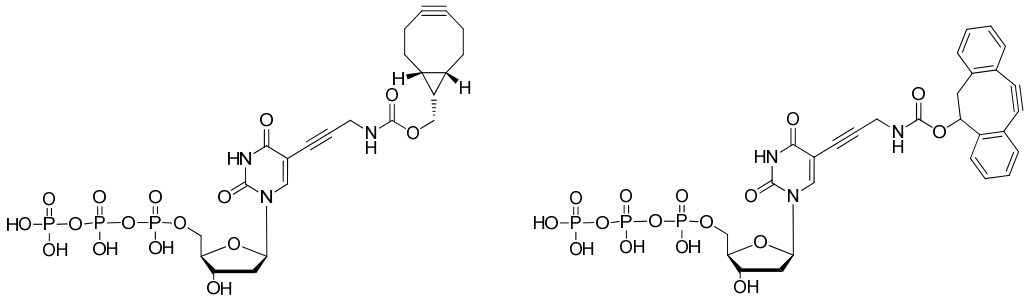

Figure 1.2 Structures of BCN and DIBO modified TTP

In addition to the C5-position of deoxyuridine, the C8-position of deoxyguanosine is another common site for DNA modification.[60] Earlier work was focused on chemical synthesis and applications in studying oligonucleotides' conformation and investigating DNA hybridization.[61-63] In 2012, Diederichsen and coworkers firstly developed a chemically

synthesized fluorescent 8-vinyl-2'-deoxyguanosine (VdGTP, Figure **1.3**, compound **6**) modified DNA for topology exploration.[64-65] Enzymatic synthesis of VdGTP-modified DNA was also reported in the same year.[66] There are other 8-styryl-2'-deoxyguanosine (SdGTP, Figure **1.3**, compound **7**) modified DNA reported, which focuses on its unique photochemically reversible isomerization potential.[67] Experiments showed that these guanosine derivatives had no or minimal effect on the B-form structure of DNA.

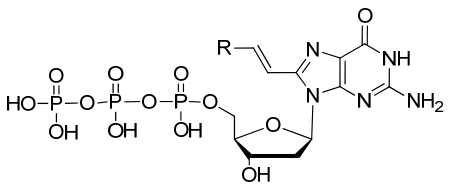

VdGTP, 6, R= H,
SdGTP, 7, R= ph

Figure 1.3 Structures of modified GTP

Among the different modification sites of nucleosides, deoxyadenine modification and enzymatic fluorescent labeling were also examined. As discussed above, inverse electron demand Diels–Alder (IEDDA) has been applied in DNA modifications because of its reaction rate and bio-compatibly. Marx and co-worker reported vinyl-modified DNA and its labeling using IEDDA in 2014.[68] 7-vinyl-7-deaza-2'-deoxyadenosine ($d^{vin}A$) and 5-vinyl-2'-deoxyuridine ($d^{vin}U$) were synthesized following a known procedure[69] for further enzymatic incorporation and post-synthesis labeling.

Hocek's group reported a fluorophore-labeled nucleotide, $dN^{API\ (or\ DAPI)}TP$ (Figure **1.4**, compound **8, 9**)[70] for DNA-protein interaction studies in 2012. In further studies of DNA-protein interaction using fluorophore-labeled DNA molecules, Hocek and co-workers designed and synthesized a GFP-like fluorophore-labeled DNA.[71] Specifically, 4-hydroxy-benzylideneimidazolinone (HBI) is a fluorophore in GFP,[72-73] which shows weak fluorescence as

a free molecule form in denatured protein.[74] The fluorescence of HBI can be significantly increased by restricting its conformational freedom, as is in the situation of binding to a protein.[75] Developed from previous reported work on HBI linked with RNA,[75] 3,5-difluoro-4-hydroxybenzylideneimidazolinone (FBI) and 3,5-bis(methoxy)-4-hydroxybenzylideneimidazolinone (MBI) were conjugated with cytosine triphosphate (CTP) to label DNA molecules (Figure **1.4**, compound **10, 11**).[71]

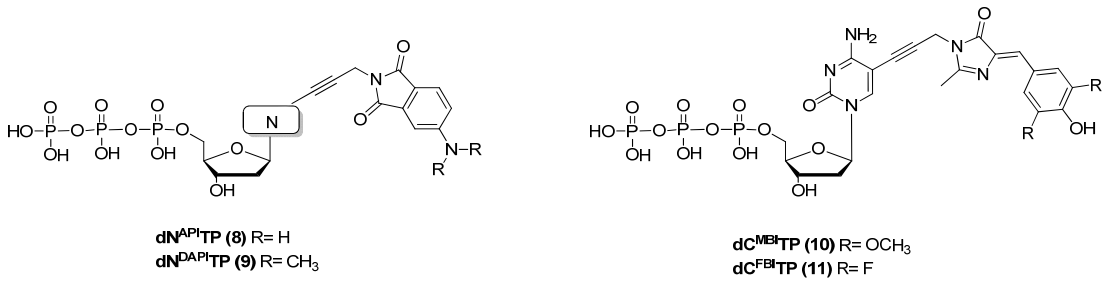

Figure 1.4 Structures of (D)API and M/FBI modified CTP

From the examples above, it is clear that modifications on the nucleobase of deoxynucleoside triphosphates allow for the creation of very useful probes in studying DNA replication and binding with proteins. Conceivably, sugar modifications represent possibilities. However, the deoxyribose portion does not have many positions that allow for modification without fundamentally changing its properties. The only position, which might allow for the modification with halogenation such as "fluorination" and the introduction of a protected hydroxyl group, is the 2'-position. Those with a free 2'-hydroxy group have similar structures with RNA monomers, and are hardly recognized by DNA polymerase.[76] In 2009, Wagenknecht and coworkers reported the chemical synthesis of sugar modification site on 2'-O position of ribose.[77] In 2013, the same group reported enzymatic synthesis and fluorescent labeling of 2'-O-propargyl-TTP.[78] This RNA-type 2'-O-propargyl nucleoside triphosphate (pNTP, Figure **1.5**,

compound **12**) is recognized by DNA polymerase and forms duplex structures with its complementary sequences.

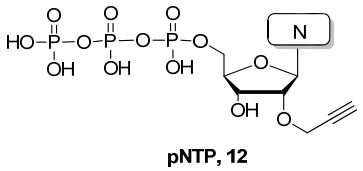

Figure 1.5 Structure of pNTP

There have been other sites modifications, like backbone modifications that use chemical synthesis instead of enzymatic incorporations.[79-80] They will be very useful as well. In addition to enzymatic incorporation of modified nucleotides into DNA, a number of chemical syntheses of modified DNA have been published. For example, Wagenknecht's group published work on post-synthetic fluorophore labeling using copper-free click[81] and photoclick reactions.[82] Diederichsen and coworkers have developed a fluorescent DNA probe, 8-vinyl-2'-deoxyguanosine, and applied it in DNA structural studies[64] and peptide nucleic acid (PNA) building blocks.[65] Such work has been reviewed recently, and thus is not discussed in detail.[12, 14, 53-54]

Aptamers are mostly single strands of oligonucleotides capable of binding to the intended targets[7-9] from small molecules to living cells with high affinity and specificity.[83-84] It have been recognized as useful tools in developing diagnostic and therapeutic agents.[85-86] Their diverse three-dimensional structures provide the possibility for developing aptamer-based molecular probes that are able to recognize biomarkers of great clinical diagnostic value.[87] In recent years, cell-based systematic evolution of ligands by exponential enrichment (cell-SELEX) has been extensively used to select aptamer candidates, which can distinguish the cell type of interest, or recognize the biomarkers of interest on cell surface.[88-91] The aptamer candidates go through

partitioning and will be remained on the target cell due to their higher binding affinity to the target. The surviving candidates can be collected and amplified by PCR and further go through several rounds of partitioning. Thus, the sequences with high binding affinity are enriched in the process of SELEX. However, the cell-SELEX method is usually involving a number of cumbersome steps and lack of efficiency. Usually, aptamers can be selected from all natural DNA/RNA pool. However, modifications with appropriate functional groups could endow these aptamers with special properties for enhanced affinity and/or selectivity. Recently, Krishnakumar's group reported an aptamer with fluorophore modification, which can recognize epithelial cell adhesion molecule (EpCAM).[92] Specifically, the EpCAM aptamer sequence SYL3C[93] with a terminal azido group can be conjugated to Alexa-fluor 594 (AF594) with a DIBO handle. Such modified aptamer was used in cell labeling studies. Flow cytometry analysis demonstrated successful labeling and obvious fluorescence improvement. Further live cell incubation and imaging was conducted using MCF7 (high EpCAM expression), Weri-RB1 (moderate EpCAM expression) and MIO-M1 (low EpCAM expression) cells. The aptamer fluorescence can be visualized and measured by fluorescent microscopy and flow cytometry. The mean fluorescence intensity (MFI) of the total population correlated with different cell line EpCAM expression. Cytotoxicity of EpDNA-DIBO-AF594 was also explored with various cells. No significant toxicity was observed at 1 μM after 48 h incubation. This is yet another example of the usefulness of DNA modification.

1.1.2 Boronic acid-based chemosensors and applications in DNA modification

Boronic acid is known as one of the most common moieties in chemosensors design because of its affinity for diols,[94-101] α-hydroxyl acids,[102-103] α-aminoacids,[104] aminoalcohols,[105-106] alcohols,[107-109] even cyanide[110-111] and fluoride.[112-113] Especially after Czarnik[114] and

Shinkai[115] reported using boronic acids as chemosensors for diols in early 1990s' (Scheme **1.1**), the boronic acid group has been widely used as the building blocks of chemosensors targeting saccharides,[95, 114, 116-120] carbohydrate transporters[121-127] and affinitive ligands for affinity chromatography.[128-130] Our group has been interested in using the boronic acid moiety for sensing applications, especially for carbohydrates chemosensors.[97, 101, 118-120, 131-137]

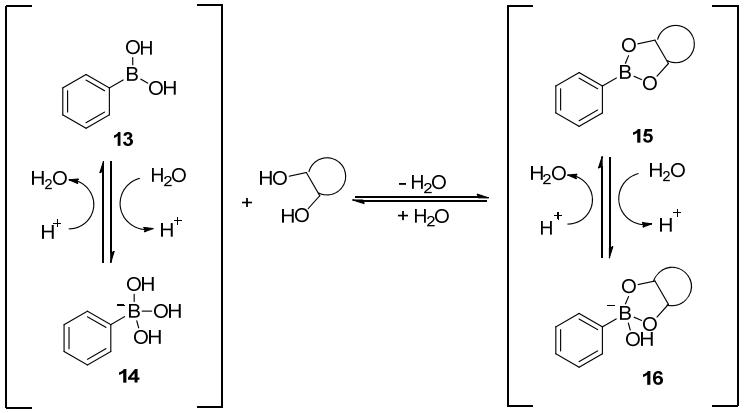

Scheme 1.1 Binding equilibrium of phenylboronic acid with a diol

Our group has had a long-standing interest in using the boronic acid moiety for various sensing applications.[97, 131-132, 138] Along this line, we have been working on the incorporation of the boronic acid functional group into DNA for aptamer selection[139-140] and other applications.[141-144] In incorporating the boronic acid group into DNA, there are special considerations because of the hygroscopic properties and Lewis acidity of this functional group. We have recently demonstrated the feasibility of direct PCR incorporation of boronic acid-modified TTP (Scheme **1.2**, Route A)[139] and post-PCR incorporation of the boronic acid group into DNA (Scheme **1.2**, Routes B).[142, 144] In post PCR DNA modification work, it is critical that the reaction goes to completion within a short period of time for various practical reasons. Thus it would be desirable to use click reactions that are fast enough so that completion of the reaction is assured on the scale of minutes. With most of the DNA click-modification reactions reported,

one fast condensation reaction of 1, 2-aminothiol with 2-cyanobenzothiazole (CBT) has a second-order rate constant of 22 $M^{-1} \cdot s^{-1}$.[48, 144] This means that at 1 μM, the reaction's first half-life ($t_{1/2}$) would be more than 12 h. One would have to force the reaction by increasing the concentration of the non-DNA click partner agent because the concentrations of the DNA product from PCR amplifications are limited by PCR efficiency at high concentrations and primer concentrations, and are generally in the low μM range. Even under forcing conditions, it would still take hours for the reaction to go to completion. Thus, we set out to develop modification chemistry, which would give a shorter half-life. Tetrazine-*trans*-cyclooctene cycloaddition is recognized as one of the fastest click reactions, with second-order rate constant being up to 22000 $M^{-1} \cdot s^{-1}$, which would give a first half-life of 45 second at 1 μM concentration.[40, 141, 145-147] Thus in this study, we examined the feasibility of using the tetrazine-*trans*-cyclooctene chemistry for the post-PCR labeling of DNA with the boronic acid moiety (Route C, Scheme **1.2**).

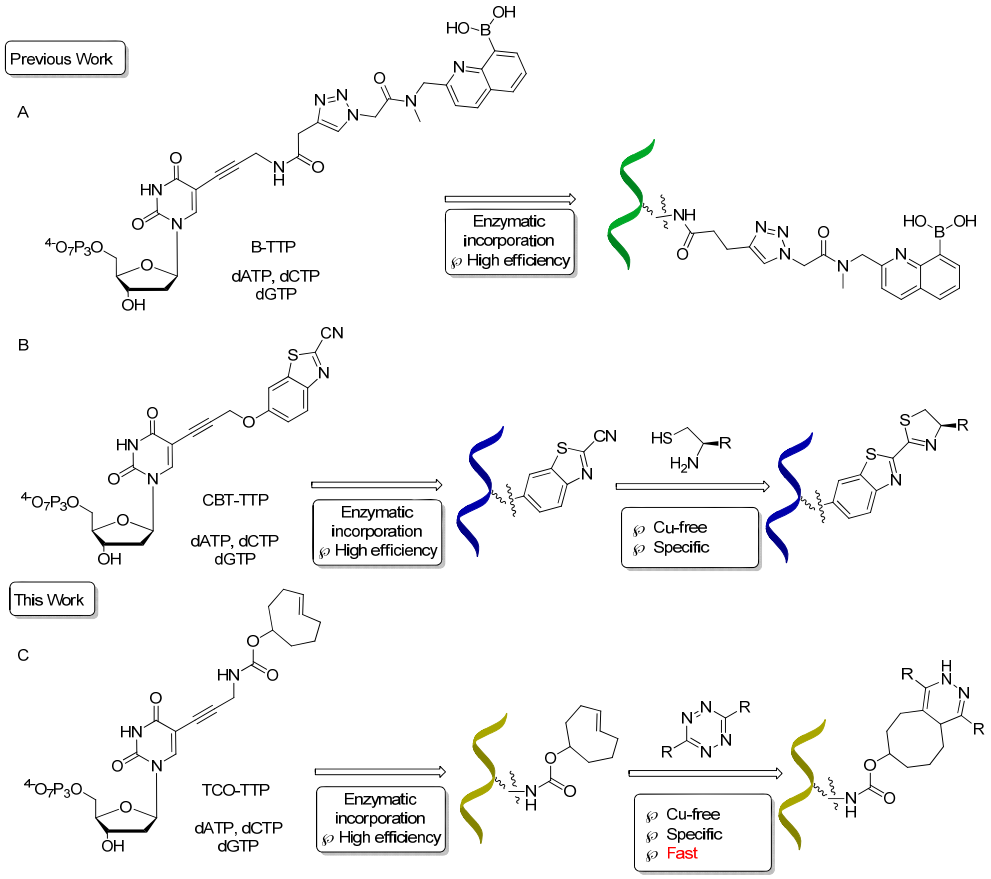

Scheme 1.2 A schematic representation of strategies for DNA modifications with a boronic acid A). Enzymatic incorporation of boronic acid-modified nucleotides; B). Enzymatic incorporation of CBT modified nucleotides, followed by post-PCR modification; C). Enzymatic incorporation of *trans*-cyclooctene modified nucleotides, followed by Cu-free post-PCR modification

1.1.3 Cell-based SELEX

Following the research on TCO-TTP incorporation into DNA molecules and subsequent boronic acid labeling, we preceded with cell-based SELEX to select aptamers targeting glycoproteins on the cell surface. We developed boronic acid-modified aptamers that target mucin 13 (MUC13), a transmembrane glycoprotein expressed in a variety of epithelial carcinomas. Mucin proteins are known for its protection and lubrication effect on the epithelial surfaces.[148] Mucin 13, a transmembrane type of mucin, has been implicated in cancer development based on laboratory findings of a malignant phenotype of MUC13-transfected cell

lines.[149-150] Thus, mucin 13 is a potential early marker of epithelial cancer and a promising target for anti-cancer drug delivery. In this study, we used HPAF II, a pancreatic cancer cell line that highly expresses MUC13 as our selection target in the cell-SELEX. Another pancreatic cancer MUC13-null cell line, MIA Paca, was used as a control cell line in the selection process.

1.2 Results and discussion

1.2.1 Synthesis of TCO-TTP

It has long been demonstrated that modification at the C5-position of deoxyuridine can be tolerated by various polymerases and such modified nucleotide triphosphates can be incorporated as a thymidine surrogate into DNA.[51-52] Thus we chose to install a click handle at the C5-position of deoxyuridine for further modifications. The *trans*-cyclooctene moiety can be introduced into compound **21** using amidation chemistry.[151] Then subsequent triphosphorylation followed a one-pot three-step method[152] to generate the final compound *trans*-cyclooctene triphosphate (**6**) in 32 % yield (Scheme **1.3**).

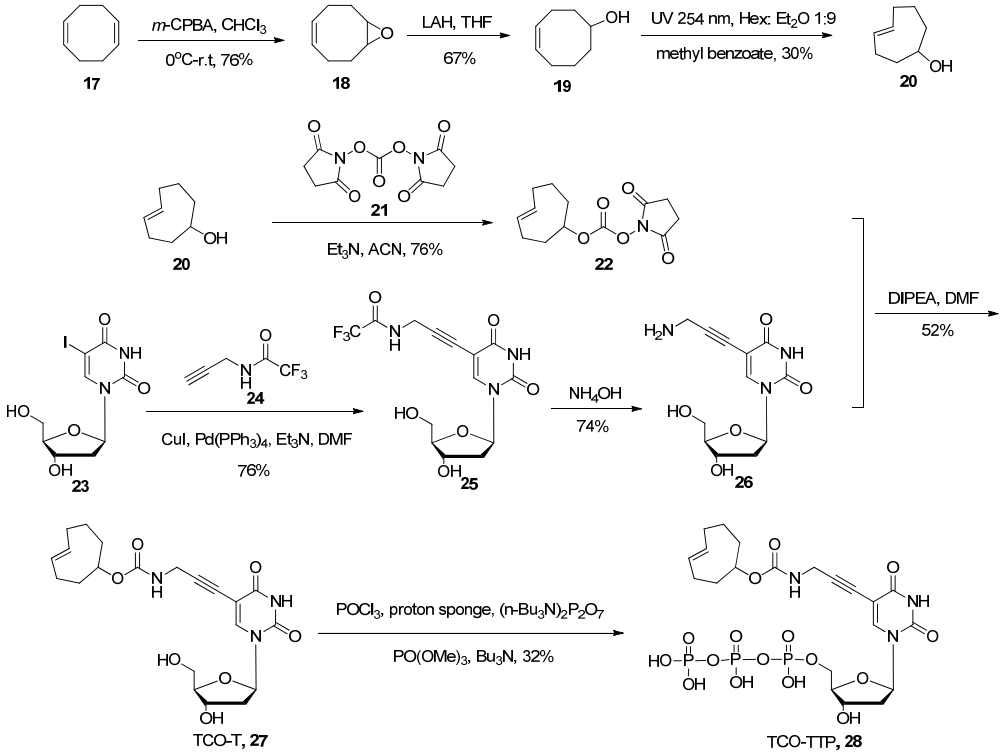

Scheme 1.3 Synthesis of trans-cyclooctene-modified deoxyuridine/thymidine triphosphate

1.2.2 Thermo-stability Studies of trans-Cyclooctene

Before PCR incorporation studies, we examined the stability of *trans*-cyclooctene modified nucleotide at high temperature using NMR and HPLC. To investigate *trans*-cyclooctene stability at high temperature, *trans*-cyclooctene sample was dissolved and heated in DMSO-*d6* at 90 ^{o}C. NMR spectra were scanned and recorded every 10 min to observe the isomerization from *trans*-isomer to *cis*-isomer. Isomerization percentage was calculated based on peak area of the peak at δ 5.55 ppm. Compared to the *cis*-cycloocetene peak, only 2% and 10% of *trans*-cyclooctene changed to the *cis*-isomer after heating at 90 ^{o}C for 20 min and 70 min (Figure **1.6**). In addition to the NMR studies, TCO thermo-stability was further examined with HPLC. As shown in Figure **1.7**, there was no noticeable difference after heating the TCO at 90 ^{o}C for 20 min (Figure **1.7**C). After heating at 90 ^{o}C for 70 min, almost 20% of TCO underwent

isomerization to give the *cis*-isomer (Figure **1.7**D). Thus *trans*-cyclooctene is generally stable under PCR conditions, which normally take 30 cycles (denaturing at 90 ^{o}C for 20 s each cycle) to complete the PCR step and would subject the sample to 90 ^{o}C for no more than 15 min.

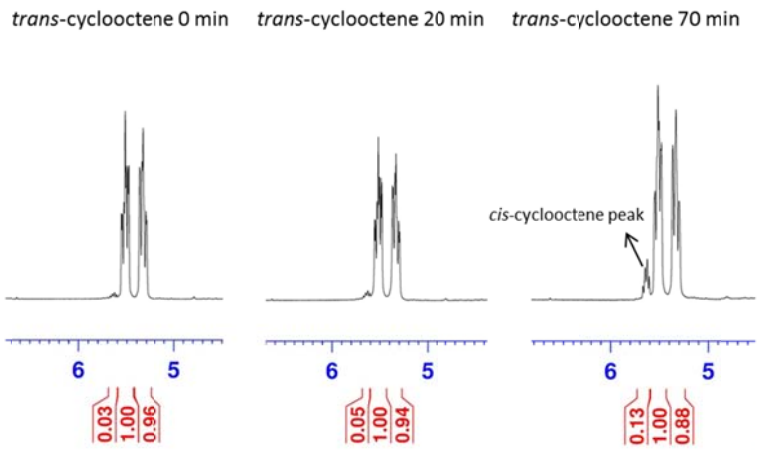

Figure 1.6 NMR study of thermo-stability of trans-cyclooctene

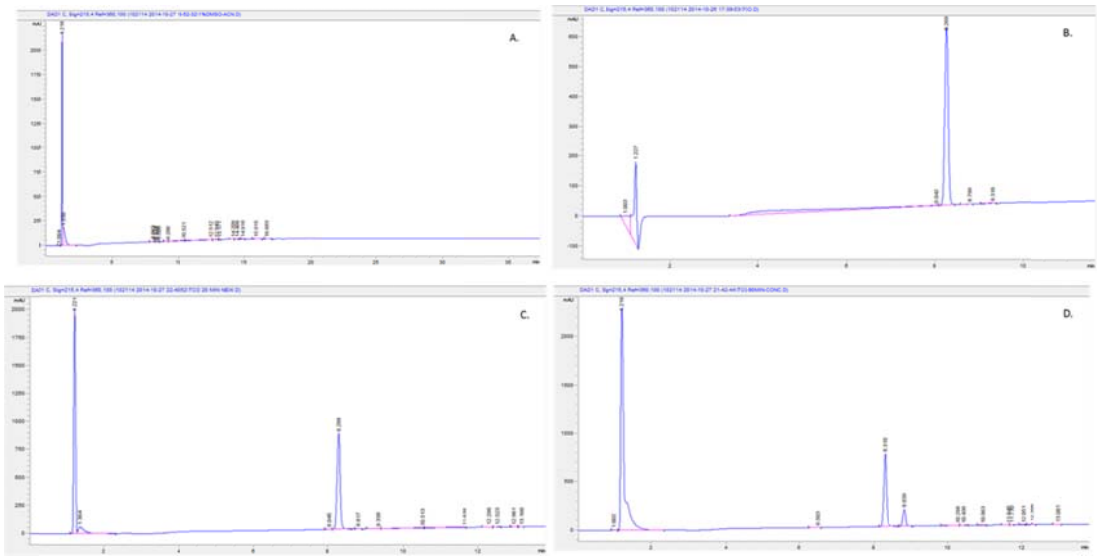

Figure 1.7 HPLC studies of the thermo-stability of trans-cyclooctene.
A). Background, ACN+ 1%DMSO; B). TCO dissolved in ACN; C). TCO heated at 90 ^{o}C for 20 min; D). TCO heated at 90 ^{o}C for 70 min

1.2.3 Enzymatic incorporation and post-synthesis labeling of TCO-TTP

To study whether the modified nucleotide **28** can be recognized by a polymerase, we first incorporated *trans*-cyclooctene thymidine triphosphate (TCO-TTP) into a short DNA via primer extension using the Klenow fragment-catalyzed reaction. Based on previous successful incorporation studies,[141, 144] we used a 21-mer oligonucleotide (nt) template-1 (5'-GGT TCC ACC AGC AAC CCG CTA-3'), a 14-mer primer (5'-TAG CGG GTT GCT GG-3') for the primer extension work (See experimental section for details). The template and primer were designed in such a way that the first incorporated nucleotide would be a T. Thus if TCO-TTP cannot be successfully recognized by the polymerase, there would be no primer extension. The extension products were examined by polyacrylamide gel electrophoresis (PAGE) (Figure **1.8**). The experiments included several negative controls: (1) primer extension with all the necessary components except TTP (Lane 1, Figure **1.8**A) (This is to make sure that enzyme fidelity would not be an issue and mis-matched incorporation does not happen), (2) primer extension with all the necessary components except the enzyme (Lane 2, Figure **1.8**A), (3) primer extension only in the presence of the template and primer without the dNTPs and the enzyme (Lane 3, Figure **1.8**A), and (4) primer only without the other necessary components (enzyme, template, and dNTPs) (Lane 4, Figure **1.8**A). Positive control was Klenow fragment catalyzed primer extension using natural dNTPs (Lane 5, Figure **1.8**A). TCO-TTP incorporation product was studied under Klenow fragment catalysis (Lane 6, Figure **1.8**A). , It is clear that primer extension with all natural dNTPs (Lane 5) and TCO-TTP (Lane 6) showed similar full-length double stranded DNA bands, demonstrating successful incorporation of TCO-TTP. Next, we wanted to explore the feasibility of post-PCR modification with the incorporation of a boronic acid. Thus, tetrazine-bisboronic acid (Tz-BBA, Figure **1.8**C) was synthesized for click-modification of the

DNA product. In doing the modification work, we ran the reaction for 15 min. As shown in Figure 1B, similar full-length 21-bp DNA bands were observed from primer extension reaction (Figure **1.8**B) using natural dNTPs (Lane 1), TCO-TTP (Lane 2), TCO-TTP labeled with Tz-BBA (Lane 3), and dNTP primer extension product reacting with Tz-BBA (Lane 4). There were some mobility differences among Lanes 1-3 with the click product (Lane 3) having the lowest mobility indicating increased molecular weight and the presence of the boronic acid group, which is a Lewis acid and can put a drag on mobility. However, the difference was small. Thus we sought additional evidence in support of successful incorporation of TCO-TTP and successful click modification.

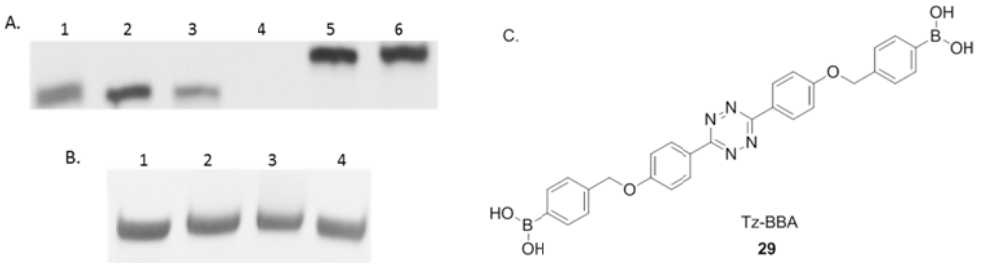

Figure 1.8 Primer extension and post-synthesis boronic acid labeling using TCO-TTP. A). Primer extension using dNTP or TCO-TTP replacing TTP catalyzed by the Klenow fragment, 20% PAGE analysis: 1. primer extension with all the other necessary components except TTP, 2. primer extension with all the necessary components except the enzyme, 3. primer extension in presence of template-1 and primer only, 4. primer extension in presence of primer only without the other components, 5. primer extension with dNTPs, 6. primer extension using TCO-TTP instead of dTTP; B). Post-synthesis boronic acid incorporation using TCO-TTP primer extension product and Tz-BBA, 20% PAGE analysis: 1. primer extension product using dNTPs, 2.primer extension product using TCO-TTP instead of dTTP, 3. primer extension product using TCO-TTP after reaction with Tz-BBA, 4. primer extension product using dNTPs after reacting with Tz-BBA; C). Structure of Tz-BBA.

The primer extension products were studied using MALDI mass spectrometry. The TCO-TTP primer extension product (Lane 2, Figures **1.8**B and Appendix) showed a molecular ion of *m/z* 6710.2 (calculated: 6710.4, [M+ H^+]). Tz-BBA click labeling product (Lane 3, Figures **1.8**B

and Appendix) showed a molecular ion of *m/z* 7237.6 (calculated: 7238.6, [M+ Na^+]). The primer extension product using dNTPs was also reacted with Tz-BBA (Lane 4, Figure **1.8**B). The product gave a molecular ion of *m/z* of 6520.0 (calculated: 6519.3, [M+ H^+]), which is the same as the original extension product, suggesting no reaction with Tz-BBA, as one would have expected. The mass spectrometric results further support the successful incorporation of one TCO-TTP moiety into DNA molecule and boronic acid labeling of DNA.

To further explore the feasibility of incorporating multiple TCO-TTP into DNA, we designed two more 21-mer templates complementary to the same 14-mer primer, template-2 (5'-TCA GTC ACC AGC AAC CCG CTA-3') and template-3 (5'-CAC GAC ACC AGC AAC CCG CTA-3'). These templates contained 2 or 3 A in the sequence, respectively, that can incorporate 2 or 3 TCO-TTP moieties into DNA. Based on previous optimization work using the Klenow fragment,[144] incorporation of additional modified TTP required higher temperature and longer incubation time than incorporating a single modified TTP. Under harsh conditions, Klenow fragment catalysis would give incomplete extension products and several blunt bands on gel. As a result, we chose the KOD-XL DNA polymerase, a family B polymerase from *thermococcus kodakaraensis*, which is more tolerant of unnatural TTP.[153] Analysis using 20% PAGE indicated successful primer extensions with the incorporation of both 2 and 3 Ts (Figure **1.9**). Template-1 primer extension using dNTPs (Lane 1, Figure **1.9**A) was conducted as positive control. Primer extension products using TCO-TTP in place of dTTP were obtained with template-1 (Lane 2, Figure **1.9**A), template-2 (Lane 3, Figure **1.9**A) and template-3 (Lane 4, Figure **1.9**A). As seen in Figure 2A, the electrophoretic mobility of primer extension products decreased progressively with increasing number of TCO-TTP moieties, indicating successful incorporation of multiple TCO-TTP units into DNA. To further confirm TCO-TTP's

incorporation and successful boronic acid labeling work, the extension product using template-3 was further studied through reaction with Tz-BBA in a similar fashion as the results described in Figure 1. As shown in Figure 2B, Tz-BBA-labeled primer extension products led to a slow-moving band (Lane 5). Such results are consistent with previous findings in similar studies.[144] It is well known that H_2O_2 can oxidatively cleave the boronic acid moiety leaving a phenol group behind.[154] Thus we also treated the boronic acid labeled primer extension product with H_2O_2 (Lane 6, Figure **1.9**B). The faster moving band after H_2O_2 treatment was presumably due to decreased molecular weight as well as the lack of the boronic acid group, which tends to interact with Lewis bases in the matrix and thus provide a drag on mobility.

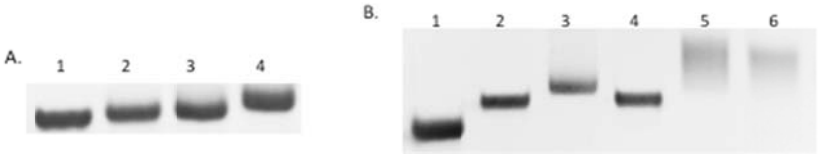

Figure 1.9 Primer extension incorporating multiple TCO-TTP and post-synthesis boronic acid labeling.

A). Primer extension incorporating multiple TCO-TTP catalyzed by KOD-XL DNA polymerase, 20% PAGE analysis: 1. primer extension using template-1 with dNTPs, 2. primer extension using template-1 with TCO-TTP in place of TTP, 3. primer extension using template-2 with TCO-TTP in place of TTP, 4. primer extension using template-3 with TCO-TTP in place of TTP; B). Post-synthesis boronic acid labeling of primer extension product using template-3 with TCO-TTP incorporation, 20% PAGE analysis: 1. primer extension with all the necessary components except TTP, 2. primer extension with dNTPs, 3. primer extension using TCO-TTP in place of TTP; 4. primer extension product using dNTPs reacted with Tz-BBA, 5. primer extension product using TCO-TTP reacted with Tz-BBA, 6. Tz-BBA labeled primer extension product (from lane 5) treated with H_2O_2.

After successful incorporation of TCO-TTP into short DNA sequences using primer extensions, we conducted PCR amplifications of a 90-mer DNA template (See experimental section for details). Before the incorporation work, we investigated amplification efficiencies of three commercially available polymerases, KOD-XL, *Taq* and Deep $Vent_R$ exo^-. PCR amplifications were examined under the same conditions for three polymerases. The screening

results showed the highest efficiency by KOD-XL (Lane 2, Figure **1.10**A). Such results are consistent with previous work on using other 5-modified deoxyuridine-5'-triphosphates.[139, 144] As a result, further PCR amplifications were conducted with the KOD-XL polymerase. According to the TCO-TTP thermo-stability test, optimized PCR amplification method was built based on an improvement of the CBT-TTP incorporation work.[144] With TCO-TTP modified DNA, 30 thermal cycles were run with 20 s melting at 90 ^{o}C, 20 s annealing at 48 ^{o}C, and 30 s extension at 72 ^{o}C, which gave 10-min exposure at 90 ^{o}C. Under this PCR condition, TCO-TTP can be introduced into DNA sequences in place of TTP. Following similar conditions as in the boronic acid labeling of primer extension products, PCR-amplified product was also reacted with Tz-BBA for boronic acid labeling. As shown in Figure **1.10**B, TCO-TTP was successfully incorporated into 90-nt PCR product (Lane 3). Experiments using dATP, dCTP, and dGTP, without dTTP for PCR amplification were used as a negative control (Lane 1) and dNTPs PCR amplification as a positive control (Lane 2). PCR-amplified TCO-TTP product was reacted with Tz-BBA (Lane 4), leading to a slow mobility band. Boronic acid labeling control experiment was performed with the dNTPs PCR amplification product by reacting with Tz-BBA (Lane 5). As expected, dNTP-PCR product didn't react with Tz-BBA and gave the same mobility as dNTP-PCR amplification product (Lane 2). The results demonstrate successful TCO-TTP incorporation during PCR and successful boronic acid labeling by reacting with Tz-BBA.

Figure 1.10 Post-PCR boronic acid labeling of amplified DNA with TCO-TTP incorporation. A). Polymerase screening for TCO-TTP incorporation, 15% PAGE analysis: 1. KOD-XL catalyzed PCR product using dNTPs, 2. KOD-XL catalyzed PCR product using TCO-TTP in

place of TTP, 3. *Taq* catalyzed PCR product using dNTPs, 4. *Taq* catalyzed PCR product using TCO-TTP in place of TTP; 5. Deep $Vent_R$ catalyzed PCR product using dNTPs, 6. Deep $Vent_R$ catalyzed PCR product using TCO-TTP in place of TTP. B). Post-PCR boronic acid labeling of amplified DNA product with TCO-TTP incorporation, 15% PAGE analysis: 1. PCR amplification in absence of TTP, 2. PCR amplification with dNTPs, 3. PCR amplification using TCO-TTP in place of TTP; 4. PCR amplification product using TCO-TTP reacted with Tz-BBA, 5. PCR amplification product using dNTPs reacted with Tz-BBA.

Encouraged by the results from TCO-TTP incorporation into a 90-nt DNA sequence and successful post-PCR boronic acid labeling, we further explored incorporating TCO-TTP into a published aptamer to see whether we can use the TCO-TTP handle for labeling DNA sequences with other structural moieties, such as fluorophore. N37 is a known aptamer selectively targeting the thrombospondin-1 (TSP-1) protein on the surface of inflamed endothelial cells with high potential of atherosclerosis.[155-156] Using the same PCR amplification conditions described above, N37 was used as new template for amplifications. Tetrazine-FITC (fluorescein isothiocyanate reacting with an amino handle of tetrazine, Tz-FITC, Figure **1.11**B) was synthesized for post-PCR fluorescent labeling of TCO-TTP modified DNA. We studied the incorporation of fluorescein into a known aptamer[155] N37 and the applicability of using such a fluorophore-labeled DNA for binding applications. TCO-TTP modified N37 (TCO37) (Lane 3, Figure **1.11**A) was obtained and analyzed with 15% PAGE after KOD-XL catalyzed PCR. This amplification product generated fluorescein-labeled N37 aptamer (Lane 4, Figure **1.11**A) after reacting with Tz-FITC. Natural N37 aptamer (Lane 2, Figure **1.11**A) was used as positive control. The product of N37 (generated using dNTPs) reacting with Tz-FITC (Lane 5, Figure **1.11**A) was used as negative control for the fluorescein labeling experiments. As shown in Figure 4A, only the PCR product with the *trans*-cyclooctene moiety reacted with Tz-FITC as indicated by the fluorescent band (FITC channel, λ_{em}: 520 nm, Lane 4, Figure **1.11**A). No fluorescence was detected in other

lanes. Ethidium bromide (EB) staining results were consistent with successful incorporation of TCO-TTP and boronic acid labeling with 90-mer DNA template.

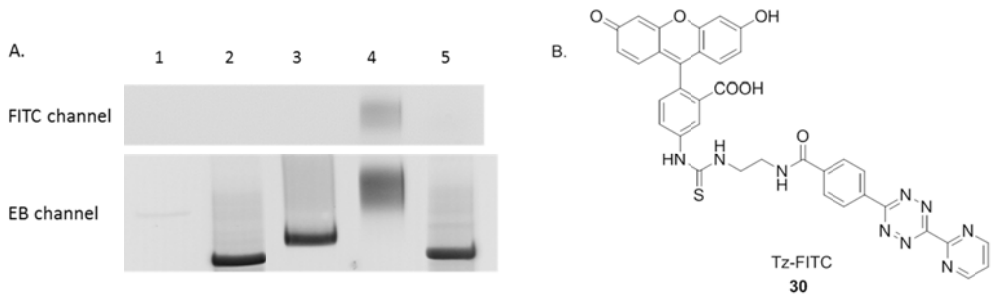

Figure 1.11 Post-PCR FITC labelling of TCO-TTP incorporation products using N37 template
A). Post-PCR FITC labeling of TCO-TTP incorporation products using N37 template, 15% PAGE analysis: 1. PCR amplification with all the essential components except TTP, 2. PCR amplification with dNTPs, 3. PCR amplification using TCO-TTP in place of dTTP; 4. PCR amplification product using TCO-TTP reacted with Tz-FITC, 5. PCR amplification product using dNTPs reacted with Tz-FITC; B). Structure of Tz-FITC.

1.2.4 Cell imaging study of TCO-TTP modified aptamer

Based on the successful incorporation of a fluorophore into a known N37 aptamer, we wanted to explore its *in vitro* cell fluorescent imaging applications. In natural N37 aptamer studies, the binding affinity with TSP-1 was determined with 5'-FAM labeled primer, which has a single fluorophore attached in each aptamer sequence.[155] However, with the ability to incorporate a fluorophore using the tetrazine-*trans*-alkene chemistry, it was possible to introduce a fluorophore in multiple positions of the TCO-modified aptamer N37 (TCO37). Such labeled aptamers could have higher fluorescent intensity without losing binding affinity. Thus fluorescent labeling studies were conducted using Hela cells, which express TSP-1 on the surface.[157] After incubation with 1 μM of 5'-FAM N37 aptamer (Figure **1.12**B) and FITC-labeled TCO37 aptamer (Figure **1.12**D) at 37 ^{o}C for 30 min, the cells were examined under a fluorescent microscope (see experimental section for details). Two control experiments were

conducted with cell only (Figure **1.12**A) and N37 (no click handle) reacted with Tz-FITC (Figure 5C). 4',6-Diamidino-2-phenylindole (DAPI) staining (for nuclei) was also used. Cells were examined using three channels (Figure **1.12**): (1) DAPI channel (λ_{em}: 461 nm; first row) for nuclear staining; (2) FITC channel (λ_{em}: 520 nm, second row) for detecting the fluorescein signal; (3) phase contrast channel for morphological observations (third row); and (4) Merged channel, with images of DAPI, FITC and phase merged into one (fourth row). As one can see, all cells stained normally with DAPI and have normal morphology under phase contrast, indicating normal cell growth. However, only the cells treated with FITC-labeled TCO37 aptamer showed significant fluorescent labeling in the fluorescein channel. Interestingly, the FAM-N37 labeled cells did not show the same significant fluorescent labeling. The results so far indicate that replacing T with TCO-T in aptamer N37 didn't affect its binding affinity to TSP-1 and allowed for fluorescent labeling of cells after the incorporation of a fluorophore. The ability to incorporate multiple fluorophores could provide enhanced sensitivity for labeling. Conceivably, the same approach can be used in other known aptamers for binding studies.

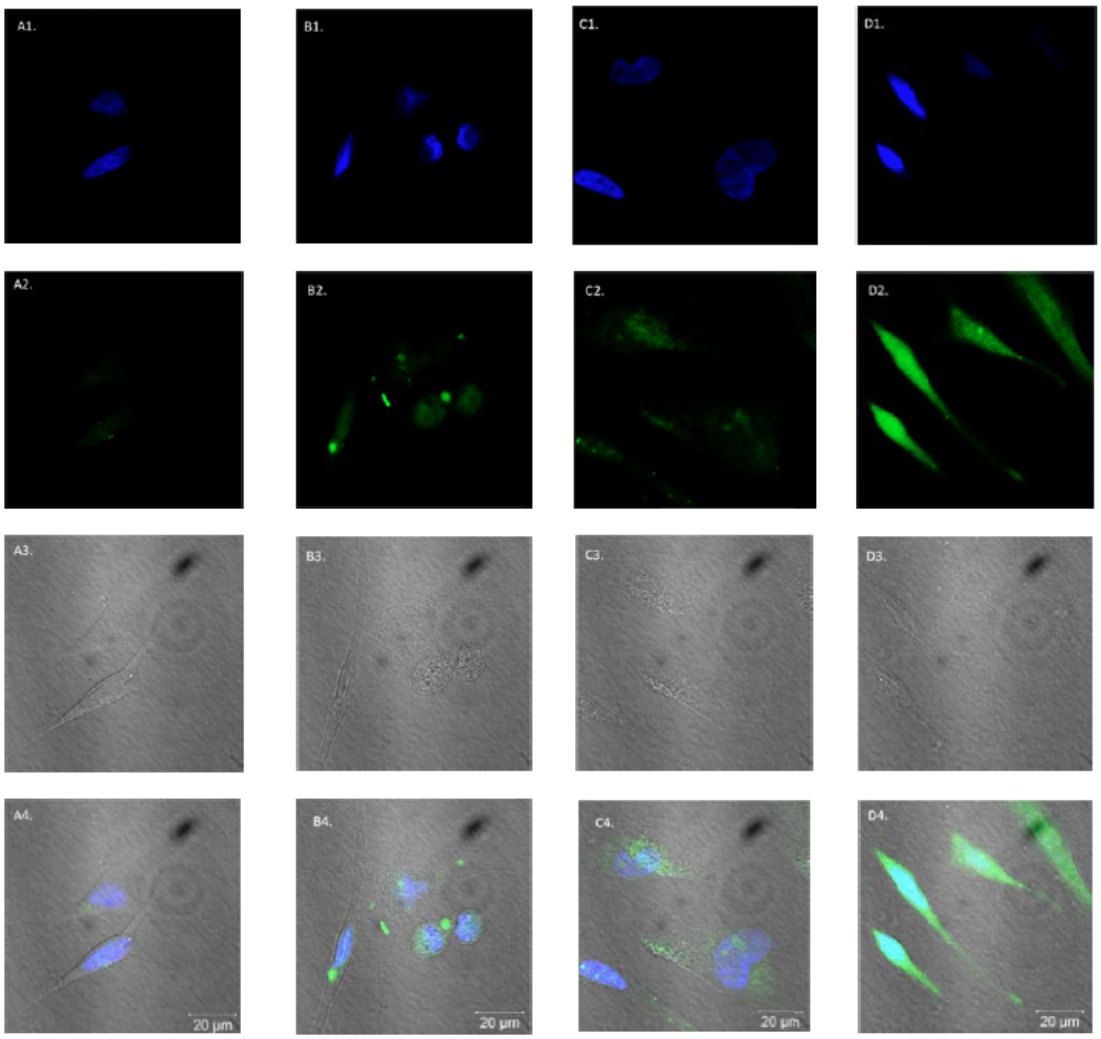

Figure 1.12 Images of Hela cells were taken using a confocal microscope.
Fluorescent images of four samples were shown: A column: blank, cell only; B column: FAM-N37 aptamer; C column: product of N37 aptamer reacting with Tz-FITC (negative control); D column: FITC-labeled TCO37 sequence. Images were taken with 3 channels: 1. DAPI channel (λ_{em}: 461 nm, first row); 2. FITC channel (λ_{em}: 520 nm, second row); 3. Phase contrast channel (third row); 4. Images from the DAPI channel merged that of the FITC channel and phase channel (fourth row)

1.2.5 Cell-SELEX using boronic acid modified DNA

1.2.5.1 Selection procedure[61]

Boronic acid-modified DNA molecules can be obtained by first incorporating a general handle (TCO-TTP) on a natural nucleotide base and then conduct PCR synthesis using KOD-XL-DNA polymerase. Subsequently, the TCO group was reacted with a tetrazine tethered to boronic acids through a fast copper-free click reaction (Scheme **1.4**).[158] An initial library is 80-nt DNA pool containing 40 randomized sites in the center, flanked by 20-mer primers at each end. For aptamer selection work, single-stranded DNA (ssDNA) is critical for binding because of their unique three-dimensional conformations.[159-160] There are several methods reported to generate ssDNA, including biotin–streptavidin separations methods,[161] lambda exonuclease digestion[162] and asymmetric PCR.[163] However, according to previous reports, asymmetric PCR has better performance compared to the conventional streptavidin pull-down method.[164-166] Thus in our study, we utilized 20:1 concentration ratio of FAM-labeled primer 1 (sense) to primer 2 (antisense) in PCR and obtained single-stranded sequences as the majority component. DNA pools were generated using TCO-TTP and other natural nucleoside triphosphates with catalysis of KOD-XL DNA polymerase (see experimental section for details). PCR-amplified products were reacted with boronic acid conjugated to tetrazine (Tz-BBA, 1 mM) at room temperature for 1 h. The post-PCR modification products of each round were examined with 15% polyacrylamide gel electrophoresis (PAGE).

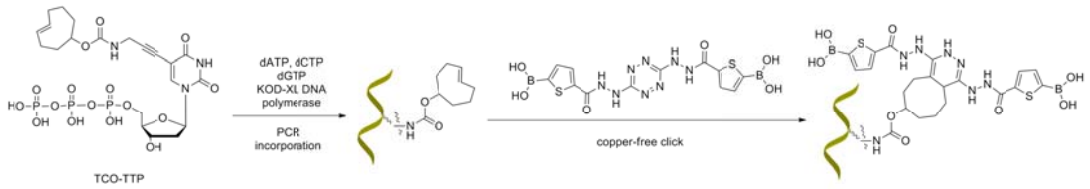

Scheme 1.4 A schematic representation of DNA modifications with a boronic acid

HPAF II and MIA Paca cell lines were chosen to be the target and control cells respectively in the selection. HPAF II and MIA Paca are both human pancreatic cancer cell lines, which share many common features. However, one distinct difference between these two cell lines is that HPAF II highly expresses MUC13 but MIA Paca is a MUC13-null cell line.[167] This makes them suitable for being a target cell line and a control cell line in the cell-SELEX selection. The single-stranded sequences pool selected from each round was amplified with FAM-labeled primer, which gave fluorescent sense ssDNA molecules. When the FAM-labeled sequences bound to glycoprotein on cell surface, it would show obvious fluorescence enrichment on cell surface under fluorescence microscope. Thus, binding of the selected sequence pool to the target cell and control cells was monitored by fluorescent imaging after each round.

Starting from an initial 80-mer DNA pool, we synthesized ssDNA (4 μM), incorporated boronic acid groups and incubated with target cell HPAF II for 30 min at 37 ^{0}C. After incubation, we discarded unbound sequences in buffer and collected cells that bound the target cells. Then we heated the cell suspension to release the bound ssDNA through protein denaturation. The sequences collected were used as the template in the next round PCR amplification. In order to maximize the number of sequences that survives at the beginning of selection, the first three rounds were performed without counter selection (no control cells involved). According to the fluorescent images, fluorescence on cell surface progressively increased with each round of selection, indicating that binding obviously increased after 3 rounds of selection (Figure **1.13**), which seems to be more efficient compared with previous reports.[168-170]

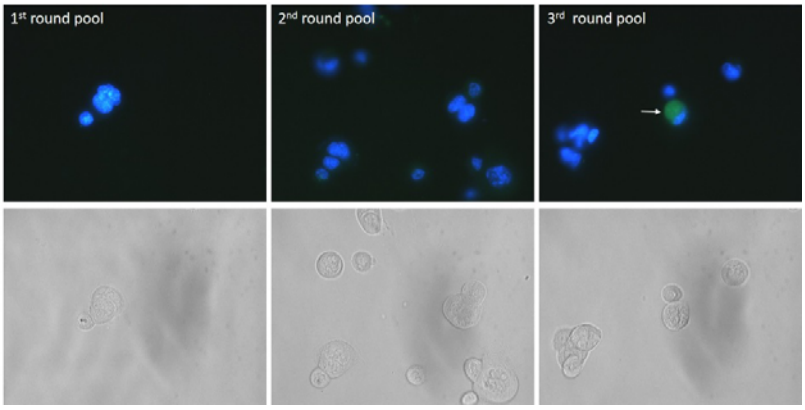

Figure 1.13 Fluorescent image of the first 3 selected pool binding to the target cell.
The second raw is the phase contrast images of the first raw. (The boronic-acid modified sequences have a FAM fluorophore at the 5' end. The selected pool after 3 rounds showed binding, which is indicated with a white arrow in the figure.)

From the 4th round, the control cells were used in counter selections to remove the sequences that also bind to the control cells, as well as to increase the specificity of selection. Selected single-stranded sequences from the 3rd round were amplified with PCR and modified with boronic acids. These modified ssDNA was firstly incubated with control cells to remove sequences bound to MIA Paca, and followed by incubation with target cell line. As shown in Figure **1.14**, after the counter selection was introduced, binding intensity decreased substantially, indicating a reduction in the number of sequences that bind to the target cells. Again, after three additional rounds of selection, the binding appeared at 7th round and could be observed obviously on cell surface (Figure **1.14**). Analysis using 15% PAGE indicated successful incorporation of boronic acid in the selected sequences after the 7th round (Figure **1.15**b). As seen in Figure **1.15**b, the boronic acid-modified sequences (Lane 2) showed decreased electrophoretic mobility compared to non-click DNA molecules (Lane 1), presumably because of the presence of the boronic acid group and increased molecular weight and affinity to the gel matrix materials. These results further suggest the high efficiency of selection using boronic-acid modified

aptamer in cell-SELEX. The sequences collected from the 7th round of selection were then sequenced. Purity of sample for sequencing was analyzed with 15% PAGE (Figure **1.15**c). Compared to negative control sample (no template added, Lane 1), selected pool amplification product (Lane 2) had a clear fluorescent band on gel, indicating pure product prepared for sequencing.

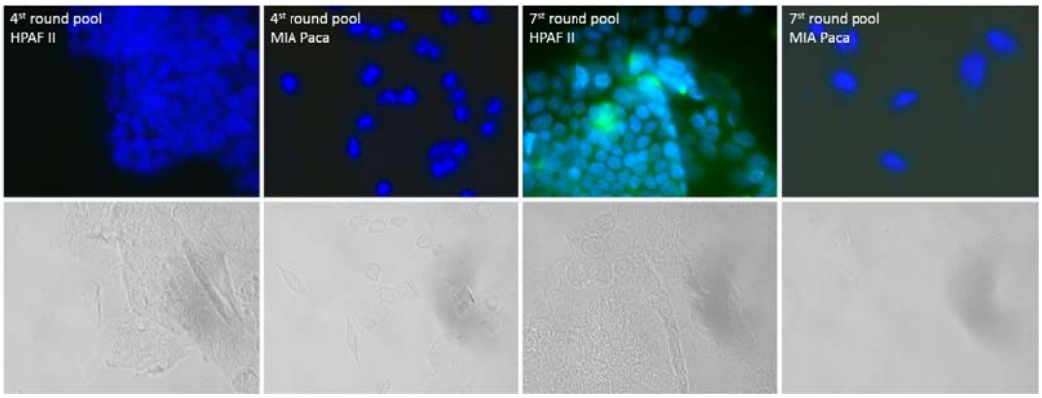

Figure 1.14 Fluorescent image of the 4th and 7th selected pools binding to the target cell and the control cell.
The second raw is the phase contrast images of the first raw.

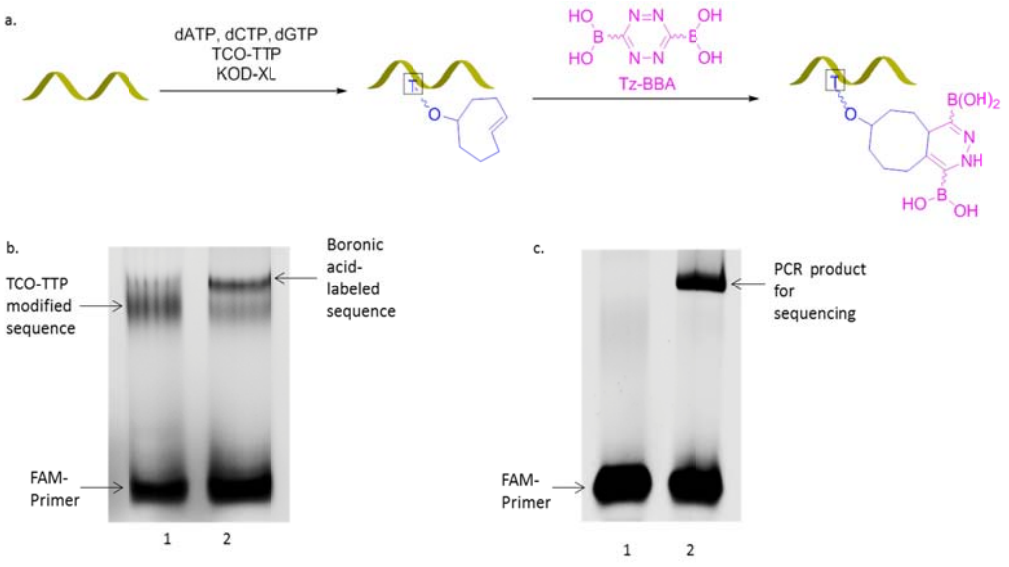

Figure 1.15 Schematic representations and gel images for the 7th round.

a. A schematic representation of boronic acid incorporated in DNA; b. 15% PAGE analysis of boronic acid-modified sequences collected from 7th round; c. 15% PAGE analysis of PCR product prepared for sequencing.

1.2.5.2 Sequencing and binding results

The selected DNA library was cloned into *E. coli* and sequenced (see experimental section for details). Next-generation (Nextgen) sequencing was also used to analyze the enriched library (Tables **1.1** and **1.2**). The sequencing results were analyzed with sequence alignment. To avoid misinterpretation, any sequence with fewer than 70 nucleotides in the library was discarded. Interestingly, sequences randomly selected from colonies and those obtained from Nextgen sequencing showed several identical sequences (highlighted in red). The identical high abundance sequences were the major components in selected pool and were considered potential aptamer candidates. Furthermore, these results indicated that the selection and enrichment progress approached to the end point of selection. As the result, the three identical as well as the most abundant sequences (3UB2, 3B6, 7UB4) were examined as for binding studies. The binding affinity towards HPAF II and MIA Paca cell lines were analyzed by flow cytometry and calculated by measuring fluorescence per cell as increasing concentration of selected sequences.[161]

Table 1.1 Sequencing results from cloning

Name	Sequence
3B4	CCT TCG TTG TCT GCC TTC GTG ACC ATG TGA CTG CAG CAC CCA GAC GGC CGC CAC CCT TCA GAA TTC GCA CCA
3B6	CCT TCG TTG TCT GCC TTC GTG GGC CGA GGC TGG GCG GCG GGC GCG GCC ATG TGG GGG GGG ACC CTT CAG AAT TCG CAC CA
3UB2	CCT TCG TTG TCT GCC TTC GTG GGC CGG GTG GAC CGA GCA TAA GGC GGG GGA GGT GGC GGC ACC CTT CAG AAT TCG CAC CA

7UB4	CCT TCG TTG TCT GCC TTC GTA CCC CAC ACG AAC CCC GAC GCG CCC GGG CAT CCT GGC TGC ACC CTT CAG AAT TCG CAC CA
7UB5	CCT TCG TTG TCT GCC TTC GTG CGC CGT GCA GAC GGT ACC CGA CCC CCG CCT CCG GCC ACC ACC CTT CAG AAT TCG CAC CA

Table 1.2 Sequencing results from Nextgen sequencing

Name	Sequence	Abundance
3UB2	CCT TCG TTG TCT GCC TTC GTG GGC CGG GTG GAC CGA GCA TAA GGC GGG GGA GGT GGC GGC ACC CTT CAG AAT TCG CAC CA	4.63%
3B6	CCT TCG TTG TCT GCC TTC GTG GGC CGA GGC TGG GCG GCG GGC GCG GCC ATG TGG GGG GGG ACC CTT CAG AAT TCG CAC CA	2.25%
7UB4	CCT TCG TTG TCT GCC TTC GTA CCC CAC ACG AAC CCC GAC GCG CCC GGG CAT CCT GGC TGC ACC CTT CAG AAT TCG CAC CA	0.70%
Oligo4	CCT TCG TTG TCT GCC TTC GTG GGC CGG GGT GGA CCG AGC ATA AGG CGG GGG AGG TGG CGG CAC CCT TCA GAA TTC GCA CCA	0.70%
Oligo5	CCT TCG TTG TCT GCC TTC GTG GGC CGG GTG GAC CGA ACA TAA GGC GGG GGA GGT GGC GGC ACC CTT CAG AAT TCG CAC CA	0.28%
Oligo6	CCT TCG TTG TCT GCC TTC GTG GGC CGA GGC TGG GCG GCG GGC GCG GCC ATG TGG GGT GGG ACC CTT CAG AAT TCG CAC CA	0.28%
Oligo7	CCT TCG TTG TCT GCC TTC GTG GGC CGA GGC TGG GCG GCG GGC GCG GCC ATG TGG GGG GGG GAC CCT TCA GAA TTC GCA CCA	0.28%

To obtain sense ssDNA and control the concentration of single-stranded sequence for bind studies, lambda exonuclease digestion was used to remove antisense sequences.[162] Conceivably, enzyme digestion of phosphate-labeled sequences and followed by 10k cut-off filtration would gave more accurate concentration of single-stranded sequences of aptamer candidates compared to asymmetric PCR.[166] Thus, the sequences were synthesized using phosphate-modified complementary template, FAM-labeled sense primer 1 and TCO-TTP

through primer extension. Lambda exonuclease cleaved and digested phosphate-labeled antisense sequence, resulting in FAM-labeled single strand of aptamer candidates (Figure **1.16**). As seen in gel, with treatment of lambda exonuclease, double-stranded sequences bands disappeared and new low mobility bands emerged. It has been reported that ssDNA moved slower than dsDNA because of its secondary structure.[171] So the gel results represented the successful digestion of antisense sequences and generation of aptamer candidates. Then, the single-stranded sequences were incorporated with boronic acid through click reaction under room temperature. Stock solutions of aptamer candidates were prepared with series dilution from 2 μM.

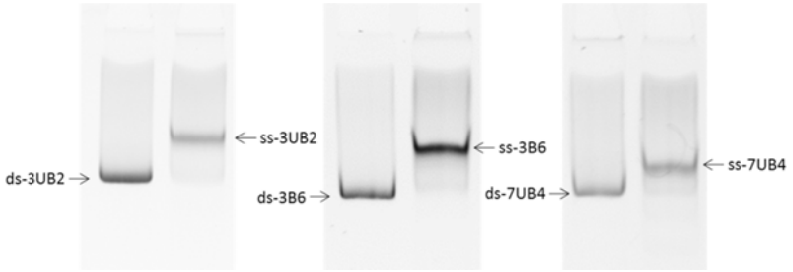

Figure 1.16 15% PAGE analysis of dsDNA and ssDNA obtained from lambda exonuclease treatment of aptamer candidates

Stock solutions at different concentrations of aptamer candidates were incubated with HPAF II for 30 min at 37 ^{0}C. Washing buffer was used to wash out non-bound sequences, leaving FAM-labeled aptamer candidates bound on cell surface. Thus the cells that had sequences bound to surface would have strong fluorescence. The fluorescence changes per cell as increasing concentration of selected sequences were monitored by flow cytometer. Ten thousand of cells were counted in each experiment. The fluorescence intensities of cells, which were incubated with different concentration of sequences, were recorded (row 2-8, Figure **1.17**). Binding studies were designed to examine the binding affinity and specificity of aptamer

candidates. Taking the most abundant sequence 3UB2 as an example, four sets of experiments were included. Binding studies of boronic acid-modified aptamer candidate (3UB2-BBA, column 5, Figure **1.17**) and non-click, TCO-modified aptamer candidate (3UB2, column 4, Figure **1.17**) were expected to show good affinity, especially boronic acid modified sequences. Two control experiments were designed to confirm binding efficiency and specificity. Because of low PCR efficiency in incorporating modified thymidine, the selected aptamer candidates only had 3 thymidine nucleosides among 40-nt randomized sites. Thus one control sequence was AT-rich sequence synthesized with natural nucleosides triphosphate (control sequence, column 2, Figure **1.17**). Another control sequence (nT-3UB2, column 3, Figure **1.17**) was the same sequence as aptamer candidate except using natural TTP instead of TCO-TTP. As shown in Figure 5, TCO-modified aptamer candidate 3UB2 (column 4) and boronic acid-modified aptamer candidate 3UB2-BBA (column 5) had obvious increased binding fluorescence peak starting at 125 nM. The newly appearing fluorescence binding peak indicated up to 15% of cells were bound with FAM-labeled sequences. The binding peak fluorescence percentage increased to more than 90% at 500 nM of sequences binding, which demonstrated strong binding between aptamer candidates and target cells. Under the same conditions, control sequence (column 2) didn't have obvious fluorescence increases compared to aptamer candidates. These binding results confirmed that selected sequences would have binding affinity to target cells. Another control nT-3UB2 (column 3) also didn't show high fluorescence intensity compared to aptamer candidates, which demonstrated only TCO-TTP incorporated DNA molecules have strong binding to HPAF II. Other aptamer candidates (3B6 and 7UB4) binding affinity were also tested under the same condition (Figure **1.18**). The binding results indicated good binding affinity of aptamer candidates to target cells. Compared to the data above, 3UB2 had the highest binding

affinity to HPAF II, while 3B6 and 7UB4 had little lower affinity. This conclusion was correlated to the abundance of each aptamer candidate in selected pool.

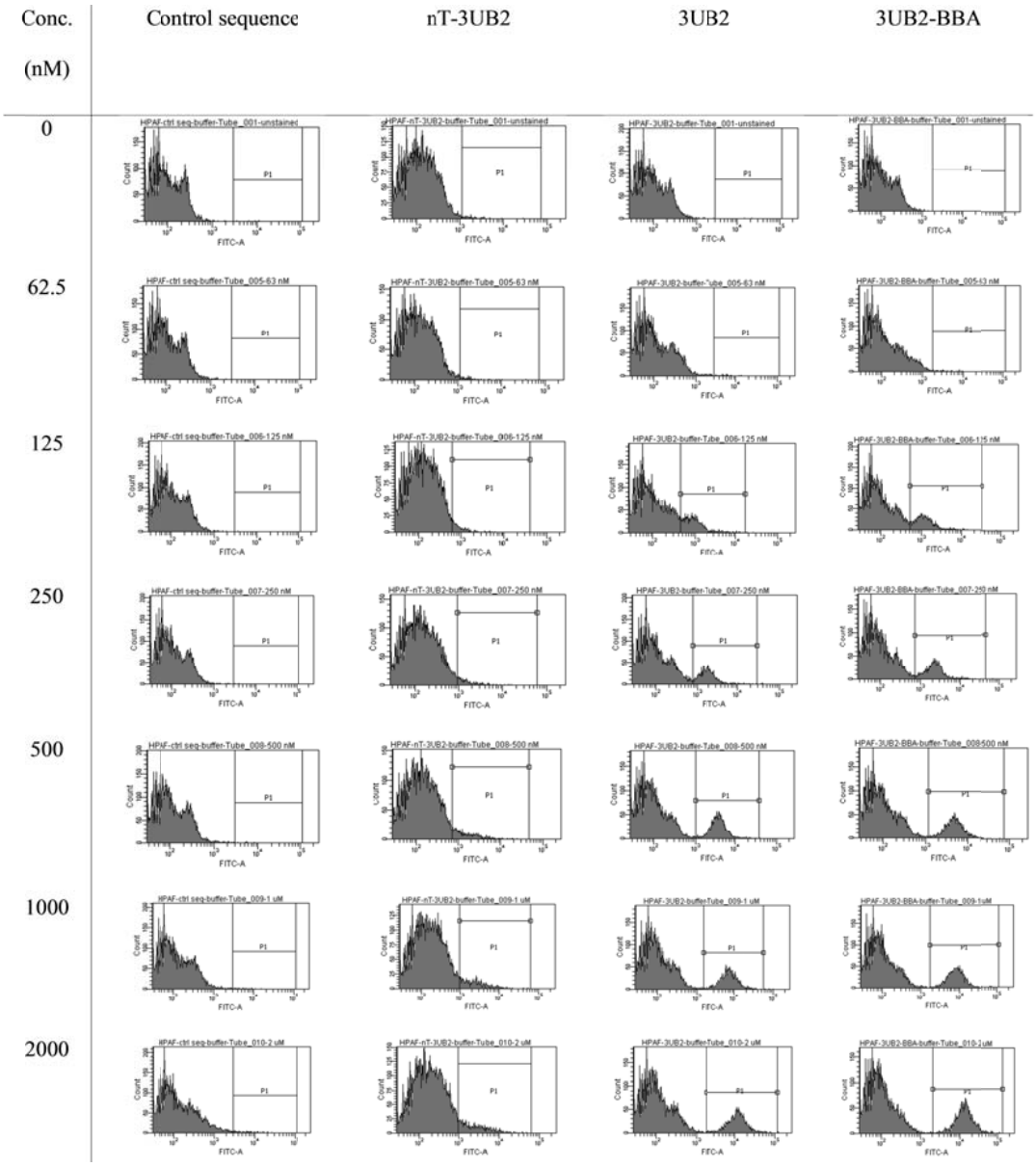

Figure 1.17 Binding studies of 3UB2 aptamer candidate to HPAF II cell using flow cytometry. Flow cytometer results of four sets of experiments were shown: 1. AT-rich control sequence (column 2); 2. 3UB2 aptamer candidate using natural TTP instead of TCO-TTP (column 3); 3. TCO-TTP incorporated 3UB2 aptamer candidate (column 4); 4. Boronic acid-incorporated 3UB2 aptamer candidate (column 5). Data represents the average of three independent experiments.

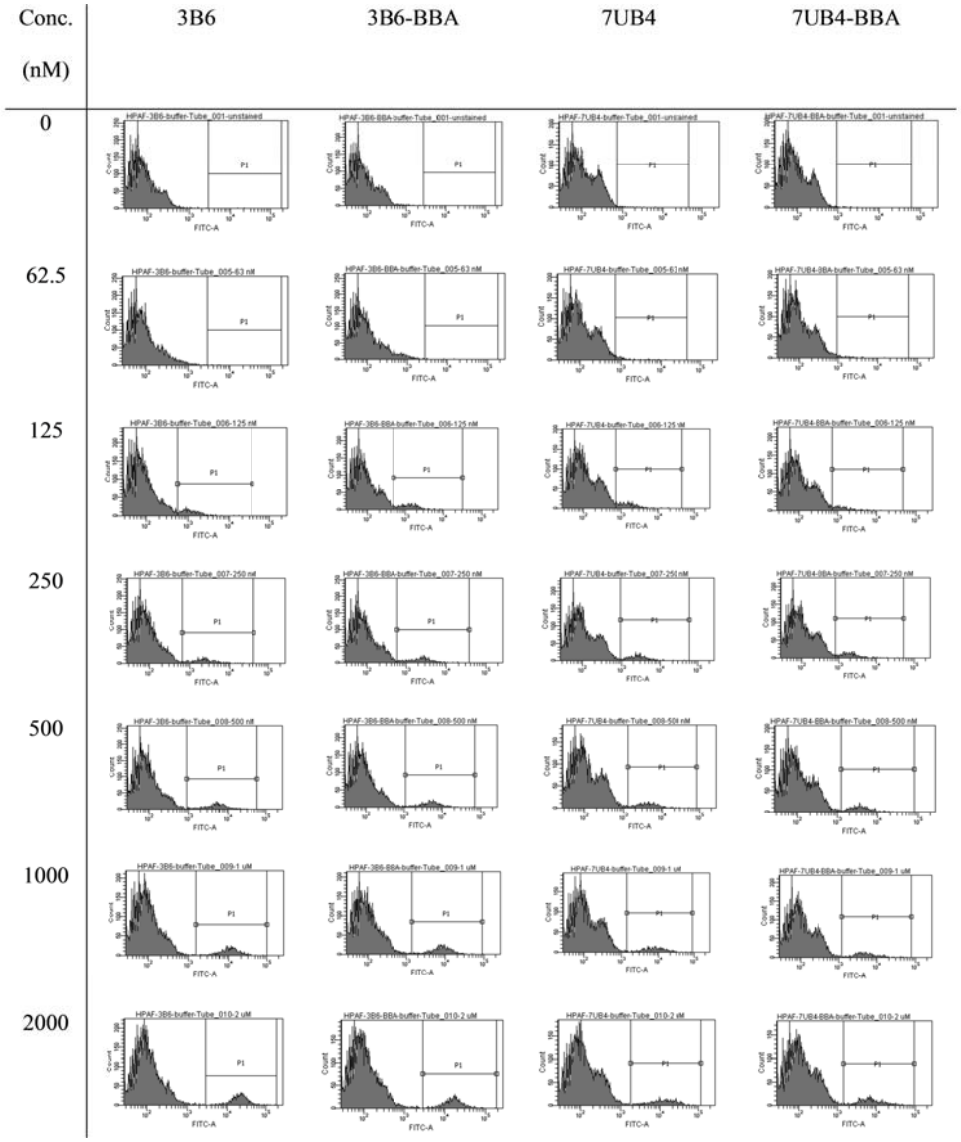

Figure 1.18 Binding studies of 3B6 and 7UB4 aptamer candidates to HPAF II cell using flow cytometry.

Flow cytometer results of four sets of experiments were shown: 1. TCO-TTP incorporated 3B6 aptamer candidate (column 2); 2. Boronic acid-incorporated 3B6 aptamer candidate (column 3); 3. TCO-TTP incorporated 7UB4 aptamer candidate (column 4); 4. Boronic acid-incorporated 7UB4 aptamer candidate (column 5). Data represents the average of three independent experiments.

During the selection process, we applied negative selection against control MUC13-null cell line (MIA Paca) to increase the selection stringency. The binding affinities of aptamer candidates to control cells were also evaluated by flow cytometer. As mentioned above, four sets

of binding studies were conducted: 1. AT-rich control sequence (control sequence, column 2, Figure **1.19**); 2. 3UB2 aptamer candidate using natural TTP instead of TCO-TTP (nT-3UB2, column 3, Figure **1.19**); 3. TCO-TTP incorporated and non-click 3UB2 aptamer candidate (3UB2, column 4, Figure **1.19**); 4. Boronic acid-incorporated 3UB2 aptamer candidate (3UB2-BBA, column 5, Figure **1.19**). As seen in Figure **1.19**, the aptamer candidate didn't show obvious binding peak and fluorescence increase with incubation of control cell up to 2 μM. The control cell binding studies indicated that the aptamer candidates had good specificity between two pancreatic cancer cell lines as expected, resulting in the capability to recognize and differentiate these two cancer cell lines.

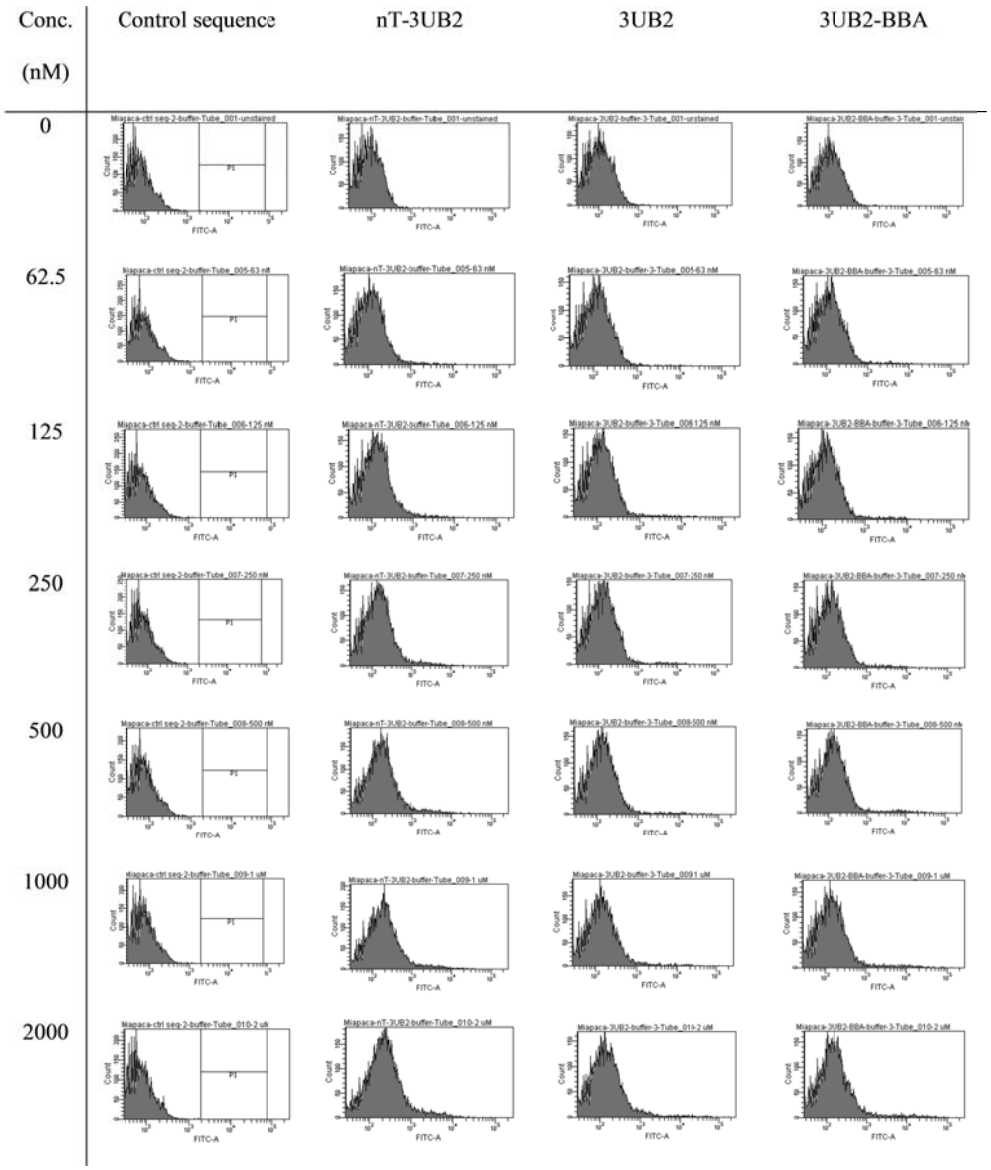

Figure 1.19 Binding studies of 3UB2 aptamer candidate to MIA Paca cell using flow cytometry. Flow cytometer results of four sets of experiments were shown: 1. AT-rich control sequence (column 2); 2. 3UB2 aptamer candidate using natural TTP instead of TCO-TTP (column 3); 3. TCO-TTP incorporated 3UB2 aptamer candidate (column 4); 4. Boronic acid-incorporated 3UB2 aptamer candidate (column 5). Data represents the average of three independent experiments.

It needs to be noted that boronic acid-modified sequences didn't show obvious difference compared to those without in binding studies. We would think these results might because of the binding buffer we used in selection process. As it known, boronic acids have good binding

affinity to carbohydrates. Although glucose is not as a good binder as fructose, in the presence of 25 mM of glucose in the buffer, most of boronic acids would be saturated by glucose binding. As a result, it might be hard to select sequences that can bind differently to target cells with boronic acid-modified and TCO-TTP modified. The data above demonstrated that selected modified sequences are potential aptamers for pancreatic cancer cell recognition, the target MUC13. Further structural studies and target identification work need to be conducted.

1.3 Experimental Section

1.3.1 General Information

Solvents and reagents were purchased from VWR International, Oakwood Product Inc., or Sigma-Aldrich Co. and used without purification unless specified otherwise. When necessary, solid reagents were dried under high vacuum. Reactions with compounds sensitive to air or moisture were performed under argon. Solvent mixtures are indicated as volume/volume ratios. Thin layer chromatography (TLC) was run on Sorbtech W/UV254 plates (0.25 mm thick), and visualized under UV-light. Flash chromatography was performed using Fluka silica gel 60 (mesh size: 0.040-0.063 mm) using a weight ratio of ca. 30:1 for silica gel over crude compound. ^{1}H, ^{13}C, and ^{31}P-NMR spectra were recorded on a Bruker Avance 400 spectrometer (400, 100, and 166 MHz, respectively) in deuterated chloroform ($CDCl_3$), methanol-d_4 (CD_3OD), and DMSO-d_6 with either tetramethylsilane (TMS) (0.00 ppm) or the NMR solvent as the internal reference. HPLC purification for *trans*-cyclooctene triphosphate (TCO-TTP) was carried out using a Shimadzu LC-20AT VP system with a Zobax C18 reversed-phase column (9.4 mm × 25 cm). The sample was eluted (3 mL/min) with buffer A (20 mM triethylammonium acetate, pH 6.9-7.1) and buffer B (50% acetonitrile, 20 mM triethyl ammonium acetate) with the following: 0 min 0% B; 20 min 20% B; 30 min 100% B; 38 min 100% B; 40 min 0% B; and 45 min 0% B.

DNA primers and templates were purchased from Integrated DNA Technologies. Klenow fragment (3'-5' exo), *Taq.* DNA polymerase and Deep $Vent_R$ (exo-) DNA polymerase were purchased from New England Biolabs. KOD-XL DNA polymerase was purchased from EMD Chemicals. Reaction buffers were used as provided. Reaction buffers were used as provided. SELEX binding buffer contained: 4.5 g/L glucose, 5 mM $MgCl_2$, 100 mg/L yeast tRNA, 1g/L bovine serum albumin in phosphate-buffered saline.[161] SELEX washing buffer components are: 4.5 g/L glucose and 5 mM $MgCl_2$ in phosphate-buffered saline.[161]

HPAF II and MIA Paca cell lines were obtained from Dr. Subhash Chauhan's lab (University of Tennessee, Health Science Center). Cells were grown in DMEM culture medium supplemented with 10% fetal bovine serum and 1% penicillin-streptomycin. Fluorescent imaging was conducted using Zeiss fluorescent microscope. The Qiagen PCR cloning kit was obtained from Qiagen. The flow cytometer used is BD LSRFortessa.

1.3.2 Experimental Procedure for the Synthesis of TCO-TTP

Synthesis of (*E*)-Cyclooct-4-en-1-yl (2,5-dioxopyrrolidin-1-yl) carbonate **22**: Compound **22** was prepared starting from cyclooctadiene (**17**) in four steps following literature procedures.[172]

Synthesis of 5-(3-Aminoprop-1-yn-1-yl)-1-((2R,4S,5R)-4-hydroxy-5 (hydroxyl-methyl) tetrahydrofuran-2-yl)pyrimidine-2,4(1H,3H)-dione **26**: Compound **26** was synthesized starting from 5-odo-2'-deoxyuridine (**23**) in two steps following literature procedures.[139, 173]

Synthesis of TCO-T, (*E*)-Cyclooct-4-en-1-yl(3-(1-((2R,4S,5R)-4-hydroxy-5-(hydroxylmethyl)tetrahydrofuran-2-yl) 2,4-dioxo-1,2,3,4-tetrahydropyrimidin-5-yl)prop-2-yn-1-yl) carbamate **27**: To a mixture of succimidyl ester **22** (134 mg, 0.5 mmol) and amine modified deoxyuridine **26** (168 mg, 0.6 mmol) in DMF 10 mL was added DIPEA (129 mg, 1 mmol). The

reaction mixture was wrapped in foil and stirred in r.t. for 12 h. Reaction solution was concentrated under reduced pressure and purified with silica gel chromatography (12% MeOH in DCM) to give a white solid (108 mg, yield 52%). ^{1}H NMR (methanol-*d*4): 8.25 (s, 1H), 6.25 (t, *J* = 6.4 Hz, 1H), 5.58-6.20 (m, 1H), 5.47-5.57 (m, 1H), 4.05 (s, 2H), 3.95-3.81 (m, 1H), 3.73-3.77 (m, 2H), 3.24-3.37 (m, 2H), 2.26-2.37 (m, 4H), 2.21-2.25 (m, 1H), 1.99-2.00 (m, 4H), 1.93-1.98 (m, 2H). ^{13}C NMR (methanol-*d*4): 163.1, 149.8, 144.0, 134.7, 132.4, 128.4, 98.6, HRMS (ESI) for $C_{21}H_{27}N_3O_7$ $[M+H]^+$ Cacld: 434.1849; Found: 434.1899.

Synthesis of TCO-TTP, (*E*)-Cyclooct-4-en-1-yl(3-(1-((2R,4S,5R)-4-hydroxy-5-(((hydroxyl((hydroxy(phosphonooxy)phosphoryl)oxy)phosphoryl)oxy)methyl)tetrahydrofuran-2-yl)-2,4-dioxo-1,2,3,4-tetrahydropyrimi-din-5-yl)prop-2-yn-1-yl)carbamate **28**: To a solution of TCO-T **26** (69 mg, 0.16 mmol) and proton sponge (42 mg, 0.19 mmol, pre-dried in vacuum over P_2O_5 overnight) in anhydrous trimethylphosphate (0.6 mL) was added freshly distilled $POCl_3$ (18 μL, 0.19 mmol) dissolved in anhydrous trimethylphosphate (0.2 mL) dropwise via a syringe with stirring under argon at 0 °C. The reaction mixture was further stirred in an ice-bath for 2 h and then a solution of tributylammonium pyrophosphate (226 mg, 0.48 mmol) and tri-*n*-butylamine (0.4 mL,) in 1.0 mL of anhydrous DMF was added in one portion. The mixture was stirred at RT for 10 min and then triethylammonium bicarbonate solution (0.1 M, pH 8, 11 mL) was added. After stirring at r.t. for an additional 1 h, the resulting reaction mixture was transferred to a 50-mL centrifuge tube. Then EtOH (33 mL) was added followed by 3 M NaCl solution (1.0 mL). After vortexing for 10 sec, the centrifuge tube was placed at -80 ^{o}C for 1 h, and then centrifuged at 5000 rpm for 20 min. After removing the supernatant, the resulting pellet was purified by HPLC and lyophilized to give a pale white powder (32 mg, 32%). ^{1}H NMR (D_2O): 8.06 (s, 1H), 6.18 (t, *J* = 6.8 Hz, 1H), 5.58-6.20 (m, 1H), 5.47-5.57 (m, 1H), 4.16-4.25 (m, 2H), 4.08-4.12 (m,

3H), 4.0 (d, *J* = 7.2 Hz, 1H), 2.25-2.34 (m, 5H), 1.88-1.98 (m, 3H), 1.35-1.86 (m, 4H). ^{13}C NMR (D_2O):179.7, 164.6, 158.0, 150.0, 144.8, 135.6, 133.4, 99.2, 82.4, 73.2, 70.5, 65.3, 46.6, 40.4, 38.7, 37.8, 33.7, 32.0, 30.6, 22.2, 8.2; ^{31}P NMR (D_2O) -10.9, -11.6, -23.3. MS (ESI) for $C_{21}H30N_3O_{16}P_3$ $[M-H]^-$ Cacld. 672.08; Found: 672.1

1.3.3 Experimental Procedure for the Synthesis of Tz-BBA

Synthesis of 4,4'-(1,2,4,5-tetrazine-3,6-diyl)diphenol: Compound was prepared starting from 4-hydroxybenzonitrile in two steps following literature procedures.[174]

Syntheis of Tz-BBA (**29**): To a solution of diphenol compound (133 mg, 0.5 mmol) was added 4-(bromomethyl) phenylboronic acid (219 mg, 1.3 mmol), $CsCO_3$ (488 mg, 1.5 mmol), and NaI (30 mg, 0.2 mmol) in acetone (20 mL). The mixture was heated to reflux and stirred at 56 ^oC overnight. The solution was concentrated under vacuum and acidified with 1M HCl. The residue was washed with EtOAc and MeOH to afford Tz-BBA **29**. ^{1}H NMR (DMSO-*d6*): 8.47 (d, *J* = 8 Hz, 4H), 7.83 (d, *J* = 8 Hz, 4H), 7.46 (d, *J* = 8 Hz, 4H), 7.31 (d, *J* = 8 Hz, 4H), and 5.28 (s, 4H). HRMS (ESI) for $C_{28}H_{24}B_2N_4O_6$ $[M+H]^+$ Cacld: 534.1882; Found: 535.1965.

1.3.4 Experimental Procedure for the Synthesis of Tz-FITC

Synthesis of 2,5-Dioxopyrrolidin-1-yl 4-(6-(pyrimidin-2-yl)-1,2,4,5-tetrazin-3-yl) benzoate: Compound was prepared starting from pyrimidine-5-carbonitrile in three steps following literature procedures.[175]

Synthesis of 5-(3-(2-Aminoethyl)thioureido)-2-(6-hydroxy-3-oxo-3H-xanthen-9-yl) benzoic acid: Compound was prepared starting from commercially available fluorescein isothiocyanate (FITC) in one step following literature procedures.[176]

Synthesis of Tz-FITC (**30**): To a mixture of tetrazine benzoate compound (188 mg, 0.5 mmol) and FITC compound (112 mg, 0.25 mmol) in MeOH (20 mL) was added Et_3N (55 mg,

0.5 mmol). The mixture was stirred at r.t. overnight. The reaction mixture was acidified to pH 2 and extracted with DCM. Residue was concentrated in *vacuo* and purified with silica gel chromatography (20% MeOH in DCM) to give solid product with 40% yield. ^{1}H NMR (DMSO-*d6*): 10.42 (s, 1 H), 9.21 (d, *J* = 4.8, 2 H), 8.97 (s, 1 H), 8.67 (d, *J* = 8.2, 2 H), 8.48 (br, 1 H), 8.30 (s, 1 H), 8.21 (d, *J* = 8.2, 2 H), 7.85 (t, *J* = 4.8, 1 H), 7.80 (d, *J* = 7.9, 1 H), 7.18 (d, *J* = 8.4, 1 H), 6.69 (s, 2 H), 6.59 (m, 4 H), 3.78 (s, 2 H). HRMS (ESI) for $C_{36}H_{25}N_9O_6S$ $[M-H]^-$ Cacld: 710.1549; Found: 710.1589.

1.3.5 Studies of the reaction kinetics between TCO-TTP and Tetrazine

1.3.5.1 Study of reaction kinetics between TCO-TTP and 4-(6-(pyrimidin-2-yl)-1,2,4,5-tetrazin-3-yl) benzoic acid

To a solution of TCO-TTP in H_2O was added a solution of 4-(6-(pyrimidin-2-yl)-1,2,4,5-tetrazin-3-yl)benzoic acid (**31**, Tz-pym, core structure of Tz-FITC) aqueous solution to afford a final concentration of 20, 25, 30, and 40 μM for TCO-TTP, and a final concentration of 2 μM for Tz-pym. The resulting mixture was examined by monitoring its absorption at 327 nm. Using established procedures,[147] the second-order rate constant was determined to be 1087 $M^{-1}\cdot s^{-1}$.

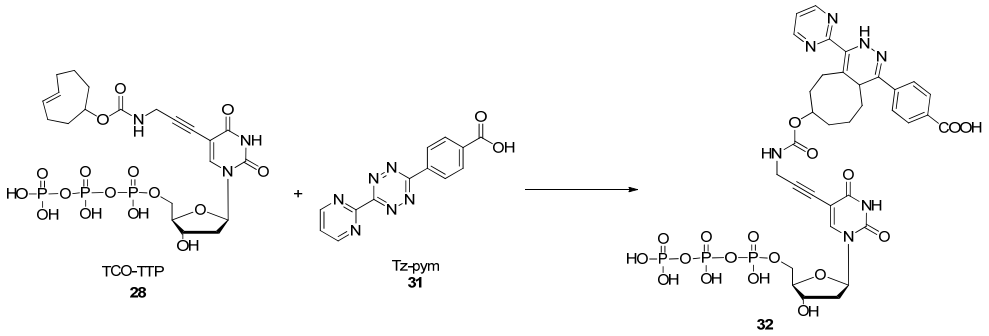

Scheme 1.5 Reaction between TCO-TTP and Tz-pym

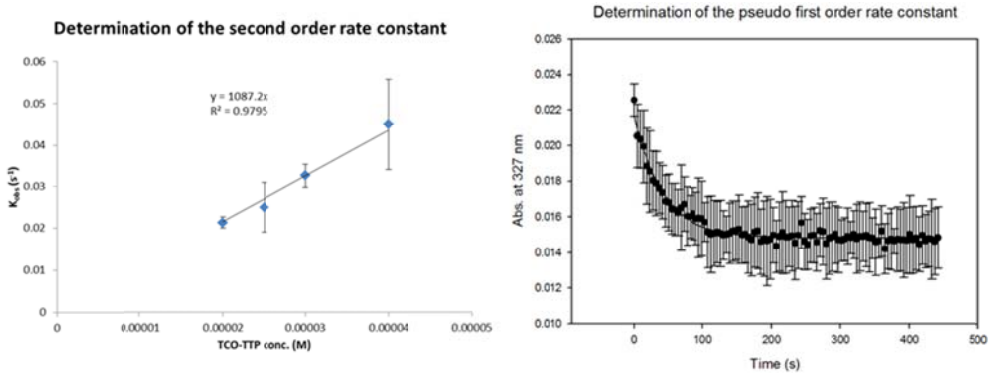

Figure 1.20 Determination of the second order rate constant for the reaction in Scheme 1.5. Left: Determination of the second order rate constant for the reaction in Scheme **1.5**: TCO-TTP final concentration: 20, 25, 30, 40 μM; Tz-pym final concentration: 2 μM. Second order rate constant K_2= 1087 $M^{-1}{\cdot}s^{-1}$. Right: Determination of the pseudo first order rate constant at 25 μM TCO-TTP. Data represents the average of three independent experiments.

1.3.5.2 Study of reaction kinetics between TCO-TTP and 3,6-diphenyl-1,2,4,5-tetrazine

To a solution of TCO-TTP in H_2O was added an aqueous solution of 3,6-diphenyl-1,2,4,5-tetrazine (**33**, Tz-ph, core structure of Tz-BBA) to afford a final concentration of 30, 40, 50 and 60 μM for TCO-TTP, and a final concentration of 3 μM for Tz-ph. The resulting mixture was examined by monitoring its absorption at 391 nm. Using established procedures,[147] the second-order rate constant was determined to be 27 $M^{-1}{\cdot}s^{-1}$.

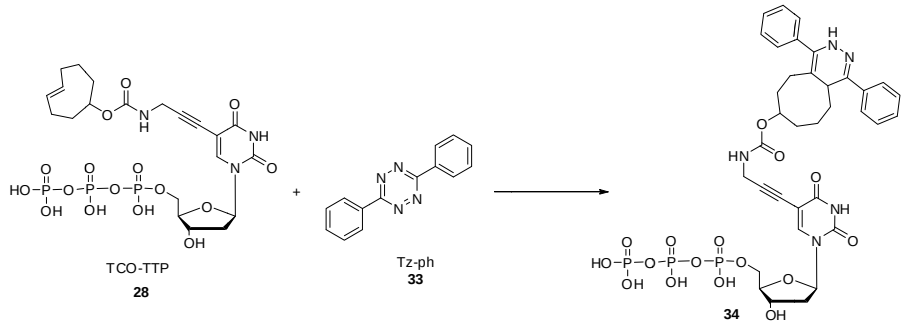

Scheme 1.6 Reaction between TCO-TTP and Tz-ph

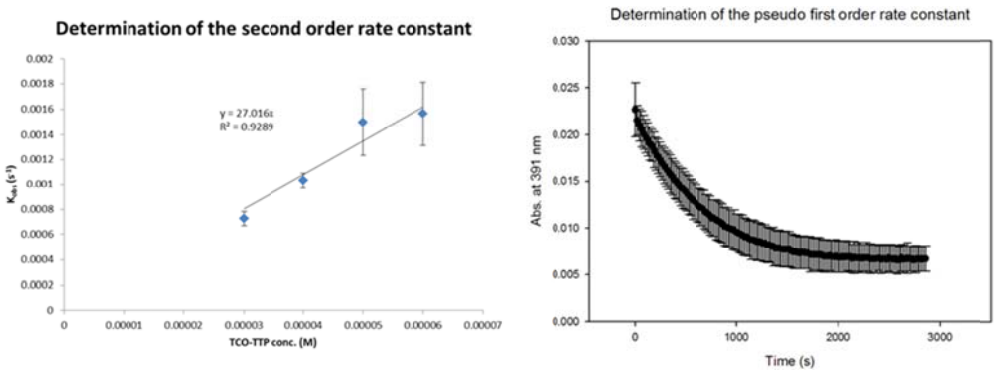

Figure 1.21 Determination of the second order rate constant for the reaction in Scheme 1.6. Left: Determination of the second order rate constant for the reaction in Scheme **1.6**: TCO-TTP final concentration: 30, 40, 50, 60 μM; Tz-ph final concentration: 3 μM. Second order rate constant K_2= 27 $M^{-1}s^{-1}$. Right: Determination of the pseudo first order rate constant at 60 μM TCO-TTP. Data represents the average of three independent experiments.

1.3.6 Experimental Procedure of enzymatic incorporation of TCO-TTP and boronic acid labeling

1.3.6.1 Experimental Procedure for Klenow Fragment Catalyzed Primer Extension:

A 50 μL reaction mixture of contained 21-nt template (5'-GGT TCC ACC AGC AAC CCG CTA-3' (20 μM)), 14-nt primer (5'-TAG CGG GTT GCT GG-3' (20 μM)), Tris-HCl (10 mM), NaCl (50 mM), $MgCl_2$ (10 mM), dithiothreitol (1 mM) at pH 7.9, Klenow fragment (0.5 U μL^{-1}), dATP, dCTP, dGTP, and dTTP (or TCO-TTP) (200 μM). Reactions were performed by incubating the prepared solutions at 25 ^oC for 30 min. The primer extension products were analyzed by 20 % PAGE.

1.3.6.2 Experimental Procedure for KOD-XL Catalyzed Primer Extension:

A 50-μL reaction mixture contained 21-nt template (Template-2: 5'-TCA GTC ACC AGC AAC CCG CTA-3', Template-3: 5'-CAC GAC ACC AGC AAC CCG CTA-3' (20 μM)), 14-nt primer (5'-TAG CGG GTT GCT GG-3' (20 μM)), Tris-HCl (10 mM), NaCl (50 mM), $MgCl_2$ (10 mM), dithiothreitol (1 mM) at pH 7.9, KOD-XL (0.5 U μL^{-1}), dATP, dCTP, dGTP,

dTTP, or TCO-TTP (200 μM). Reactions were performed by incubating the prepared solutions at 90 ^{o}C for 1 min, 20 ^{o}C for 1 min, and 66 ^{o}C for 20 min. The primer extension products were analyzed by 20 % PAGE.

1.3.6.3 Experimental Procedure for Post-synthesis Labeling of Primer Extension Products with Tz-BBA:

The primer extension product TCO-DNA_{21} was purified using Millipore Amicon 3 kDa spin column. 2 μL of 10 mM Tz-BBA in DMSO was added into pre-purified TCO-DNA_{21} (20 μL). The reaction was allowed to vortex at r.t. for 15 min. The negative control experiment was performed following the same procedure except using dNTPs-DNA_{21}, the primer extension product using dNTPs and other reagents. The resulting DNA products after post-synthesis modification were purified with Millipore Amicon 3 kDa spin column and analyzed by 20 % PAGE.

1.3.6.4 Experimental Procedure for PCR Incorporation and Post-PCR Labeling of TCO-TTP:

A 50-μL PCR mixture contained DNA 90-nt template (PBA, 5'-CCT TCG TTG TCT GCC TTC GTG AGC GGA GTC AGA CGC ACG CTC GTA CCT GTG CGC AAG CAC TAT GAC GGA CAC CCT TCA GAA TTC GCA CCA-3', 10 nM), 20-nt primer 1 (5'-TGG TGC GAA TTC TGA AGG GT-3', 1 μM), 20-nt primer 2 (5'-CCT TCG TTG TCT GCC TTC GT-3', 1 μM), dATP, dCTP, dGTP, dTTP or TCO-TTP at a concentration of 200 μM, 0.5 U μL^{-1} KOD-XL DNA polymerase and 1× reaction buffer as provided by vender. Thirty thermal cycles were conducted with melting at 90 °C for 20 s, annealing at 48 °C for 20 s, and extending at 72 °C for 30 s with initial denaturing at 90 °C for 2 min and final extension at 72 °C for 5 min. The PCR products were then analyzed by 15% PAGE.

Post-synthesis labeling of the PCR products was performed using similar procedures as those for primer extension. Specifically, TCO-DNA_{90} prepared from PCR was purified using Millipore Amicon 10 kDa spin column. Pre-purified TCO-DNA_{90} (20 μL) was then added to the 2 μL of 10 mM Tz-BBA DMSO solution, which was further reacted at r.t. for 30 min. The negative control experiment was performed following the same procedure except using dNTPs-DNA_{90}, the PCR product using dNTPs and other reagents. The resulting DNA product after post-synthesis modification was purified with Millipore Amicon 10 kDa spin column and analyzed by 15% PAGE.

1.3.6.5 Experimental Procedure of Fluorescence Labeling and Cell Imaging Studies:

The PCR mixture of a final volume of 50 μL contained DNA 86-nt template (N37, 5'-ATA CCA GCT TAT TCA ATT CTG CCG GGA ACA CCG CGT GGC TCT CTG CAA CGC CCA GGA CAT ACC ACA TTA GAT AGT AAG TGC AAT CT-3' 10 nM each), 18-nt primer 1 or 5'-FAM 18-nt primer 1 (5'-(FAM)-ATA CCA GCT TAT TCA ATT-3', 1 μM), primer 2 (5'-AGA TTG CAC TTA CTA TCT-3', 1 μM),[155] dATP, dCTP, dGTP, dTTP or TCO-TTP at a concentration of 200 μM, 0.5 U μL^{-1} KOD-XL DNA polymerase and 1× reaction buffer as provided by vender. PCR thermal cycles were conducted as previous incorporation. Post-PCR labeling using Tz-FITC was performed with similar procedures as previous incorporation. The FITC-labeled DNA product was purified with Millipore Amicon 10 kDa spin column and analyzed by 15% PAGE.

HeLa cells were seeded on rectangular coverslips in a 6-well plate until it achieved 90% coverage on surface before the imaging experiment and were grown in Dulbecco's modified Eagle's medium (DMEM) supplemented with 10% fetal bovine serum (FBS) and 1% PNS at 37 °C with 5% CO_2. The cells were then incubated with either FAM-N37 aptamer, or FITC-labelled

TCO37 aptamer at the same concentration in SELEX binding buffer[161] for 30 min at 37 °C. After washing with phosphate buffered saline (PBS) for 2 times, the cells were fixed with ice-cold methanol for 5 min. Thereafter, the coverslips containing the cells were mounted onto the slides and imaged with a fluorescent microscope.

1.3.7 Experimental procedure of cell-based SELEX using boronic acid-modified DNA molecules

1.3.7.1 Initial DNA pool preparation

The initial ssDNA library comprised of 80 bp, with a random 40 bp sequence in the middle flanked by 20 bp primers at 5' and 3' ends (5'-CCT TCG TTG TCT GCC TTC GTN NNN NNN NNN NNN NNN NNN NNN NNN NNN NNN NNN NNN ACC CTT CAG AAT TCG CAC CA-3'). The initial DNA pool was dissolved in DI water to make 1 μM stock solution. The initial pool was first amplified with FAM-labeled primer (5'-FAM-CCT TCG TTG TCT GCC TTC GT-3') and TCO-TTP to incorporate TCO-TTP into the sequences through PCR. Asymmetric PCR condition and amplification cycle program were as following: DNA library template (40 nM), FAM-labeled primer (4 μM), reverse primer (5'-TGG TGC GAA TTC TGA AGG GT-3', 200 nM), dATP (396 μM), dCTP (396 μM), dGTP (396 μM), TCO-TTP (1.188 mM), and KOD XL DNA polymerase (0.025 U/μL) in 500 μL. Thirty thermal cycles were conducted with melting at 90 °C for 20 s, annealing at 48 °C for 20 s, and extending at 72 °C for 30 s with initial denaturing at 90 °C for 2 min and final extension at 72 °C for 5 min. TCO-modified sequences prepared from PCR was purified using Millipore Amicon 10 kDa spin column. Pre-purified sequences solution (480 μL) was then added to the 24 μL of 10 mM Tz-BBA DMSO solution, which was further reacted at r.t. for 1 h. The boronic modified products were then analyzed by 15% PAGE. This is the "0 round pool".

1.3.7.2 Preparation of target cell and control cell

The HPAF II cells (target cell) and MIA Paca cells (control cell) were cultured in DMEM/F-12 media and DMEM media, respectively, supplemented with 10% fetal bovine serum and 1% penicillin-streptomycin at 37 °C with 5% CO_2. The cells were cultured in the 5.0 cm diameter cell culture dish until it achieved 90% coverage on surface before incubation.

1.3.7.3 General selection procedure

The target cell was incubated with the "0 round pool" (450 μL) in 10 mL SELEX binding buffer for 30 minutes at 37 °C. The cells were then washed 3 times with SELEX washing buffer and collected using a cell scraper. The collected cells were re-suspended in 250 μL DIH_2O and heated for 10 minutes at 90 °C to release the sequences. The suspension was centrifuged at 1500 rpm for 4 minutes. The supernatant collected was the template for the "1st round pool". Next round sequence was synthesized using template selected from last round (100 μL), FAM-labeled primer and TCO-TTP through similar procedure stated above.

1.3.7.4 Negative selection procedure

After 3 rounds, a counter selection was introduced by incubating the sequence pool with the control cells (MIA Paca) for 30 minutes at 37 °C. Discard the bound sequences that are attached to control cells. The sequences that remained unbound to the control cells were further incubated with the target cells following the similar procedure as described above. Fluorescence imaging was used to monitor the binding of each round pool selected against the target cells.

1.3.7.5 Monitoring the progress of selection

The cells were cultured on coverslips in a 6-well plate until it achieved 90% coverage on surface before the imaging experiment. 100 μL of the selected pool was dissolved in 2 mL of

culture medium and incubated with the cells for 30 minutes at 37 °C. The cells were then washed 2 times with PBS and fixed with 4% paraformaldehyde for 30 minutes at room temperature. The coverslips with the cell sample were mounted onto glass slides by using hard set mounting medium containing DAPI. The slides were imaged under FITC, or DAPI, or phase contrast channel by fluorescent microscope.

1.3.7.6 Cloning and sequencing of enriched pools

After binding was observed by fluorescent imaging, the sequences in the selected pool was cloned and sequenced for identification. The selected pool was prepared with the same procedure in pool amplification, except using non-labeled primer instead of FAM-labeled primer. 2 μL of the PCR product was added into the ligation-reaction mixture and incubated at 4 °C for 30 minutes. The competent cells were thawed on ice and incubated for 5 minutes on ice after adding 2 μL of the ligation mixture. The competent cell tubes were then heat-shocked in 42 °C water bath for 1 minute, followed by incubation on ice for 2 minutes. 500 μL of the SOC medium was added into the competent cell tube and 50 μL was spread onto one LB plate. The colonies were allowed to grow for 16 hours at 37 °C in an inverted plate position. The white colonies on the LB plate was picked and suspended into 5 mL of liquid LB medium and shaken vigorously for 12 hours. The *E. Coli* bacteria pallet was then collected by centrifuging at 10k rpm for 3 minutes. The plasmid of the bacteria was extracted using QIAprep® Miniprep kit and sent for sequencing in DNA core facility at Georgia State University. Meanwhile, the PCR product of the selected pool was also sent for next-generation sequencing (Core Facilities at the University of Florida).

1.3.7.7 Synthesis of potential single-stranded aptamer candidates

The sequences of the highest abundance from the sequencing data were selected as the top aptamer candidates. The sequences were synthesized using phosphate-modified complementary template (5-phosphate C3UB2, 5'-phosphate-TGG TGC GAA TTC TGA AGG GTG CCG CCA CCT CCC CCG CCT TAT GCT CGG TCC ACC CGG CCC ACG AAG GCA GAC AAC GAA GG-3'), FAM-labeled sense primer 1 and TCO-TTP through similar PCR procedures. The product mixture was purified using Millipore Amicon 10 kDa spin column. The double strand was then incubated with lambda exonuclease for 4 hours at 37 °C to remove the phosphorylated strand. The remained single-stranded TCO-modified DNA (500 μL) was further reacted with 1mM BBA4 (25 μL) at r.t. for 1 hour. The boronic acid-modified product mixture then purified with spin column.

1.3.7.8 Binding studies of aptamer candidates to cells

The binding affinity was measured using fluorescence from FAM-labeled sequences by flow cytometry. 2 μM stock solution of selected sequences was prepared. Series diluted stock solution to 31.25 nM. HPAF II cells were dissociated with trypsin. Cells were washed with SELEX washing buffer and incubated with various concentration of sequences in 50 μL of binding buffer. After 30 minutes incubation, cells were washed and re-suspended with washing buffer, and further analyzed by flow cytometer.

1.4 Conclusion

A fast and efficient approach of post-PCR DNA modification is described. The modified TTP (TCO-TTP) has a click handle for reaction with tetrazine, which can be used for tethering other functional groups. Compared to previously reported methods, the approach described uses a very fast click reaction and has the advantage of significantly improved reaction kinetics. The

incorporation of a boronic acid functional group or a fluorophore has been described after the successful incorporation of TCO-TTP. The boronic acid-labeled DNA can be used for aptamer selection against carbohydrates and glycoproteins, while the fluorophore-labeled DNA can be used for cell labeling studies among other applications. Following labeling work, boronic acid-modified aptamers that can selectively target HPAF II cell line was successfully selected and examined. Taking advantage of high binding affinity between boronic acid and glycoproteins, the selection efficiency is highly improved and selection rounds are decreased. This approach provides an efficient way to generated aptamer for glycoprotein on cell surface. In addition, the *trans*-alkene functional group in the modified DNA can also be used to tether other functional group for various purposes.

1.5 Statements

The much of the results described in this chapter has been published in *Org. Biomol. Chem* (Wang, K.; Wang, D.; Ji, K.; Chen, W.; Zheng, Y.; Dai, C.; Wang, B., Post-synthesis DNA modifications using a trans-cyclooctene click handle, *Org. Biomol. Chem*. **2015**, *13* (3), 909-915, DOI: 10.1039/C4OB02031F) and *Curr. Org. Chem.* (Wang, K.; Wang, D.; Wang, B., Modified nucleosides that can be incorporated into DNA enzymatically or in live cells, *Curr. Org. Chem.* **2015**, *19* (11), 1011-1020, DOI: 10.2174/1385272819111506101011 41). In this chapter, my contributions include the synthesis of *trans*-cyclooctene-modified thymidine triphosphate (TCO-TTP), enzymatically incorporation of modified thymidine into DNA molecules through PCR, fluorophore and boronic acid functional groups labeling of DNA, aptamer-cell binding studies and partially on aptamer selection and cloning process.

2 DEVELOPMENT OF FLUORESCENT CHEMOPROBES FOR MOLECULES OF BIOLOGICAL IMPORTANCE

2.1 Development of fluorescent chemoprobes for hydrogen sulfide (H_2S)

2.1.1 Introduction

The past decade has seen a boost of research interest in hydrogen sulfide (H_2S), which has been recently recognized as one of the three important gasotransmitter, including nitric oxide (NO)[177] and carbon monoxide (CO).[178] H_2S is synthesized endogenously in the cell by enzymes such as cystathionine β-synthase (CBS)[179] and cystathionine γ-lyase (CSE).[180] And it is involved in the regulations of a series of important genes. Endogenous concentrations of H_2S is related to a number of diseases such as Down syndrome[181] and lung diseases.[182] H_2S was also found to show protective effects in the cardiovascular (CV)[183] and central nervous systems (CNS)[184] and to play a regulatory role in inflammation.[185-186] Regulation of H_2S levels is also a potential drug development strategy.[187-188] The importance of accurate detection of H_2S has been greatly emphasized. However, this is not a trivial issue mainly due to the low stability of this gaseous molecule. H_2S is volatile and prone to oxidation. Considering the features of hydrogen sulfide, such as reducing ability and duo-nucleophilicity (can undergo nucleophilic addition or substitution twice), current detection for hydrogen sulfide uses either sulfide specific chemosensor (methylene blue method),[189] electrochemical methods (sulfide selective electrodes or polarographic methods)[190-191] and gas chromatography (GC).[192] However, none of these methods is compatible with detection and imaging in cells. These methods also show problems such as narrow linearity ranges (methylene blue method) and complicated sample preparations (chromatography). Fluorescent probes are emerging as important tools for the selective and sensitive detection of H_2S.[193-195] Chang and our group first reported that the reduction of an azido

group attached to a fluorophore could be utilized for the design of H_2S-selective fluorescent probes.[196-197] Recently, a number of fluorescent probes have been developed, including probes based on nucleophilic cyclization,[198-202] redox reactions,[197, 203-206] and metal-sulfide formation.[207-209] A few reviews have been published discussing H_2S probes.[210-213] Some recently published probes are discussed below (Table **2.1**).

Table 2.1 Properties of hydrogen sulfide probes

Probe	Wavelength (λ_{ex}/ λ_{em}, nm) or Abs.	Reaction time (min)	Temperature (^{0}C)	pH	Medium	LOD	Application in biological system
Lyso-NHS	450/ 555	20	37	7.4	ACN/ PBS 1: 9	0.48 uM	serum and live cells
CouMC	475/ 510& 652	0.5	r.t.	7.4	2% DMSO-PBS	1 uM	live cells
probe **40**	450/ 485& 690	0.17	r.t.	7.4	ACN/ PBS 1: 3.3	0.14 uM	live cells
HS-Cy	510& 700/ 625& 780	35	37	7.4	HEPES	5-10 nM	live cells
probe **46**	350/ 440, 510, & 570	30	37	7.4	DMSO: phosphate buffer 2: 8	10 uM	live cells
SFP-1	300/ 395	60	37	7.4	PBS	5-10 uM	live cells
SFP-2	465/ 510	240	37	7.0	PBS	6 uM	live cells
SFP-3	500/ 525	30	25	7.4	PBS	1.5 uM	plasma
SF4	496/517	60	25	7.4	HEPES	125 nM	live cells
SF5-AM	498/521	60	25	7.4	HEPES	250 nM	live cells
SF7-AM	498/526	60	25	7.4	HEPES	500 nM	live cells
SHS-M1	365/500	90	r.t.	7.4	HEPES	200 nM	live cells, tissue
SHS-M2	383/545	90	r.t.	7.4	HEPES	400 nM	live cells, tissue
MPhSe-BOD	460/ 510	30	r.t.	7.4	PBS/ACN	<10 μM	live cells
probe **68**	440/544	180	r.t.	7.4	Phosphate buffer	500 nM	live cells

2.1.1.1 Probes based on nucleophilic reactions

In aqueous solution, H_2S dissociates to form nucleophilic anion HS^-, which can react with a variety of electrophiles. Taking advantage of this feature, a number of probes have been developed. One of the examples is reported by Cui and co-workers with specific subcellular localization property[214] (Figure **2.1**). This lysosome-targetable probe Lyso-NHS consists of a 1,8-naphthalimide fluorophore, a 4-(2-aminoethyl)morpholine moiety (the lysosome targeting group), and a dinitrophenyl ether as the H_2S reactive site.

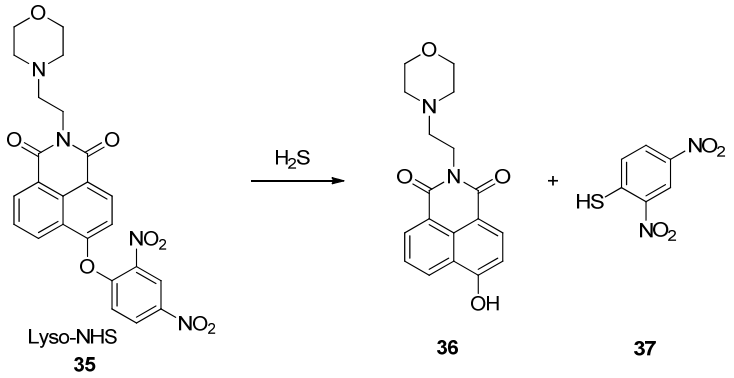

Figure 2.1 Structure of probe Lyso-NHS and its mechanism of action

Among all fluorescent probes, ratiometric probes afford easy quantification due to the advantage of self-calibration. In 2013, Z. Guo and co-workers reported a ratiometric H_2S probe CouMC (Figure **2.2**), for detection in mitochondria.[215] The selectivity for H_2S over Cys, Hcy and GSH is achieved due to differences in pK_a values. Biothiols have a higher pK_a (> 8.5)[216] than H_2S (7.0), which makes H_2S a better nucleophile in neutral medium. Another ratiometric fluorescent probe flavylium derivative (compound **40**) was reported by W. Guo and co-workers recently (Figure **2.2**).[217] With a similar strategy, this probe featured a fast detection response (< 10 s) and NIR property (λ_{em}: 485 and 690 nm) in ACN/PBS (1: 3.3). MTT cytotoxicity studies using HeLa cells showed 80% cell viability after incubation with 10 μM probe for 24 h.

Further increased sensitivity was achieved by a NIR probe HS-Cy reported by the Tang group (Figure **2.2**)[218] This probe takes advantage of the duo-nucleophilicity of hydrosulfide anion. It undergoes a nucleophilic addition by sulfide, followed by a thiolactone formation releasing a cyanine fluorophore.

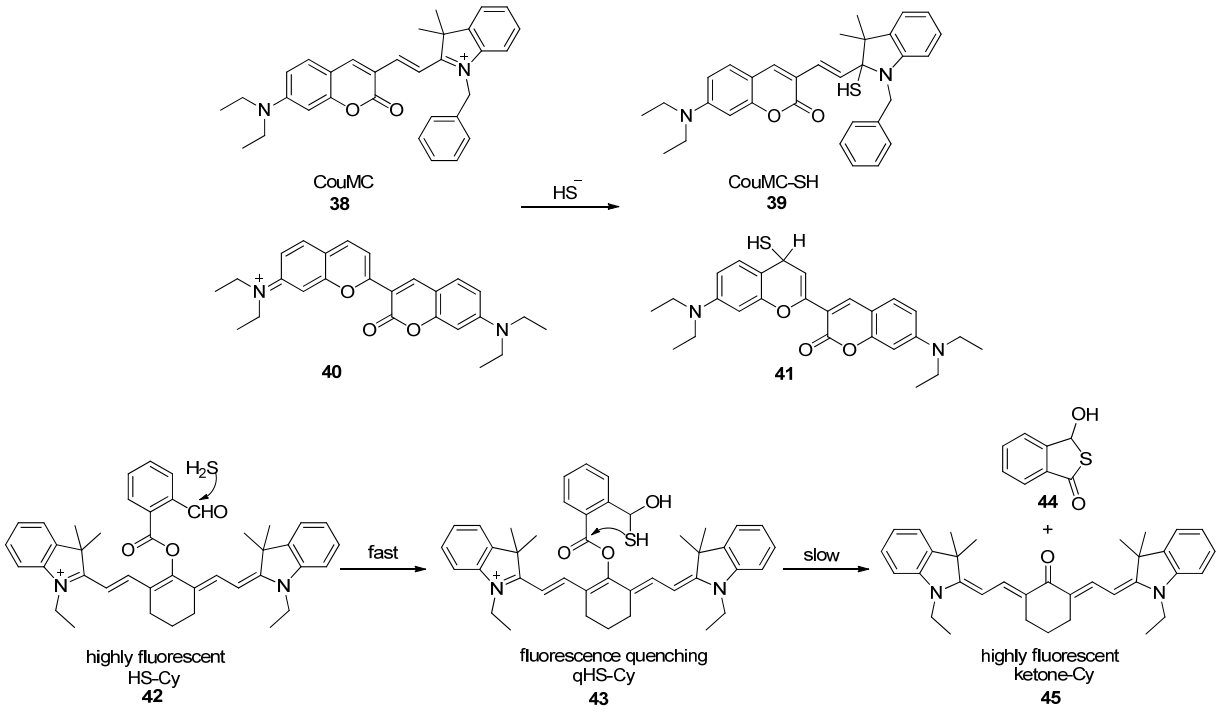

Figure 2.2 Structure of ratiometric H_2S probes and their mechanisms of actions

A white light-emitting fluorescent probe (**46**) reported by Lin and co-workers shows advantages of low-background multi-channel detection (Figure **2.3**).[219] This probe was constructed by conjugating a blue fluorescent dye and with an ESIPT (excited-state intramolecular proton transfer) dye, which is modified by a 2,4-dinitrophenyl group as the reactive site. This probe can be utilized to detect endogenous H_2S in living cells with three-channel monitoring. Although this probe is not as sensitive as some aforementioned probes, it features a new multi-channel sensor for hydrogen sulfide.

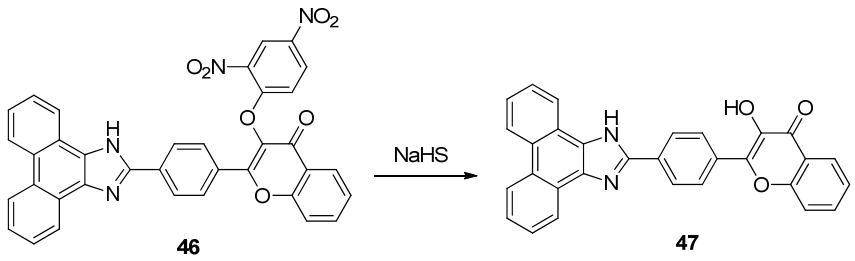

Figure 2.3 Structure of probe 46 and its mechanism of action

A series of hydrogen sulfide probes (SFP1, 2, 3, Figure **2.4**) were reported by the He group.[220-221] Based on a Michael addition-cyclization mechanism, these probes (5-10 μM) selectively react with sulfide exhibiting more than 10-fold fluorescence increases. Furthermore, SFP-1 and SFP-2 can be applied in dynamic monitoring of enzymatic hydrogen sulfide biosynthesis.

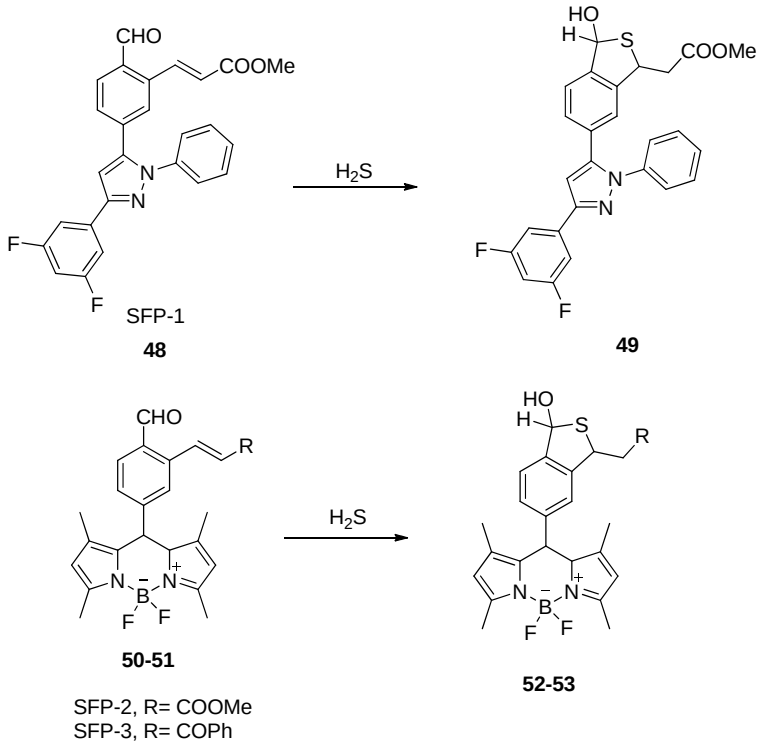

Figure 2.4 Structures of SFP probes and its mechanism of action

2.1.1.2 Probes based on redox reactions

In 2013, Chang and co-workers reported several bis-azido rhodamine analogues (SF4-SF7, Figure **2.5**) for cell imaging of hydrogen sulfide.[222] Compared to the mono-azido probes reported in 2011, these bis-azido analogues exhibit improved sensitivity with detection limits ranging from 125-500 nM. Acetoxymethyl esters (SF5-AM, SF7-AM, etc.) were synthesized to provide cell-trappability for increased imaging sensitivity by maintaining a high dye concentration in the cells. Production of H_2S was observed in HUVECs (human umbilical vein endothelial cells) using SF7-AM and it was found that H_2S generation is dependent on NADPH oxidase (Nox) derived H_2O_2, providing evidence in support of H_2S/H_2O_2 crosstalk.

Ratiometric two-photon excitation fluorescent probes SHS-M1 and SHS-M2 (Figure **2.5**) were reported recently by Kim and co-workers.[223] The reduction of the 4-azidobenzyl group to the corresponding aniline triggers the cleavage of the carbamate, releasing the *N*-methylaniline analogues and resulting in a red shift from 420 to 500 nm for SHS-M1 and 464 to 545 nm for SHS-M2. This shift in emission provides feasibility for ratiometric detection of hydrogen sulfide for cellular imaging. The positively charged TPP serves as a mitochondria-targeting moiety. SHS-M2 was used to monitor H_2S in cultured astrocytes and showed that H_2S production decreased when CBS was knocked down by siRNA. It was also found that H_2S level decreased in DJ-1-knockout astrocytes and brain slices as Parkinson's disease models.

A selenium-bearing fluorescent probe (MPhSe-BOD, Figure **2.5**) was reported by Han and co-workers.[224] It exhibits a reversible redox cycle between oxidation by hypochlorous acid (HClO) to MPhSeO-BOD (strongly fluorescent) and reduction by H_2S back to the original probe (weakly fluorescent). In a confocal imaging experiment, this probe showed good cell permeability in murine macrophage cell RAW264.7. It also showed the ability to continuously

monitor the HClO/H_2S redox cycles when the production of hypochlorous acid (HClO) in cells was stimulated by phorbol myristate acetate (PMA) or exogenous sulfide was added into the cell culture. Similar strategy was also used in a NIR fluorescent probe reported by the same group.[225]

Another redox-sensitive naphthalimide-based fluorescent probe **68**(Figure **2.5**) was reported recently by Wang and co-workers.[226] The reduction of hydroxylamine moiety by H_2S led to the production of its amino analogue as well as a dramatic increase in fluorescence intensity. A detection limit of sub-micromolar concentration was achieved. Imaging experiments in astrocytes using this probe revealed good cell membrane permeability. However, the slow kinetics (reaction requires 180 min to finish) hampers imaging applications. A fluorescent protein (FP)-based hydrogen sulfide probe cpGFP-Tyr66pAzF was recently reported by the Ai group.[227]

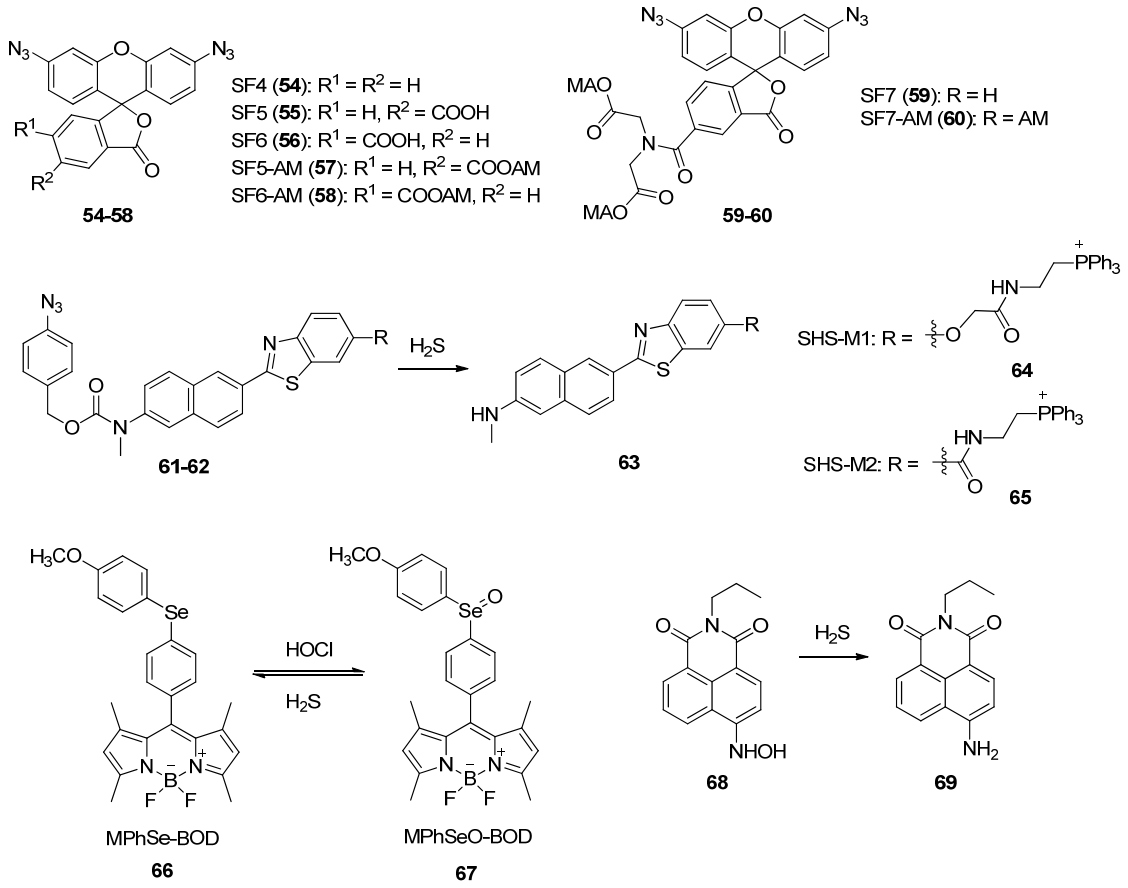

Figure 2.5 Structure of redox-based H_2S probes and their mechanism of action

2.1.2 Results and discussion

The redox-based fluorescent probe (DNS-Az), which was reported by our group, shows significant fluorescence "turn-on" effect in the presence of H_2S in aqueous solutions. Most importantly, the sensing reaction (completes in minutes) is the fastest among all redox-based fluorescent probes for H_2S. This might be attributed to the unique structure features of DNS-Az. Compared to other redox-based fluorescent probes bearing an azido group, DNS-Az includes a sulfonyl azide. We believe that the sulfonyl azide provides the probe with fast reaction rates and increased photo-stability. However, the quantum yield of the fluorescent species DNS-NH_2 is

very low (< 0.05) in pure aqueous solutions. In order to reach higher sensitivity, a surfactant Tween-20 was added in previous experiments.[196] Herein we describe the synthesis and evaluation of a new fluorescent probe, which shares structure similarity with the previously reported probe but emits a different wavelength with higher fluorescence quantum yield and detection sensitivity in phosphate buffer without addition of any surfactant.

The structure of DNS-Az is based on a 1,5-dansyl fluorophore, which is known for its large Stokes shift (λ_{ex} = 330 nm, λ_{em} = 517 nm in phosphate buffer/Tween-20). 2,6-Dansyl fluorophore has a smaller Stokes shift, however exhibits much higher fluorescence quantum yield in pure aqueous media.[228] Therefore, it is conceivable that 2,6-dansyl azide (2,6-DNS-Az, **73**) might serve as a fluorescent probe for H_2S with high detection sensitivity in pure aqueous media. Starting from commercially available 6-amino-2-naphthalenesulfonic acid (**70**), 2,6-dansyl azide was synthesized in 3 simple steps, including reductive alkylation to form dimethylamino sulfonate **71**, formation of sulfonyl chloride **72**, and substitution with sodium azide to afford the sulfonyl azide **73** in 35% overall isolated yield.

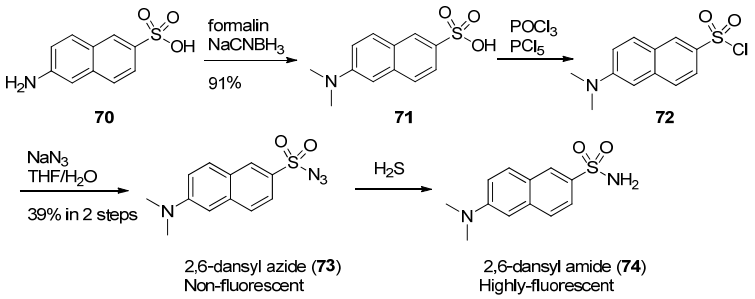

Scheme 2.1 Synthesis of 2,6-dansyl azide

2,6-Dansyl azide was evaluated as a fluorescent probe for H_2S. In all experiments, Na_2S was used as the sulfide source in aqueous solutions as reported previously[196] and elsewhere. As

expected, 2,6-DNS-Az could be easily reduced to its corresponding sulfonyl amide after sulfide addition. 2,6-Dansyl amide **74** was isolated and identified using ^{1}H NMR, ^{13}C NMR and mass spectrometry (see appendix). The quantum yield of 2,6-dansyl amide **74** was about 40-fold higher than that of 1,5-dansyl amide in deionized water (see experimental section). In a sulfide detection experiment, 20 μM of probe **73** showed an over 100-fold fluorescence increase in 60 min after addition of only 10 μM of sulfide in phosphate buffer without surfactant. This is a much more significant change compared to the 8-fold fluorescence increase observed for the first-generation probe 1,5-DNS-Az in phosphate buffer (Figure **2.7**b).

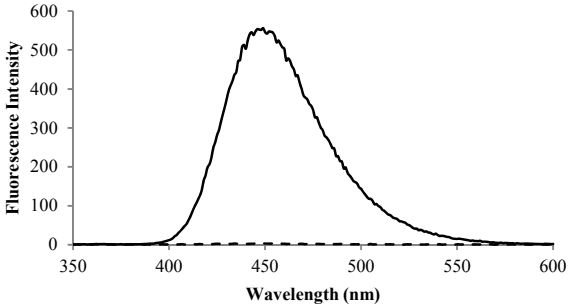

Figure 2.6 Fluorescence increase of 2,6-DNS-Az (1, 20 μM) with the addition of sulfide (10 μM) in 0.1 mM sodium phosphate buffer (pH 7.4) at room temperature.
Dashed line represents fluorescence spectrum of **1** alone. Solid line represents fluorescence spectrum of **1** with sulfide.

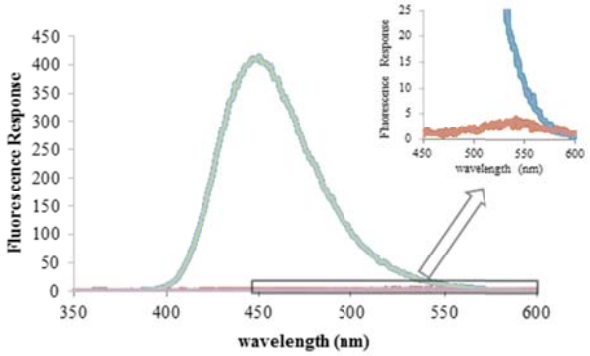

Figure 2.7 Comparison of fluorescence response of 2,6-DNS-Az and 1,5-DNS-Az in phosphate buffer.

Blue line represents fluorescence response of 2,6-DNS-Az (20 μM) to sulfide (10 μM); red line represents fluorescence response of 1,5-DNS-Az (20 μM) to sulfide (10 μM) in 0.1 M phosphate buffer (pH =7.4), λ_{ex}=325nm

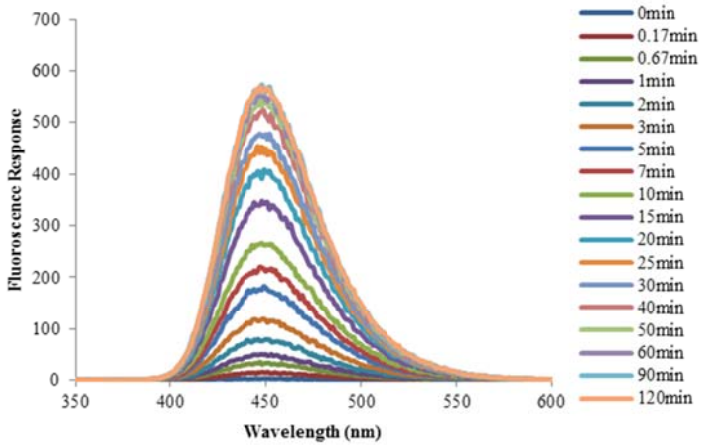

Figure 2.8 Time-dependent fluorescence response of 2,6-DNS-Az (20 μM) to hydrogen sulfide (10 μM) in 0.1 M phosphate buffer (pH =7.4).

A stock solution of 2,6-DNS-Az (10 mM in acetonitrile, 2 μL, final concentration 100 μM) was added into 1.0 mL of a solution containing 10 μM of Na_2S. Then it was mixed thoroughly and placed in a fluorometer for measurements with λ_{Ex}= 325 nm at a series of time points for 120 min (sample was not exposed to UV between these time points)

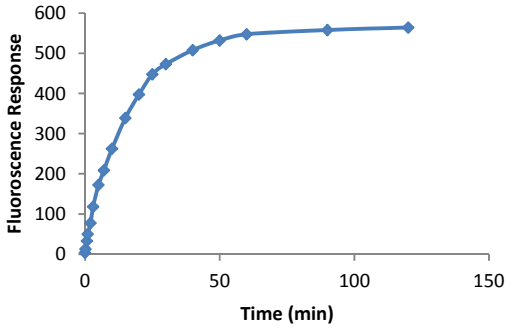

Figure 2.9 Reaction time profile of 2,6-DNS-Az (20 μM) in the presence of hydrogen sulfide (10 μM) in 0.1 M phosphate buffer (pH =7.4).

Fluorescence intensity at 445 nm was plotted against time.

After the fluorescence response of 2,6-DNS-Az to sulfide was demonstrated, a variety of 17 common anions, including sulfur-containing reducing anions, were used at concentrations

above their physiological levels, to test the selectivity of 2,6-DNS-Az. It was found that 2,6-dansyl azide showed almost exclusive response to sulfide over other anions. For strong reducing anions such as HSO_3^-, $S_2O_4^{2-}$, and $S_2O_5^{2-}$, the selectivity was found to be 30 to 44-fold. Other reducing biological species, such as cysteine (Cys) and glutathione (GSH) at 100 μM, were also tested (Figure **2.10**). The probe did not show fluorescence response to Cys and GSH. A slight increase in fluorescence response to sulfide was found in the presence of Cys and GSH. This could be due to antioxidative effect of Cys and GSH, which prevented undesired oxidation of sulfide in the reaction media. Selectivity over nucleophilic species was also tested by using high concentrations (1 mM) of glycine and lysine. These results have indicated that 2,6-DNS-Az shows sufficient selectivity for the detection of H_2S in a complex biological sample.

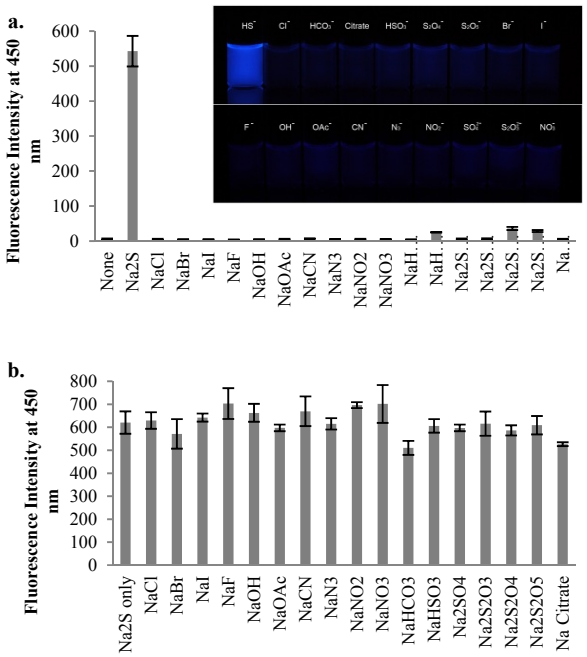

Figure 2.10 Fluorescence changes of 2,6-DNS-Az (20 μM) in the presence of (sulfide and) various anions.

a. Fluorescence changes of 2,6-DNS-Az (**1**) in the presence of various anions; b. fluorescence changes of 2,6-DNS-Az (**1,** 20 μM) in the presence of sulfide and various anions (HS^- 10 μM; HSO_3^-, $S_2O_4^{2-}$, and $S_2O_5^{2-}$ 20 μM; all other anions 1 mM in 20 mM sodium phosphate buffer (pH 7.4), λ_{ex}= 325 nm). Anions tested: Cl^-, Br^-, I^-, F^-, OH^-, OAc^-, CN^-, N_3^-, NO_2^-, NO_3^-, HCO_3^-, HSO_3^-

, SO_4^{2-}, $S_2O_3^{2-}$, $S_2O_4^{2-}$, $S_2O_5^{2-}$, and citrate. Data represents average of three independent experiments.

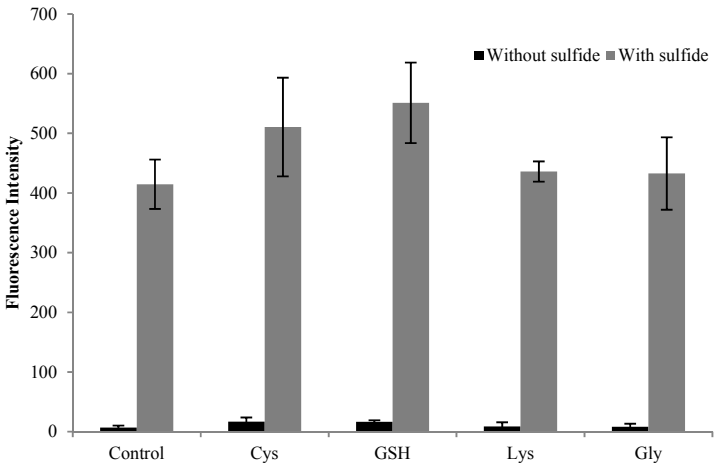

Figure 2.11 Fluorescence response of 2,6-DNS-Az to sulfide in the presence and absence of reducing agents.

Fluorescence response of 2,6-DNS-Az to sulfide in the presence and absence of reducing agents (cysteine 100 μM, GSH 100 μM) and nucleophilic amino acids (lysine 1 mM, glycine 1 mM) in 0.1 M phosphate buffer (pH =7.4).

For all quantitative analytical methods, a linear calibration curve is always preferred because it allows easy calculation. After confirming the selectivity of 2,6-DNS-Az, this probes was evaluated for quantitative measurement of H_2S by testing concentration-dependent response of 2,6-DNS-Az to sulfide. As shown in Figure 3, a linear correlation (R^2 = 0.9993) was found for sulfide in phosphate buffer. As determined by 3:1 signal/noise ratio, the detection limit for sulfide in phosphate buffer is 1 μM (Figure **2.12**). This indicates that 2,6-DNS-Az could be used for quantitative measurement of H_2S in pure aqueous media.

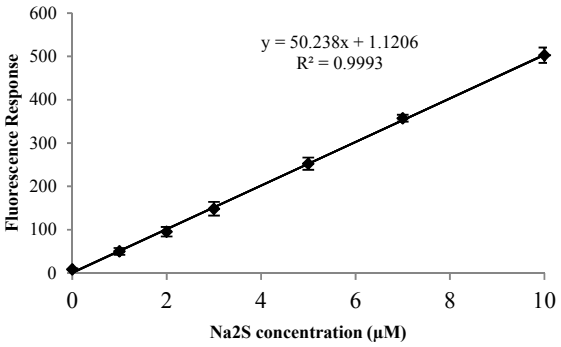

Figure 2.12 Hydrogen sulfide concentration dependent fluorescence intensity changes. 2,6-dansyl azide 20 µM, Na_2S 0-10 µM in 100 mM phosphate buffer (pH 7.4, λ_{ex}= 325 nm), Data represents average of three independent experiments.

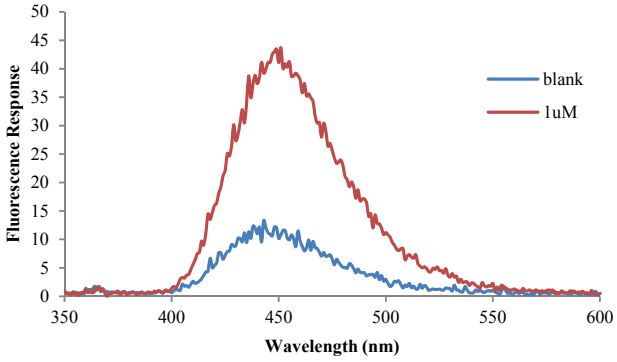

Figure 2.13 Measurement of LOD.
Red line represents fluorescence response of 2,6-DNS-Az (20 µM) to sulfide (1.0 µM). Blue line represents the background fluorescence of 2,6-DNS-Az (20 µM) in 0.1 M phosphate buffer (pH =7.4).

Due to the biological significance of H_2S, the detection of H_2S in biological systems such as blood serum is of great importance in both research and clinical applications. Therefore, we are also interested in using 2,6-DNS-Az for sulfide detection in serum. The probe was evaluated in fetal bovine serum (FBS). First, a reaction time profile was tested for 2,6-DNS-Az and sulfide. As shown in Figure **2.14**, although FBS shows some background fluorescence, a very significant increase was still observed after addition of sulfide. Over 10-fold fluorescence increase was

observed for only 10 μM of sulfide. This indicates more than 2-fold higher sensitivity compared to 1,5-DNS-Az reported earlier by our group. The reaction of 2,6-DNS-Az with sulfide is very fast and completes in about 2 minutes in FBS. This is very promising considering that H_2S is very unstable and easily consumed in biological systems. We also tested concentration-dependent fluorescence changes of 2,6-DNS-Az in FBS. The linear calibration curve (R^2 = 0.995) obtained in FBS has also indicated that 2,6-DNS-Az could serve as a useful tool for H_2S detection. The detection limit of H_2S in FBS is about 6 μM.

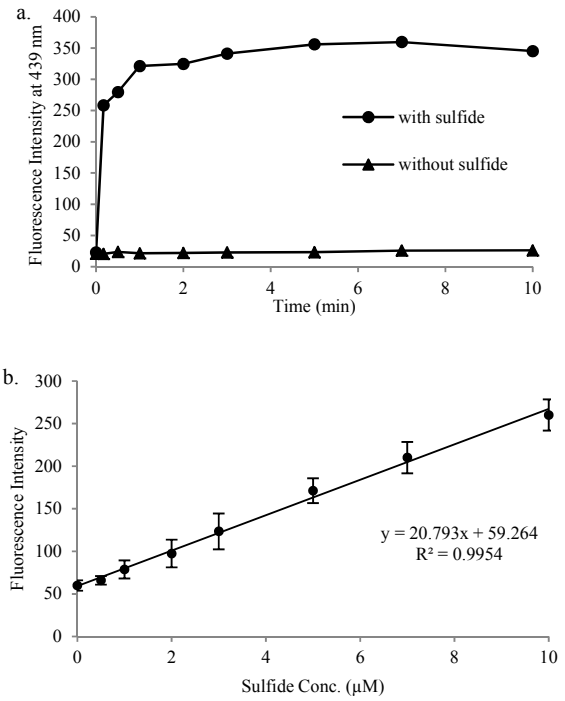

Figure 2.14 Reaction time and concentration dependent profile of 2,6-DNS-Az (20 μM) and H2S (10 μM) in FBS

a. Reaction time profile of 2,6-DNS-Az (20 μM) and H_2S (10 μM) in FBS; b. H_2S concentration dependent fluorescence intensity changes, determined using a fluorometer: 2,6-DNS-Az 20 μM, Na_2S 0-10 μM in FBS (λ_{ex}= 325 nm). Concentration dependence data represents average of three independent experiments.

2.1.3 Experimental Section

2.1.3.1 General Information

Solvents and reagents were purchased from VWR International, Oakwood Product Inc., or Sigma-Aldrich Co., and used without purification unless specified otherwise. When necessary, solid reagents were dried under high vacuum. Reactions with compounds sensitive to air or moisture were performed under argon. Solvent mixtures are indicated as volume/volume ratios. Thin layer chromatography (TLC) was run on Sorbtech W/UV254 plates (0.25 mm thick), and visualized under UV-light or by a Ce-Mo staining solution (phosphomolybdate, 25 g; $Ce(SO_4)_2.4H_2O$, 10 g; conc. H_2SO_4, 60 mL; H_2O, 940 mL) with heating. Flash chromatography was performed using Fluka silica gel 60 (mesh size: 0.040-0.063 mm) using a weight ratio of ca. 30:1 for silica gel over crude compound. ^{1}H and ^{13}C-NMR spectra were recorded on a Bruker 400 spectrometer (400 and 100 MHz, respectively) in deuterated chloroform ($CDCl_3$), methanol-d_4 (CD_3OD), or DMSO-d_6 with either tetramethylsilane (TMS) (0.00 ppm) or the NMR solvent as the internal reference. UV-Vis absorption spectra were recorded on a Shimadzu PharmaSpec UV-1700 UV-Visible spectrophotometer. Fluorescence spectra were recorded on a Shimadzu RF-5310PC spectrofluorophotometer. 96-Well plates were read and recorded on a PerkinElmer 1420 multilabel counter.

2.1.3.2 Synthesis and Characterization

6-(Dimethylamino)naphthalene-2-sulfonic acid **71**: To a solution of compound **70** (220 mg, 0.99 mmol) in acetonitrile (3 mL), formaldehyde (1 mL) was added dropwise. After the reaction mixture was stirred for 10 min, $NaCNBH_3$ (450 mg, 7.2 mmol) was added in 2 portions. Then, AcOH (1 mL) was added in 4 portions during 4 h. The reaction was stirred at r.t. for an additional 2 h. The product precipitated out from the reaction solution. The white precipitate was

filtered out, washed with H_2O and MeOH, and dried (225 mg, yield: 91%). ^{1}H NMR (CD_3OD): δ 8.17 (1H, s), 7.79 (1H,d, *J* = 8.8 Hz), 7.75 (1H, d, *J* = 8.8 Hz), 7.69 (1H, d, *J* = 8.4 Hz), 7.28 (1H, d, *J* = 8.8 Hz), 7.00 (1H, s), 3.08 (6H, s); MS (ES+) 252.1 $(M+1)^+$.

6-(Dimethylamino)naphthalene-2-sulfonyl azide **73**: To an Ar-protected solution of **71** (225 mg, 0.9 mmol) in $POCl_3$ (1.1 mL) in an ice bath, PCl_5 (832 mg, 4 mmol) was added in one portion. The reaction mixture was stirred at 0 ^oC for 2 h. Then, the reaction was stirred at r.t. for an additional 2 h. The reaction mixture was poured into 100 g ice and the product was extracted with EtOAc (100 mL × 3). The organic phase was dried over Na_2SO_4, and concentrated under vacuum to yield crude product **72**. The crude product **72** was dissolved in THF (5 mL) and added into a stirred solution of NaN_3 (580 mg, 9 mmol) in a 1:1 mixture of THF/H_2O (10 mL). The reaction mixture was stirred at room temperature for 2 h. Organic solvent was evaporated to obtain light yellow solid. The crude product was purified by flash chromatography purification (Hex: EtOAc, 20: 1) to give compound **73** as light yellow solid (134 mg, 54%). ^{1}H NMR ($CDCl_3$): 8.33 (1H, s), 7.82 (1H, d, *J* = 9.2 Hz), 7.72 (2H, s), 7.24 (1H, t, *J* = 9.2 Hz), 6.88 (1H, s), 3.14 (6H, s); ^{13}C NMR ($CDCl_3$): 151.0, 138.0, 130.7, 129.6, 127.5, 124.2, 122.5, 117.2, 104.9, 40.3; IR 2133, 1614 1507, 1361, 1069, 840, 812, 739; MS (ES+) 277.1 $(M+1)^+$.

6-(Dimethylamino)naphthalene-2-sulfonamide **74**: To a stirred solution of 2,6-DNS-Az (19.8 mg, 0.072 mmol) in 1.44 mL acetonitrile was added dropwise a solution of Na_2S (51.6 mg, 0.22 mmol) in H_2O. The solution was stirred at r.t. for 30 min and was dried under vacuum. The crude product was purified by column chromatography to give compound **74** as white solids (13 mg, 72%). ^{1}H NMR (DMSO-d_6, 400 MHz): 8.18 (1H, s), 7.90 (1H, d, *J* = 9.2 Hz), 7.78 (1H, d, *J* = 8.8 Hz), 7.68 (1H, d, *J* = 8.8 Hz), 7.31 (1H, d, *J* = 9.2 Hz),7.24 (2H, s), 6.99 (1H, s), 2.50 (6H, s); MS (ES+) 251.08 $(M+1)^+$.

2.1.3.3 Relative quantum yield determination of 2,6-DNS-Az and 2,6-DNS-NH_2

1,5-DNS-NH_2 was used as the reference for relative quantum yield determination. Absorption and emission (λ_{Ex}= 325 nm) spectra were recorded for a series of concentrations (16 µM, 12 µM, 8 µM, 4 µM and 0 µM in deionized water) of 1,5-DNS-NH_2, 2,6-DNS-NH_2, and 2,6-DNS-Az. Integrated fluorescence intensity was plotted against the absorption values at each concentration (Figures **2.15** and **2.16**).[229] Relative quantum yield values can be calculated using slopes of each compound.

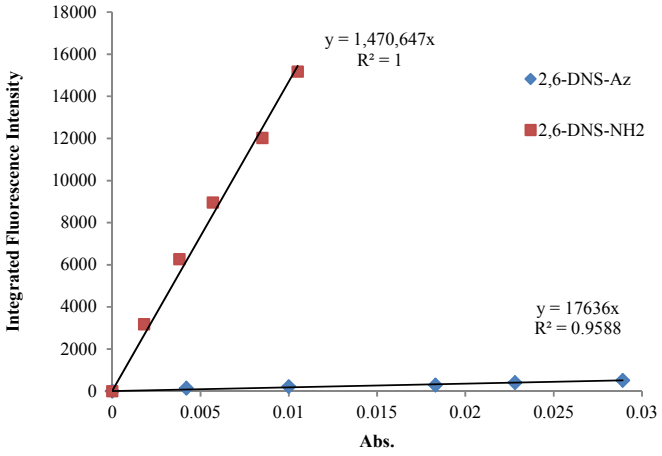

Figure 2.15 Quantum yield determination of 2,6-DNS-Az (0-20 µM) in H2O

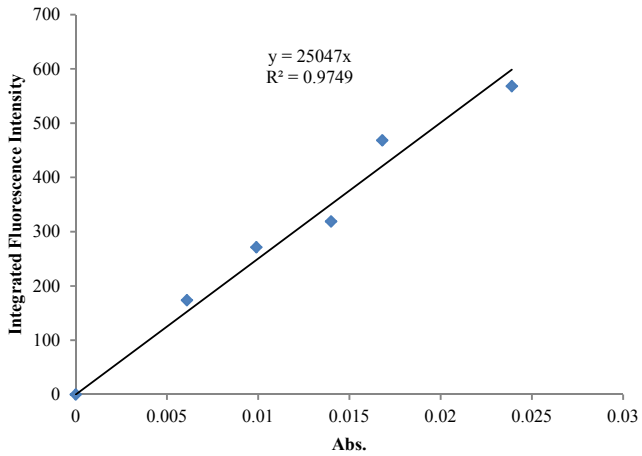

Figure 2.16 Quantum yield determination of 1,5-DNS-NH2 (0-20 µM) in H_2O

2.1.4 Conclusions

The biological significance as well as difficulty in accurate detection of H_2S urged chemists to find new detection methods. We have reported previously a fluorescent probe (1,5-DNS-Az) for H_2S detection, but requires the addition of Tween-20 to achieve sufficient sensitivity when used in buffer solutions. The present work reports the development and evaluation of a new fluorescent probe for H_2S, 2,6-DNS-Az. This probe shows much higher fluorescence change in pure aqueous media (>100-fold for 10 μM of sulfide) compared to the probe described earlier (8-fold) without addition of any surfactant. High detection sensitivity, almost exclusive selectivity and excellent linear correlation for sulfide in aqueous solution and blood serum make this probe a useful tool for quantitative detection of H_2S.

2.1.5 Statements

The much of the results in this chapter has been published in *J. Fluoresc.* (Wang, K.*; Peng, H.*; Ni, N.; Dai, C.; Wang, B., 2,6-Dansyl azide as a fluorescent probe for hydrogen sulfide. *J. Fluoresc.* **2014,** *24* (1), 1-5, DOI: 10.1007/s10895-013-1296-5) and *J. Cell. Biochem.* (Wang, K.; Peng, H.; Wang, B., Recent advances in thiol and sulfide reactive probes. *J. Cell. Biochem.* **2014,** *115* (6), 1007-1022, DOI: 10.1002/jcb.24762). In this chapter, my contributions include fluorescence studies and quantitative determination of hydrogen sulfide probe.

2.2 Development of fluorescent chemoprobes for homocysteine (Hcy)

2.2.1 Introduction

Thiols, such as cysteine (Cys), homocysteine (Hcy) and glutathione (GSH) (Figure **2.17**), are indispensable functional molecules in the biological system due to the strong nucleophilicity

and redox reactivity of the sulfhydryl group.[230] Thiols are ideal nucleophiles in enzyme functions, excellent sensors[231] and mild buffering molecules for maintaining cellular redox states.[232-233] Biological thiols play versatile roles in various processes, including protein structure and functions, antioxidant activity, and redox signaling. Hcy is a key intermediate generated during the biosynthesis of Cys.[234-235] Plasma Hcy exists in three major forms including free reduced (~1%), free oxidized (30%) and protein-bound oxidized (70%) forms.[236-237] Fluctuations in thiol concentrations can indicate or even lead to a variety of cardiovascular disorders and neurodegenerative diseases. For example, circulating Hcy has been correlated with Alzheimer's disease[238] and coronary artery diseases,[239-240] Excessive amount of total Hcy (tHcy) in the blood,[241] hyperhomocysteinemia (HHcy), is related to folate deficiency, which can lead to miscarriage[242] and various tumors.[243] According to the American Heart Association (AHA) advisory statement, normal tHcy concentrations range from 5-15 μM; moderate, intermediate, and severe hyperhomocysteinemia refer to concentrations between 16 and 30, between 31 and 100, and >100 μM, respectively, and are essentially pathognomonic.[244] Cys deficiency is associated with slow growth, and liver and skin damage.[245] High Cys concentration exhibits neurotoxicity.[246] Decrease in GSH concentration was also shown to be associated to Parkinson's disease.[247] As a result, accurate determination of these biological thiols, especially of Hcy in biological systems such as blood plasma and urine are of great importance in both clinical and research practice.

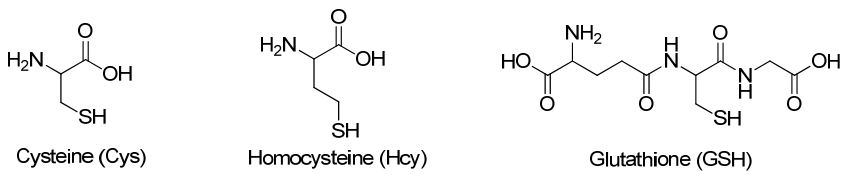

Figure 2.17 Structures of Cysteine (Cys), Homocysteine (Hcy) and Glutathione (GSH)

By taking advantage of the unique chemical properties of the sulfhydryl group, such as strong nucleophilicity and low redox potential (-0.2~-0.3 V),[248-249] general detection of thiols can be achieved using thiol reactive probes and electrochemical probes.[250] For determination of specific thiols, both detection methods can be coupled with different separation technology, such as chromatography and capillary electrophoresis (CE). Chemically derivatized thiols can also be selectively detected using mass spectrometry (MS). Due to the low redox potential of the sulfhydryl group, thiols (R-SH) are readily oxidized to their disulfide state. For example, more than 95% of total Hcy is in the oxidized form,[251] while only a very small amount is in the form of free thiol. Therefore, a reducing pre-treatment is usually required to convert all thiol species to their reduced forms before analysis of total thiol concentrations. Reducing agents such as dithiothreitol (DTT), tris(2-carboxyethyl)phosphine (TCEP),[252] or sodium borohydride ($NaBH_4$) can be used for the reduction of disulfide bonds. Because the chemical derivatization relies on the nucleophilicity of the sulfhydryl group (pK_a of –SH in cysteine:[253] 8.15, Hcy: 8.7, GSH: 8.56), pH of the media is also an important factor affecting the reaction rates and outcomes. Basic buffer condition is often used to deprotonate sulfhydryl group and to accelerate the sensing reaction.[254-255] For thiol reactive probes, numerous reaction types have been utilized, including nucleophilic substitution, Michael addition, cyclization, and cleavage of disulfide bond, metal complexes coordination, and redox reactions.

Normal tHcy is lower than 15 μM in plasma, which is about 1/20 of the total Cys concentration.[251] Due to high degree of similarity in both structure and chemical properties between Hcy and other thiols such as Cys, the selective detection of Hcy has never been a trivial issue. Current detection methods for Hcy involve the derivatization at the sulfhydryl group using electrophilic fluorogenic reagents.[256-258] However, due to the lack of selectivity among different

biological thiols, these methods require tedious separating techniques such as GC and HPLC. This has led to an increased cost and reduced efficiency and thus limited the applicability of Hcy as an important biomarker. Therefore, selective recognition of Hcy over other biological thiols is of great interest. In this and the following sections, Cys/Hcy-specific probes, and Hcy -specific probes (Table **2.2**) are discussed.

Table 2.2 Properties of Cys and Hcy probes

Probe	Analyte	Wavelength (λ_{ex}/ λ_{em}, nm) or Abs.	Reaction time (min)	Temperature (^{o}C)	pH	Medium	LOD	Application in biological system
CIC	Cys/ Hcy	430/547	30	37	7.2	DMSO: HEPES 9: 1	N.D.	N.D.
MV^{2+}	Hcy	510 (Abs.)	5	r.t.	7.5	Tris	N.D.	plasma
fluorone black	Hcy	510 (Abs.)	5	r.t.	7.3	phosphate buffer	N.D.	plasma
FSN-AuNPs	Hcy	370/ 485	120	r.t.	13	phosphate buffer	4.4 nM	plasma

Tris: tris(hydroxymethyl)aminomethane

In 2010, Li reported an inorganic phosphorescent imaging probe, cationic iridium (III) complex (CIC) (Figure **2.18**), for Cys and Hcy detection in living cells.[259] Upon addition of aminothiols, the probe's luminescence changes from yellow to red in DMSO-HEPES (9: 1). This makes it a "naked-eye" indicator of Cys or Hcy. With its membrane-permeable property, CIC can ratiometrically indicate the intracellular Cys and Hcy concentrations.

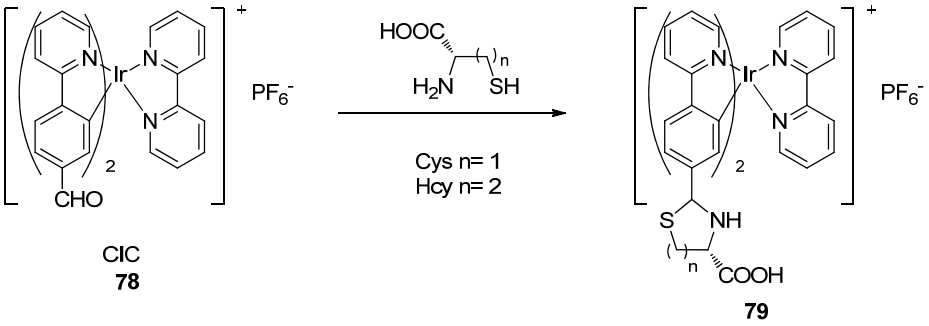

Figure 2.18 Structures of Cys/Hcy-specific probes and their mechanisms

Two Hcy-specific probes based on redox chemistry were reported by the Strongin group.[255, 260] One visual detection probe was methyl viologen (MV^{2+}) (Figure **2.19**), which responded to Hcy changing from colorless to blue in 5 min. Another commercially available probe fluorone black (Figure **2.19**) shared a similar mechanism as that of MV^{2+} with higher detection sensitivity (linearity working range 0-15 μM).

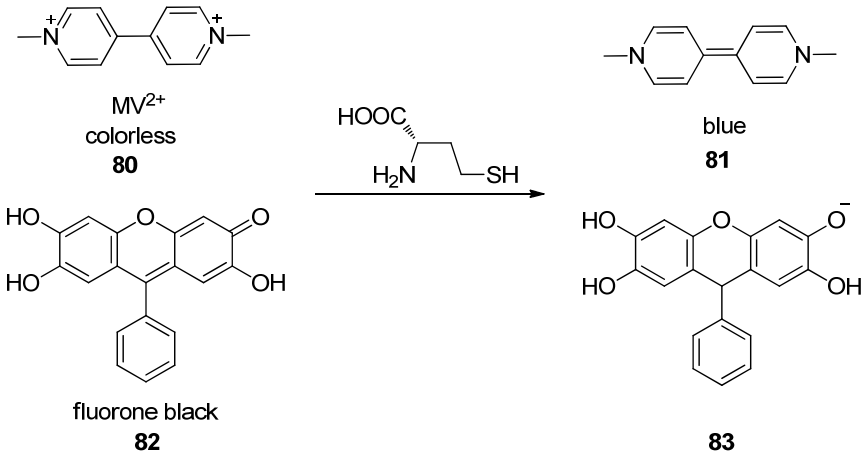

Figure 2.19 Structures of Hcy-specific probes and their mechanisms of action

Another quantitative detection method of Hcy in plasma was reported by Tseng and co-workers in 2012.[254] The combination of TCEP reduction, fluorosurfactant-capped gold nanoparticles (FSN-AuNP) extraction and subsequent *o*-phthaldialdehyde (OPA) derivatization

(Figure **2.20**) provided a selective and sensitive method for quantification of total Hcy as well as protein-bound, free, and free oxidized Hcy. To avoid the interference of Cys, particle size of FSN-AuNPs was increased from 12 nm to 40 nm, which led to a higher aggregation rate of Hcy-attached AuNPs than Cys-attached.[261] In addition, OPA can selectively react with Hcy forming a highly fluorescent (9-fold intensity increase) product emitting at 485 nm with excitation at 370 nm.[262] Within the dynamic range 0.01-1 μM, the detection limit of this method was determined to be 4.4 nM. This detection method can provide more than 100-fold selectivity toward Hcy over other aminothiols in plasma. However, the detection pH of this probe was 13, which cannot be widely used in detection in a biological system.

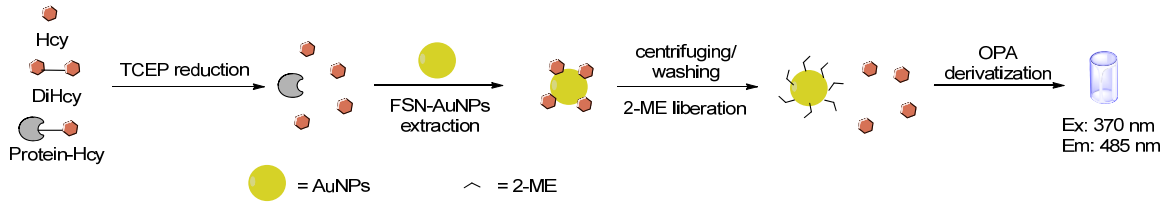

Figure 2.20 Schematic presentation of probe FSN-AuNPs assay and its mechanism of action

Fluorescent probes based on cyclization mechanisms using both the amino and sulfhydryl groups have been reported mostly selective for Cys.[263-267] The Strongin group found a colorimetric method for selective Hcy detection based on a radical mechanism.[268-271] They also reported a fluorescent probe showing different reaction profiles for Hcy and Cys and thus their simultaneous detection.[264] The Yoon lab recently reported a pyrene-based fluorescent probe functionalized with an aldehyde moiety selective for Hcy.[272] Herein we report a redox-sensitive fluorometric detection of Hcy using a dansyl azide analogue **1** (DN-2).

2.2.2 Results and discussion

During our search for redox-sensitive fluorescent probes for H_2S,[273] we discovered a dansyl-based fluorescent probe (DN-2) with selectivity towards Hcy over other biological thiols such as Cys and GSH in aqueous media. It is well known that thiols show reducing ability and help to maintain the redox states in biological systems. Redox reactions have been employed in thiol detections. For example, Ellman's reagent (5,5'-dithiobis-2-nitrobenzoic acid or DTNB)[274] is widely used in the quantitation of sulfhydryl groups through the reductive cleavage of a disulfide bond, which releases the chromogenic indicator. However, only a few studies have been reported on the difference in reducing ability among thiols.[275-276]

Specifically, we have synthesized dansyl derivative **87** (DN-2) as a fluorescent probe. The synthesis of DN-2 is accomplished in 3 steps from commercially available starting materials (Scheme **2.2**). The substitution reaction between 5-naphthol-1-sulfonate **84** and ethylene diamine was followed by reductive amination, which installed three methyl groups on the amino groups.[277] Then the sulfonate was converted to sulfonyl chloride, which reacted quantitatively with sodium azide to form the sulfonyl azide, DN-2 (**87**). This short and convenient synthetic route has provided the probe in a 37% isolated yield.

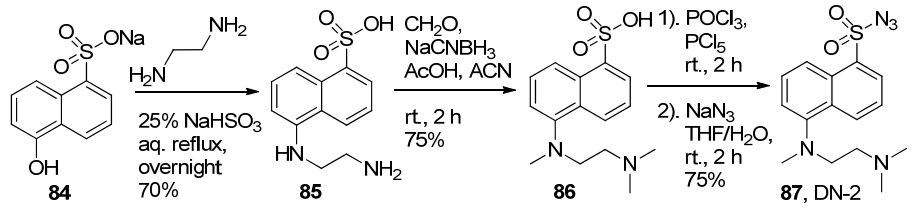

Scheme 2.2 Synthesis of the fluorescent probe DN-2

Fluorescence spectroscopy was used to monitor the reaction between DN-2 and biological thiols, Cys, Hcy, and GSH. As is shown in Figure 1, a significant fluorescence increase (~25-fold) at around 517 nm was observed for Hcy. Such fluorescent changes are also

readily visible to the naked eyes (Figure**2.21**, insert). However, with Cys and GSH, only 2 and 3-fold fluorescence intensity change was observed, respectively. Spectroscopic (^{1}H NMR, ^{13}C NMR, and MS) identification of the product confirmed that the sulfonyl azide was reduced by Hcy, forming the corresponding sulfonamide and homocystine (Scheme **2.3**). The fluorescence increase was due to the formation of highly fluorescent DA-2 (Φ_{FL} (DN-2) = 0.007 and Φ_{FL} (DA-2) = 0.58 in acetonitrile, Φ_{FL} (DN-2) = 0.02 and Φ_{FL} (DA-2) = 0.29 in water, Figure **2.22**).

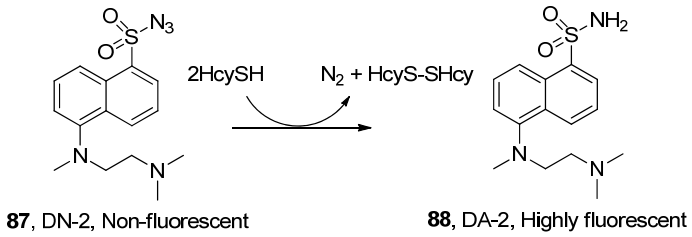

Scheme 2.3 Sensing reaction of DN-2 with Hcy

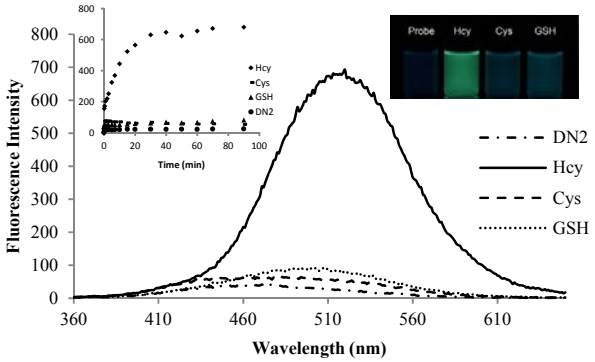

Figure 2.21 Fluorescence spectrum of DN-2 in the presence of different amino thiols.
Fluorescence spectrum of DN-2 in the absence and presence of different amino thiols; insert: time dependent fluorescence emission (517 nm) of DN-2 in the presence of different Hcy and Cys, and comparison of fluorescence intensity change with the addition of different amino thiols. (DN-2 120 μM, amino thiols 100 μM in 100 mM sodium phosphate buffer at pH 7.4 with 10% ethanol, fluorescence spectrum and pictures were recorded 1 h after the addition of thiols).

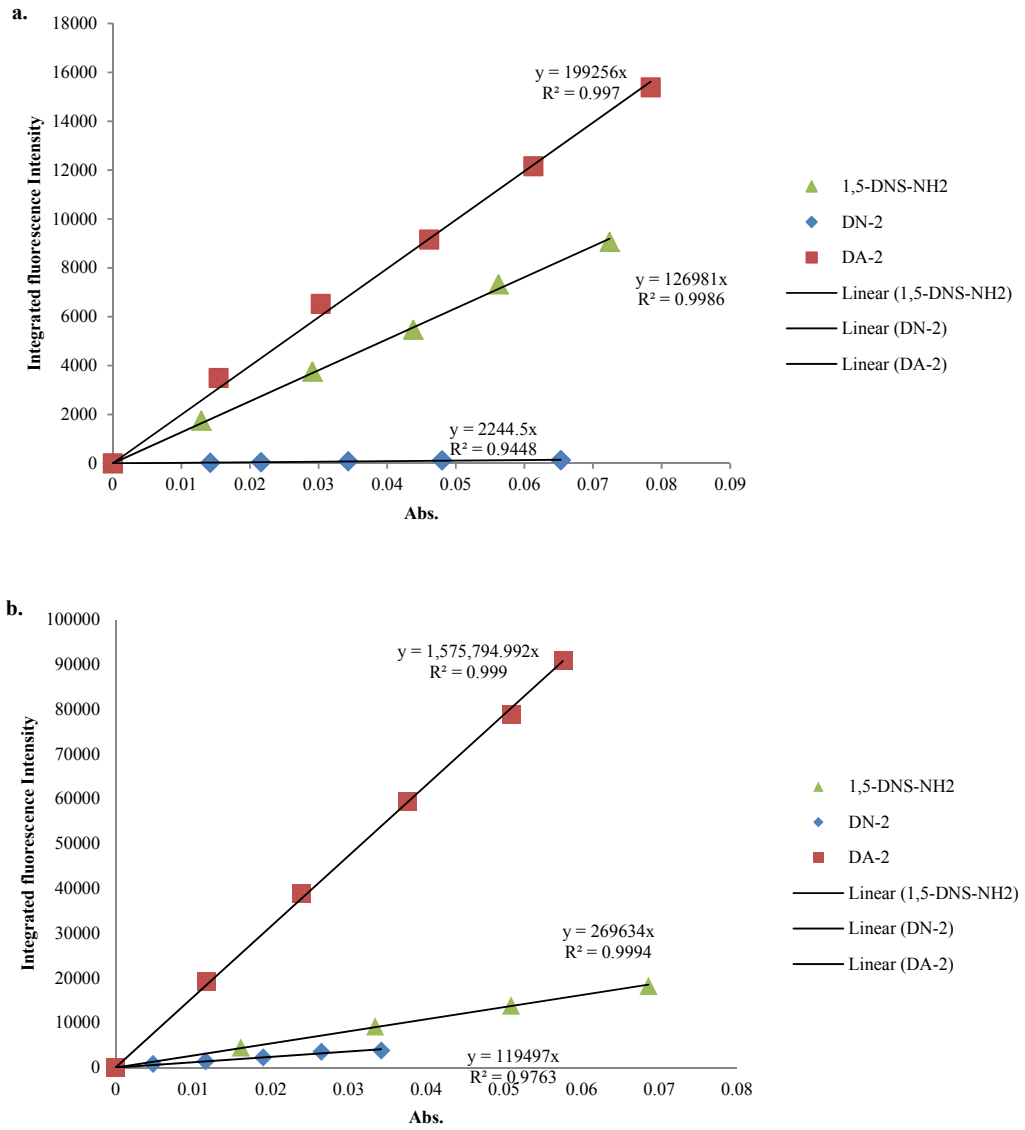

Figure 2.22 Quantum yield determination of DN-2 and DA-2.
a. Quantum yield determination of DN-2 and DA-2 in acetonitrile; b. quantum yield determination of DN-2 and DA-2 in water. 1,5-DNS-NH_2 was used as the reference for relative quantum yield determination. Absorption and emission (λ_{Ex}= 325 nm) spectra were recorded for a series of concentrations (16 µM, 12 µM, 8 µM, 4 µM and 0 µM in acetonitrile or deionized water) of 1,5-DNS-NH_2, DN-2 (**1**) and DA-2 (**2**). Integrated fluorescence intensity was plotted against the absorption values at each concentration.[229] Relative quantum yield values can be calculated using slopes of each compound

Next we compared the reaction time profile of DN-2 to thiols. Specifically, DN-2 was dissolved in the solution to a final concentration of 120 µM, while thiol concentrations were 100

μM. The probe, DN-2 was only weakly fluorescent in solvent systems, including acetonitrile (ACN), 100 mM sodium phosphate buffer at pH 7.4, and water. Immediately after the addition of thiols, an initial small increase in fluorescence was observed for all species (Figure **2.21**, left inset). However, the fluorescent intensity quickly reached a plateau for Cys and GSH. For Hcy, the fluorescence intensity reached a plateau at about 1 h point at a much higher level. The selectivity for Hcy over Cys and GSH was found to be 8-12-fold. However, since GSH concentration in plasma is as low as ~2 μM,[278] one would not expect interference problem with GSH.

To further test the feasibility of DN-2 as a fluorescent probe in a complex biological system, the selectivity of DN-2 was tested among various amino acids in phosphate buffer with 10% ethanol (Figure **2.23**). It was found that DN-2 did not respond to most amino acids. A selectivity of over 45-fold was found among these amino acids at 100 μM. The reaction between DN-2 and Hcy was carried out in the presence of various amino acids (100 μM) (Figure **2.23**b) in order to test how the presence of other amino acids affects the fluorescence response of DN-2 to Hcy. It was found that the fluorescence response of DN-2 to Hcy was elevated by ~40% in the presence of 100 μM Cys. GSH showed similar effect. In contrast, none of the other amino acids affected the detection of Hcy. In addition, other possible reducing species in biological samples, such as Fe(II), Cu(I), and ascorbate, showed no reactivity with DN-2 (Figure **2.24**)

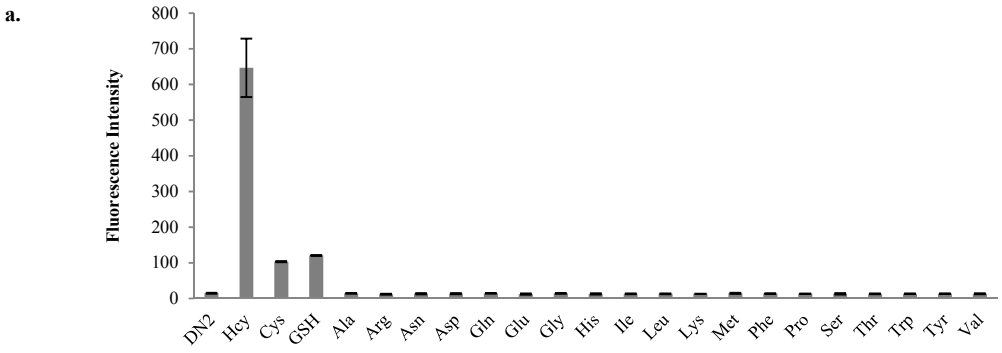

b.

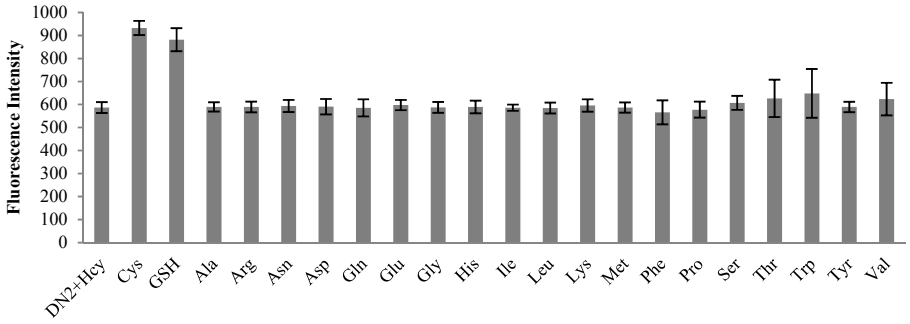

Figure 2.23 Fluorescence response of DN-2 to amino acids.

a. Fluorescence response of DN-2 to amino acids; b. fluorescence response of DN-2 to Hcy in the presence of amino acids. (DN-2 120 µM, amino acids 100 µM in 100 mM sodium phosphate buffer at pH 7.4 with 10% ethanol, fluorescence intensities were recorded 1 h after the addition of amino acids. Data represents the average of three independent experiments.)

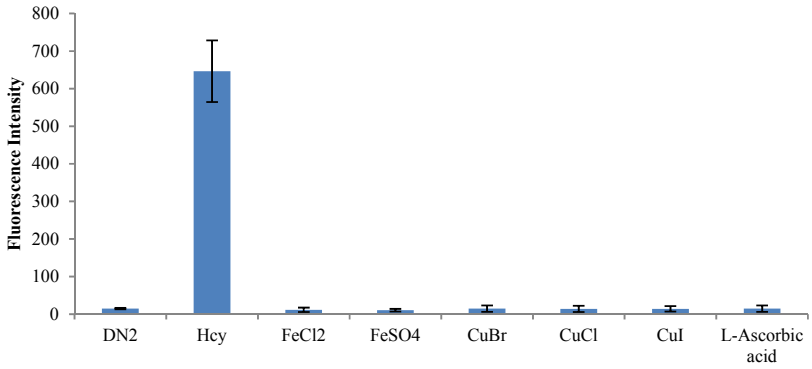

Figure 2.24 Fluorescence response of DN-2 to metal ions

Fluorescence response of DN-2 to $FeCl_2$, $FeSO_4$, CuBr, CuCl, CuI, and ascorbic acid in comparison with negative control (DN-2 alone) and positive control (Hcy addition to DN-2 solution). (DN-2 120 µM, analytes 100 µM in 100 mM sodium phosphate buffer at pH 7.4 with 10% ethanol, fluorescence intensities were recorded 1 h after the addition of reducing species. Data represents the average of three independent experiments.)

A fluorescent probe is especially useful for quantitation if a linear calibration curve could be obtained. Therefore, experiments were performed to obtain a calibration curve using a series of concentrations for Hcy. As expected, a linear calibration curve with R^2 >0.99 was obtained for Hcy (Figure **2.25**). This linearity is very important for quantitative analysis of Hcy.

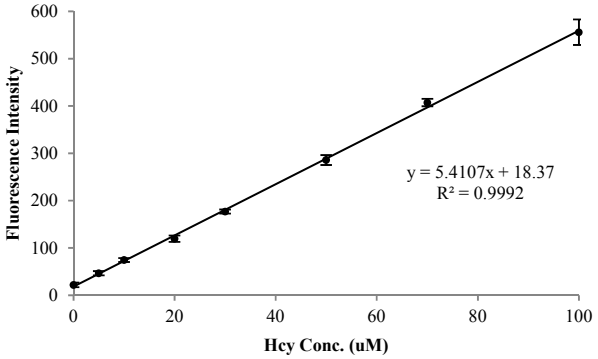

Figure 2.25 Calibration curve for Hcy.
DN-2 120 μM, Hcy 100 μM in 100 mM sodium phosphate buffer at pH 7.4, with 10% ethanol; fluorescence intensities at 517 nm were recorded 60 min after the addition of Hcy. Data represents the average of three independent experiments.

Since the presence of Cys was found to increase the fluorescence response of DN-2 to Hcy by ~40%, we were interested whether endogenous Cys fluctuations (~200-250 μM) would affect Hcy detection. In order to test the effect of Cys fluctuation, calibration curves of Hcy at 0-50 μM was generated in the presence of 200 and 250 μM of Cys (Figure **2.26**). It was found that these two curves are very close, though not identical. Therefore, the accuracy of Hcy quantitation may be affected by Cys fluctuation. However, the selectivity of DN-2 to Hcy still allows a good estimation of Hcy level with large (~50 μM) fluctuation of Cys concentrations.

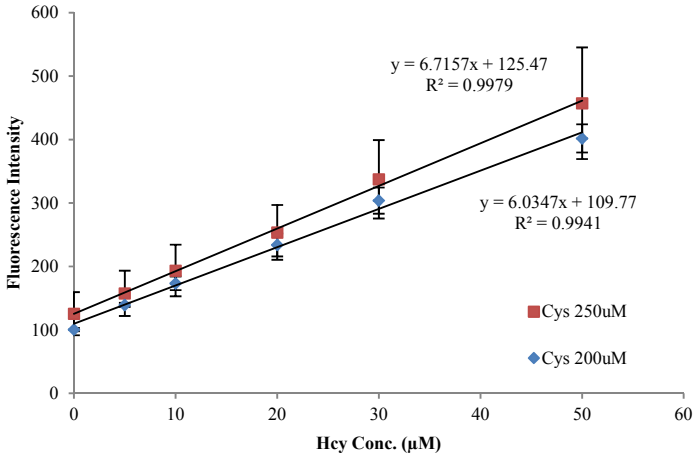

Figure 2.26 Calibration curve of homocysteine in the presence of 200 and 250 μM of cysteine.

DN-2 120 μM, Hcy 0-50 μM in 100 mM sodium phosphate buffer at pH 7.4, with 10% ethanol; fluorescence intensities at 517 nm were recorded 60 min after the addition of Hcy. Data represents the average of three independent experiments.

As arylsulfonyl azide was found to be a very sensitive fluorescent probe for sulfide,[258, 279] DN-2 also reacts with sulfide. In order to exclude the influence of sulfide in the selective detection of Hcy, a solution of $ZnCl_2$ could be added into the reaction buffer to precipitate sulfide out of the solution in the form of ZnS ($K_{sp}(ZnS)\sim2\times10^{-25}$). It was found that the presence of high concentration of Zn^{2+} (at 300 μM) shows very little interference with the fluorescence response of DN-2 to Hcy (Figure **2.27**).

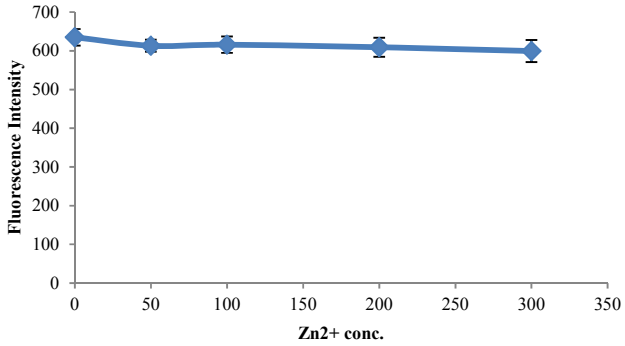

Figure 2.27 Fluorescence response of DN-2 to Hcy in the presence of different concentrations of Zn^{2+}

DN-2 120 μM, Hcy 100 μM in 100 mM phosphate buffer with 10% ethanol at pH 7.4. Fluorescence was recorded on a fluorometer after reaction for 120 min in the presence of 0, 50, 100, 200 and 300 μM of $ZnCl_2$, respectively. Data represents the average of three independent experiments.

Due to the significance of Hcy in biological system, the application of this probe in serum was examined. In diluted (10%) deproteinized fetal bovine serum (FBS), with addition of Hcy, this probe selectively responded to Hcy over Cys (Figure **2.28**, insert). Furthermore, concentration-dependent fluorescence changes of DN-2 in diluted deproteinized FBS were observed. A linear calibration curve (R^2 = 0.9997) was obtained suggesting the potential utility

of DN-2 in serum. The detection limit of Hcy in deproteinized FBS was 10 μM based on a 3-fold signal-to-noise ratio.

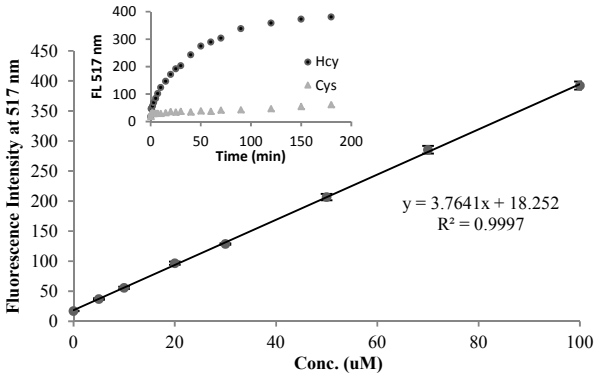

Figure 2.28 Calibration curve for Hcy

DN-2, 120 μM, Hcy, 0-100 μM in diluted deproteinized FBS, fluorescence intensities at 517 nm were recorded 180 min after addition of Hcy. Data represents the average of three independent experiments; Insert shows time-dependent fluorescence response of DN-2 (120 μM) to Hcy (100 μM) or Cys (100 μM) in diluted deproteinized FBS.

Our experiments have found that DN-2 selectively oxidizes Hcy in buffer and diluted deproteinized FBS. Although Cys is reduced by DN-2 at very high concentrations (~100 mM), there is apparently a large difference at lower concentrations. Thus, we were interested in achieving an understanding of the difference in reducing ability between Cys and Hcy. Hcy has one extra methylene group compared to Cys. However, this does not make its sulfhydryl group a stronger nucleophile since most nucleophilic substitution-based fluorescent probes show similar reactivity with both thiols. We have also examined the pK_a of the sulfhydryl groups on Cys and Hcy using pH titration.[280] It was found that the pK_a was 8.25 for Cys and 8.9 for Hcy (Figure **2.29**), similar to most previously reported values.[280-281] (In another paper, the pK_a of –SH group was reported to be as high as 10.[282]) According to these pK_a values, Cys should be deprotonated more easily than Hcy. Therefore, one would expect that Cys being a stronger reducing agent than Hcy if pK_a was the determining factor. Fluorescent/colorimetric probes with disulfide moieties show comparative or slightly higher reactivity to Cys.[283-284] This may be due to their difference

in pK_a. However, this is not the case in the redox reaction between these thiols and DN-2, where a different mechanism is indicated. In fact, it has been reported that oxidation of Hcy by albumin is faster than that of Cys and the oxidation is accelerated by basic conditions or addition of a copper catalyst.[276, 285]

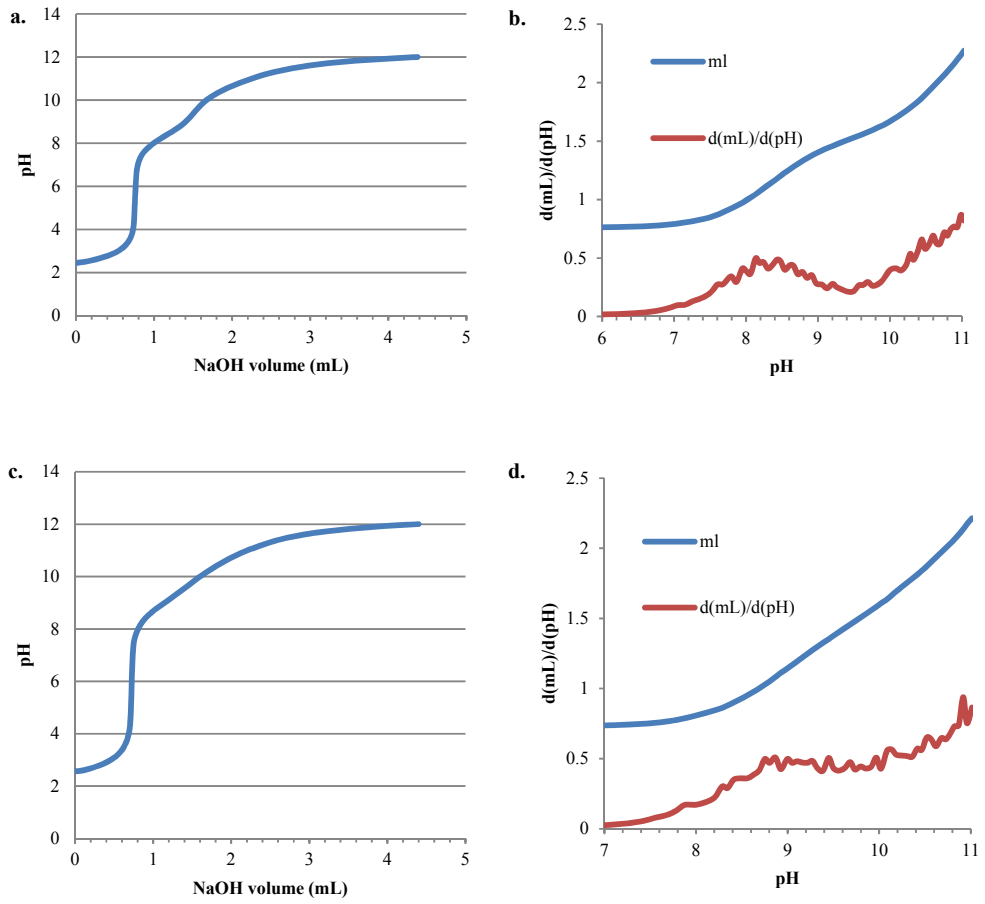

Figure 2.29 Titration curves of cysteine and homocysteine.
a. Titration curve of 5 mM cysteine hydrochloride; b. Calculation of the sulfhydryl group pKa of cysteine; c. Titration curve of 5 mM homocysteine hydrochloride; d. Calculation of the sulfhydryl group pKa of homocysteine. NaOH solution (99.35 mM) was standardized with potassium hydrogen phthalate (KHP) and used for titration of 5 mM cysteine hydrochloride and 5 mM homocysteine hydrochloride. Experiment was triplicated to obtain the average pKa values (8.25 for cysteine and 8.9 for homocysteine).

The reduction mechanism of an azido compound by a dithiol has been proposed in a previous report.[286] Based on the experimental results, we propose that the initial attack by thiol leads to the formation of an intermediate **90** (Scheme **2.4**), which is responsible for the initial 2-3-fold fluorescence increase. Proton transfer then occurs to neutralize the negatively charged nitrogen leading to intermediates **89b** and **89c**. In the case of Hcy, the amino group then attacks the sulfur to form a five-membered ring intermediate **7**, which then reacts with another molecule of thiol to form the disulfide product. The intermediate **90** then releases N_2 to provide the sulfonamide product **88**. In the case of Cys, a similar intramolecular attack would lead to a strained four membered ring **92**, which would be unstable and thus unfavorable. In addition, the reversibility of the initial step means that the intermediate (**89**) exists in equilibrium with the starting materials and thus the probe (**87**) is available to react with Hcy even in the presence of Cys. In fact, cyclic transition states/intermediates have been used to explain the mechanisms of other Cys- or Hcy-selective probes.[264, 268-269] It is entirely possible that there are other conformational factors, which affect the reactivity of intermediate **89**. In the last step, another thiol comes to attack the sulfur to form a disulfide. Although gaseous diatomic bond energy for general S-N bond is higher than S-S bond,[287] the formation of disulfide bond from the attack of sulfhydryl group on an electron-deficient S-N bond has been reported previously.[288] In this step, it is conceivable that when excessive amount of Cys exists in the reaction media, a Cys-Hcy mixed disulfide could also form. This explains why Cys alone does not trigger fluorescence increase but causes a ~40% increase in fluorescence response to Hcy. It should be noted that a previously published dansyl azide analogue, 1,5-DNS-Az also shows selectivity for Hcy (Figure **2.30**).

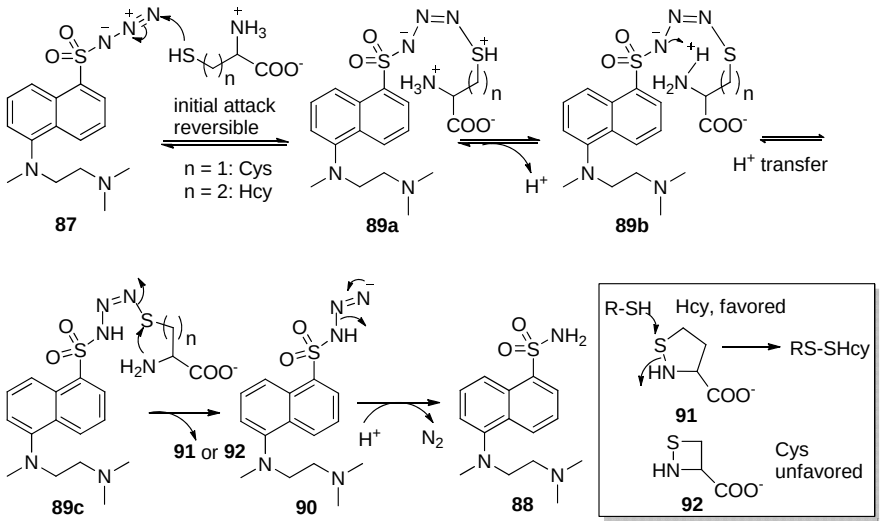

Scheme 2.4 Proposed mechanism

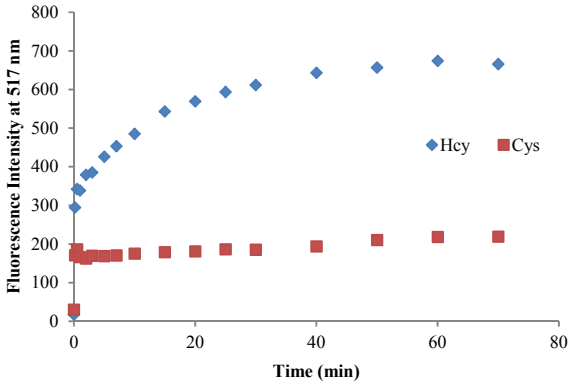

Figure 2.30 Time dependent fluorescence emission (517 nm) of 1,5-DNS-Az in the presence of Hcy and Cys

DNS-Az 120 µM, amino thiols 100 µM in 100 mM sodium phosphate buffer at pH 7.4 with 10% ethanol

In addition, the influence of pH on the selectivity has also been tested using 96-well plate and a microplate reader (Figure **2.31**). Sodium phosphate buffer (100 mM) in the pH range of 5.3-11.5 was used in the experiments. A pH dependent fluorescence response was observed for DN-2 in the presence of thiols. It was found that DN-2 itself remains fluorescently stable at pH

values lower than 10.5. The selectivity for Hcy increased with increasing pH from 5-7.4. In buffers at pH higher than 7.4, reactions with Cys and GSH were promoted. Therefore, the highest selectivity was observed at pH 7.4, which is the physiological pH. We have also examined the reaction time profile in phosphate buffer at 37 °C (Figure **2.32**). The result has suggested that heat facilitated the reaction. The reaction time for 120 μM of DN-2 and 100 μM of Hcy decreased from 60 min at room temperature (about 22 °C) to 30 min at 37 °C.

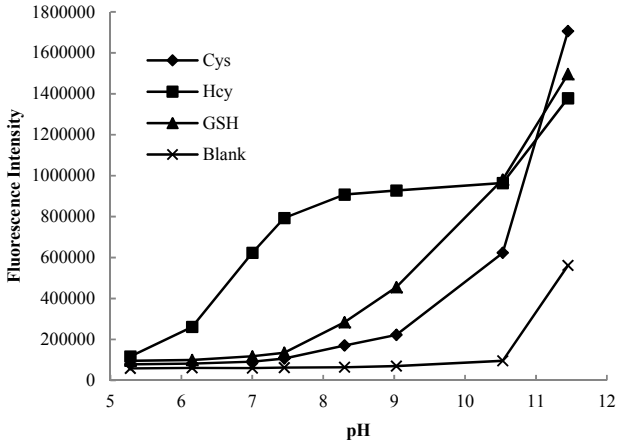

Figure 2.31 pH dependent fluorescence response of DN-2 to thiols.
Fluorescence intensity was read on a microplate reader (Excitation filter 340 nm, Emission filter 535 nm). DN-2 100 μM, thiols 100 μM in 100 mM sodium phosphate buffer at pH values of 5.3, 6.2, 7.0, 7.5, 8.3, 9.0, 10.5, and 11.5.

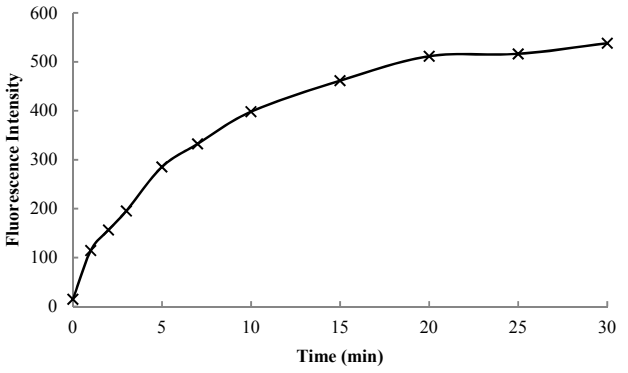

Figure 2.32 Reaction time profile at 37 °C.
DN-2 120 μM, amino thiols 100 μM in 100 mM sodium phosphate buffer at pH 7.5, 37 °C, fluorescence intensities at 517 nm were recorded at each time point

2.2.3 Experimental section

2.2.3.1 General Information

Solvents and reagents were purchased from VWR International, Oakwood Product Inc., or Sigma-Aldrich Co. and used without purification unless specified otherwise. When necessary, solid reagents were dried under high vacuum. Reactions with compounds sensitive to air or moisture were performed under argon. Solvent mixtures are indicated as volume/volume ratios. Thin layer chromatography (TLC) was run on Sorbtech W/UV254 plates (0.25 mm thick), and visualized under UV-light or by a Ce-Mo staining solution (phosphomolybdate, 25 g; $Ce(SO_4)_2.4H_2O$, 10 g; conc. H_2SO_4, 60 mL; H_2O, 940 mL) with heating. Flash chromatography was performed using Fluka silica gel 60 (mesh size: 0.040-0.063 mm) using a weight ratio of ca. 30:1 for silica gel over crude compound. ^{1}H and ^{13}C NMR spectra were recorded on a Bruker 400 spectrometer (400 and 100MHz, respectively) in deuterated chloroform ($CDCl_3$), methanol-d_4 (CD_3OD), and DMSO-d_6 with either tetramethylsilane (TMS) (0.00 ppm) or the NMR solvent as the internal reference. UV-Vis absorption spectra were recorded on a Shimadzu PharmaSpec UV-1700 UV-Visible spectrophotometer. Fluorescence spectra were recorded on a Shimadzu RF-5310PC spectrofluorophotometer. 96-Well plates were read and recorded on a PerkinElmer 1420 multi-label counter. Automatic pH titration on a Accumet$^{@}$ Research, AR10 pH meter was used to determine the pKa values of the sulfhydryl groups on cysteine and homocysteine. Titration curve was created and analyzed using TitriSoft 2.51.

2.2.3.2 Synthesis and Characterization

5-(2-Aminoethylamino)naphthalene-1-sulfonic acid **84** and 5-(*N*-(2-(dimethylamino) ethyl)-N-methylamino)naphthalene-1-sulfonic acid **85** was performed following literature reported procedures.[277]

5-(*N*-(2-(Dimethylamino)ethyl)-*N*-methylamino)naphthalene-1-sulfonyl azide **87**: To a Ar protected solution of **85** (110 mg, 0.36 mmol) in $POCl_3$ (570 μL, 6.2 mmol) was added PCl5 in 2 portions (430 mg, 2.1 mmol). The reaction was stirred on ice bath for 1 h, then warmed to room temperature, and stirred for additional 2 h. The reaction mixture was poured into 10 g ice. EtOAc extraction and evaporation gave crude intermediate 5-(*N*-(2-(dimethylamino)ethyl)-*N*-methylamino)naphthalene-1-sulfonyl chloride, which was dissolved in MeOH (2 mL) and added into a stirred solution of NaN_3 (243 mg, 3.75 mmol) in a 1:1 mixed solvent of MeOH/H_2O (4 mL). The reaction mixture was stirred at room temperature for 2 h. MeOH was evaporated and the product was extracted with EtOAc. The organic phase was washed with water and brine, and dried over Na_2SO_4. Solvent evaporation followed by flash chromatography (CH_2Cl_2:Hex:EtOAc, 1:2:0.2) gave a light yellow solid (90 mg, 75% yield). ^{1}H NMR ($CDCl_3$): 8.64 (d, *J* = 8.4 Hz, 1 H), 8.34 (d, *J* = 7.2 Hz, 1 H), 8.64 (d, *J* = 8.8 Hz, 1 H), 7.74-7.64 (m, 2 H), 7.39 (d, *J* = 7.6 Hz, 1 H), 3.59 (t, *J* = 7.0 Hz, 2 H), 3.12 (t, *J* = 7.0 Hz, 2 H), 2.91 (s, 3 H), 2.91 (s, 6 H); ^{13}C NMR ($CDCl_3$): 149.8, 134.1, 131.7, 131.0, 130.4, 129.7, 129.2, 124.0, 120.7, 118.3, 60.6, 51.1, 50.4, 45.1; IR 2916.9, 2421.7, 2130.7, 1571.2, 1465.2, 1166.6, 792.6, 743.8; MS (ES+) 333.9 $(M+1)^+$.

5-(*N*-(2-(Dimethylamino)ethyl)-*N*-methylamino)naphthalene-1-sulfonyl amide **88**: ^{1}H NMR ($CDCl_3$): 8.51-8.46 (m, 2 H), 8.26 (d, *J* = 7.2 Hz, 1 H), 7.65-7.57 (m, 2 H), 7.40-7.38 (m, 1 H), 3.52 (t, *J* = 6.0 Hz, 2 H), 3.13 (t, *J* = 6.0 Hz, 2 H), 2.84 (s, 3 H), 2.66 (s, 6 H); ^{13}C NMR

($CDCl_3$): 149.8, 139.1, 130.6, 129.5, 128.7, 127.5, 127.0, 123.7, 120.8, 117.3, 60.1, 50.2, 49.9, 43.5; MS (ES+) 308.0 $(M+1)^+$.

2.2.4 Conclusions

Hcy is a very important biomarker for the diagnosis and prognosis of various diseases. However, due to the structural similarity of Hcy and Cys, direct detection of this biomarker still remains a major challenge. We have developed a novel redox sensitive fluorescent probe for quantitative Hcy analysis. The sensing reaction is selective for Hcy over other biological thiols such as Cys and GSH. In addition, a linear calibration curve could be obtained in both buffer and diluted deproteinized FBS with a detection limit at 10 μM. Endogenous Cys level fluctuation (200-250 μM) can also be tolerated to provide a good estimation of Hcy concentration. This probe will be very useful for the selective detection of Hcy in complex biological samples.

2.2.5 Statements

The much of the results in this chapter has been published in *Chem. Commun.* (Wang, K.;* Peng, H.;* Dai, C.; Williamson, S.; Wang, B., Redox-based selective fluorometric detection of homocysteine. *Chem. Commun.* **2014**. *50* (89), 13668-13671, DOI: 10.1039/C4CC03677H) and *J. Cell. Biochem.* (Wang, K.; Peng, H.; Wang, B., Recent advances in thiol and sulfide reactive probes. *J. Cell. Biochem.* **2014,** *115* (6), 1007-1022, DOI: 10.1002/jcb.24762). My contributions include fluorescence detection and quantitative evaluation of homocysteine probe.

REFERENCES

1. Liu, J.; Lu, Y., Fast colorimetric sensing of adenosine and cocaine based on a general sensor design involving aptamers and nanoparticles. *Angew. Chem. Int. Ed.* **2006,** *45* (1), 90-94.

2. Drummond, T. G.; Hill, M. G.; Barton, J. K., Electrochemical DNA sensors. *Nat. Biotechnol.* **2003,** *21*, 1192-1199.

3. Rothemund, P. W., Folding DNA to create nanoscale shapes and patterns. *Nature* **2006,** *440* (7082), 297-302.

4. Long, X.; Thomas, A., Drug delivery trends in clinical trials and translational medicine: Challenges and opportunities in the delivery of nucleic acid-based therapeutics. *J. Pharm. Sci.* **2011,** *100*, 38-52.

5. Hurley, L. H., DNA and its associated processes as targets for cancer therapy. *Nat. Rev. Cancer* **2002,** *2* (3), 188-200.

6. Keefe, A. D.; Pai, S.; Ellington, A., Aptamers as therapeutics. *Nat. Rev. Drug Discov.* **2010,** *9* (7), 537-550.

7. Kanan, M. W.; Rozenman, M. M.; Sakurai, K.; Snyder, T. M.; Liu, D. R., Reaction discovery enabled by DNA-templated synthesis and in vitro selection. *Nature* **2004,** *431* (7008), 545-549.

8. Syed, M. A.; Pervaiz, S., Advances in aptamers. *Oligonucleotides* **2010,** *20* (5), 215-224.

9. Fang, X.; Tan, W., Aptamers generated from cell-SELEX for molecular medicine: a chemical biology approach. *Accounts Chem. Res.* **2009,** *43*, 48-57.

10. Eaton, B. E.; Gold, L.; Hicke, B. J.; Janjić, N.; Jucker, F. M.; Sebesta, D. P.; Tarasow, T. M.; Willis, M. C.; Zichi, D. A., Post-SELEX combinatorial optimization of aptamers. *Bioorg. Med. Chem.* **1997,** *5* (6), 1087-1096.

11. Sakthivel, K.; Barbas, C. F., Expanding the potential of DNA for binding and catalysis: highly functionalized dUTP derivatives that are substrates for thermostable DNA polymerases. *Angew. Chem. Int. Ed.* **1998,** *37* (20), 2872-2875.

12. Haque, M. M.; Peng, X., DNA-associated click chemistry. *Sci. China Chem.* **2013,** *57* (2), 215-231.

13. Hollenstein, M., Nucleoside triphosphates building blocks for the modification of nucleic acids. *Molecules* **2012,** *17* (11), 13569-13591.

14. El-Sagheer, A. H.; Brown, T., Click chemistry with DNA. *Chem. Soc. Rev.* **2010,** *39* (4), 1388-1405.

15. Sidman, R. L.; Miale, I. L.; Feder, N., Cell proliferation and migration in the primitive ependymal zone; an autoradiographic study of histogenesis in the nervous system. *Exp. Neurol. Suppl.* **1959,** *1* (4), 322-333.

16. Angevine Jr, J. B., Time of neuron origin in the hippocampal region: An autoradiographic study in the mouse. *Exp. Neurol. Suppl.* **1965,** *11*, 1-39.

17. Schlessinger, A. R.; Cowan, W.; Gottlieb, D., An autoradiographic study of the time of origin and the pattern of granule cell migration in the dentate gyrus of the rat. *J. Comp. Neurol.* **1975,** *159* (2), 149-175.

18. Altman, J.; Bayer, S. A., Mosaic organization of the hippocampal neuroepithelium and the multiple germinal sources of dentate granule cells. *J. Comp. Neurol.* **1990,** *301* (3), 325-342.

19. Taupin, P., BrdU immunohistochemistry for studying adult neurogenesis: paradigms, pitfalls, limitations, and validation. *Brain ReS. Rev.* **2007,** *53* (1), 198-214.

20. Gratzner, H. G., Monoclonal antibody to 5-bromo-and 5-iododeoxyuridine: a new reagent for detection of DNA replication. *Science* **1982,** *218* (4571), 474-475.

21. Freese, A.; O'Rourke, D.; Judy, K.; O'Connor, M. J., The application of 5-bromodeoxyuridine in the management of CNS tumors. *J. Neurooncol.* **1994,** *20* (1), 81-95.

22. Begg, A.; Hofland, I.; Van Der Pavert, I.; Van Der Schueren, B.; Haustermans, K., Use of thymidine analogues to indicate vascular perfusion in tumours. *Brit. J. Cancer* **2000,** *83* (7), 899-905.

23. Neef, A. B.; Samain, F.; Luedtke, N. W., Metabolic labeling of DNA by purine analogues in vivo. *ChemBioChem* **2012,** *13* (12), 1750-1753.

24. Best, M. D., Click chemistry and bioorthogonal reactions: unprecedented selectivity in the labeling of biological molecules. *Biochemistry* **2009,** *48* (28), 6571-6584.

25. Sletten, E. M.; Bertozzi, C. R., Bioorthogonal chemistry: fishing for selectivity in a sea of functionality. *Angew. Chem. Int. Ed.* **2009,** *48* (38), 6974-6998.

26. Wang, Q.; Chan, T. R.; Hilgraf, R.; Fokin, V. V.; Sharpless, K. B.; Finn, M., Bioconjugation by copper (I)-catalyzed azide-alkyne [3+ 2] cycloaddition. *J. Am. Chem. Soc.* **2003,** *125* (11), 3192-3193.

27. Saxon, E.; Bertozzi, C. R., Cell surface engineering by a modified Staudinger reaction. *Science* **2000,** *287* (5460), 2007-2010.

28. Baskin, J. M.; Prescher, J. A.; Laughlin, S. T.; Agard, N. J.; Chang, P. V.; Miller, I. A.; Lo, A.; Codelli, J. A.; Bertozzi, C. R., Copper-free click chemistry for dynamic in vivo imaging. *P. Natl. Acad. Sci.* **2007,** *104* (43), 16793-16797.

29. Ngo, J. T.; Champion, J. A.; Mahdavi, A.; Tanrikulu, I. C.; Beatty, K. E.; Connor, R. E.; Yoo, T. H.; Dieterich, D. C.; Schuman, E. M.; Tirrell, D. A., Cell-selective metabolic labeling of proteins. *Nat. Chem. Biol.* **2009,** *5* (10), 715.

30. Jao, C. Y.; Salic, A., Exploring RNA transcription and turnover in vivo by using click chemistry. *P. Natl. Acad. Sci.* **2008,** *105* (41), 15779-15784.

31. Neef, A. B.; Schultz, C., Selective fluorescence labeling of lipids in living cells. *Angew. Chem. Int. Ed.* **2009,** *48* (8), 1498-1500.

32. Ning, X.; Guo, J.; Wolfert, M. A.; Boons, G. J., Visualizing Metabolically Labeled Glycoconjugates of Living Cells by Copper-Free and Fast Huisgen Cycloadditions. *Angew. Chem., Int. Ed.* **2008,** *47* (12), 2253-2255.

33. Kolb, H. C.; Finn, M. G.; Sharpless, K. B., Click chemistry: diverse chemical function from a few good reactions. *Angew. Chem. Int. Ed.* **2001,** *40* (11), 2004-2021.

34. Rostovtsev, V. V.; Green, L. G.; Fokin, V. V.; Sharpless, K. B., A stepwise huisgen cycloaddition process: copper (I)- catalyzed regioselective "ligation" of azides and terminal alkynes. *Angew. Chem. Int. Ed.* **2002,** *114* (14), 2708-2711.

35. Seela, F.; Sirivolu, V., DNA containing side chains with terminal triple bonds: Base-pair stability and functionalization of alkynylated pyrimidines and 7-deazapurines. *Chem. Biodivers.* **2006,** *3* (5), 509-514.

36. Burley, G.; Gierlich, J.; Mofid, M.; Nir, H.; Tal, S.; Eichen, Y.; Carell, T., Directed DNA metallization. *J. Am. Chem. Soc.* **2006,** *128* (5), 1398-1399.

37. Kolb, H.; Finn, M.; Sharpless, K., Click chemistry: diverse chemical function from a few good reactions. *Angew. Chem. Int. Ed.* **2001,** *40* (11), 2004-2021.

38. Tornøe, C. W.; Christensen, C.; Meldal, M., Peptidotriazoles on solid phase:[1, 2, 3]-triazoles by regiospecific copper (I)-catalyzed 1, 3-dipolar cycloadditions of terminal alkynes to azides. *J. Org. Chem.* **2002,** *67*, 3057-3064.

39. John, C. J.; Carolyn, R. B., Cu-free click cycloaddition reactions in chemical biology. *Chem. Soc. Rev.* **2010,** *39*, 1272-1279.

40. Selvaraj, R.; Fox, J. M., trans-Cyclooctene--a stable, voracious dienophile for bioorthogonal labeling. *Curr. Opi. Chem. Bio.* **2013,** *17* (5), 753-760.

41. Juliane, S.; Manfred, W.; Andres, J. s., Post-synthetic modification of DNA by inverse-electron-demand Diels−Alder reaction. *J. Am. Chem. Soc.* **2010,** *132*, 8846-8847.

42. Kennedy, D. C.; McKay, C. S.; Legault, M. C. B.; Danielson, D. C.; Blake, J. A.; Pegoraro, A. F.; Stolow, A.; Mester, Z.; Pezacki, J. P., Cellular consequences of copper complexes used to catalyze bioorthogonal click reactions. *J. Am. Chem. Soc.* **2011,** *133* (44), 17993-18001.

43. Varizhuk, A. M.; Kaluzhny, D. N.; Novikov, R. A.; Chizhov, A. O.; Smirnov, I. P.; Chuvilin, A. N.; Tatarinova, O. N.; Fisunov, G. Y.; Pozmogova, G. E.; Florentiev, V. L., Synthesis of triazole-linked oligonucleotides with high affinity to DNA complements and an analysis of their compatibility with biosystems. *J. Org. Chem.* **2013,** *78* (12), 5964-5969.

44. Pujari, S. S.; Ingale, S. A.; Seela, F., High-density functionalization and cross-linking of DNA: “click” and “bis-click” cycloadditions performed on alkynylated oligonucleotides with fluorogenic anthracene azides. *Bioconjugate Chem.* **2014,** *25* (10), 1855-1870.

45. Arndt, S.; Wagenknecht, H.-A., “Photoclick” postsynthetic modification of DNA. *Angew. Chem. Int. Ed* **2014,** *Early View*.

46. Neef, A. B.; Luedtke, N. W., An azide-modified nucleoside for metabolic labeling of DNA. *ChemBioChem* **2014,** *15*, 789-793.

47. Bußkamp, H.; Ellen, B.; Niederwieser, A.; Abdel-Rahman, O. S.; Winter, R. F.; Wittmann, V.; Marx, A., Efficient labelling of enzymatically synthesized vinyl-modified DNA by an inverse-electron-demand Diels–Alder reaction. *Chem. Commun.* **2014,** *50*, 10827-10829.

48. Stubinitzky, C.; Cserép, G. B.; Bätzner, E.; Kele, P.; Wagenknecht, H.-A., 2′-Deoxyuridine conjugated with a reactive monobenzocyclooctyne as a DNA building block for copper-free click-type postsynthetic modification of DNA. *Chem. Commun.* **2014,** *50*, 11218-11221.

49. Pyka, A. M.; Domnick, C.; Braun, F., Diels–Alder cycloadditions on synthetic RNA in mammalian cells. *Bioconjugate Chem.* **2014,** *25*, 1438-1443.

50. Rieder, U.; Luedtke, N. W., Alkene-tetrazine ligation for imaging cellular DNA. *Angew. Chem. Int. Ed* **2014,** *126* (35), 9322-9326.

51. Ötvös, L.; Sági, J.; Kovács, T.; Walker, R. T., Substrate specificity of DNA polymerases I. Enzyme-catalysed incorporation of 5-(1-alkenyl)-2′-deoxyuridines into DNA. *Nucleic Acids Res.* **1987,** *15* (4), 1763-1777.

52. Kovács, T.; Ötvös, L., Simple synthesis of 5-vinyl-and5-ethynyl-2′-deoxyuridine-5′-triphosphates. *Tetrahedron Lett.* **1988,** *29* (36), 4525-4528.

53. Gramlich, P. M.; Wirges, C. T.; Manetto, A.; Carell, T., Postsynthetic DNA modification through the copper-catalyzed azide-alkyne cycloaddition reaction. *Angew. Chem. Int. Ed.* **2008,** *47* (44), 8350-8358.

54. Lallana, E.; Riguera, R.; Fernandez-Megia, E., Reliable and efficient procedures for the conjugation of biomolecules through Huisgen azide-alkyne cycloadditions. *Angew. Chem. Int. Ed.* **2011,** *50* (38), 8794-8804.

55. van Delft, P.; Meeuwenoord, N. J.; Hoogendoorn, S.; Dinkelaar, J.; Overkleeft, H. S.; van der Marel, G. A.; Filippov, D. V., Synthesis of oligoribonucleic acid conjugates using a cyclooctyne phosphoramidite. *Org. Lett.* **2010,** *12* (23), 5486-5489.

56. Jayaprakash, K. N.; Peng, C. G.; Butler, D.; Varghese, J. P.; Maier, M. A.; Rajeev, K. G.; Manoharan, M., Non-nucleoside building blocks for copper-assisted and copper-free click chemistry for the efficient synthesis of RNA conjugates. *Org. Lett.* **2010,** *12* (23), 5410-5413.

57. Shelbourne, M.; Chen, X.; Brown, T.; El-Sagheer, A. H., Fast copper-free click DNA ligation by the ring-strain promoted alkyne-azide cycloaddition reaction. *Chem. Commun.* **2011,** *47* (22), 6257-6259.

58. Shelbourne, M.; Brown, T.; El-Sagheer, A. H.; Brown, T., Fast and efficient DNA crosslinking and multiple orthogonal labelling by copper-free click chemistry. *Chem. Commun.* **2012,** *48* (91), 11184-11186.

59. Ren, X.; Gerowska, M.; El-Sagheer, A. H.; Brown, T., Enzymatic incorporation and fluorescent labelling of cyclooctyne-modified deoxyuridine triphosphates in DNA. *Bioorg. Med. Chem.* **2014,** *22* (16), 4384-4390.

60. Jäger, S.; Rasched, G.; Kornreich-Leshem, H.; Engeser, M.; Thum, O.; Famulok, M., A versatile toolbox for variable DNA functionalization at high density. *J. Am. Chem. Soc.* **2005,** *127* (43), 15071-15082.

61. Kool, E. T., Replacing the nucleohases in DNA with designer molecules. *Acc. Chem. Res.* **2002,** *35* (11), 936-943.

62. Wilson, J. N.; Kool, E. T., Fluorescent DNA base replacements: reporters and sensors for biological systems. *Org. Biomol. Chem.* **2006,** *4* (23), 4265-4274.

63. Greco, N. J.; Tor, Y., Simple fluorescent pyrimidine analogues detect the presence of DNA abasic sites. *J. Am. Chem. Soc.* **2005,** *127* (31), 10784-10785.

64. Nadler, A.; Strohmeier, J.; Diederichsen, U., 8-Vinyl-2′-deoxyguanosine as a fluorescent 2′-deoxyguanosine mimic for investigating DNA hybridization and topology. *Angew. Chem. Int. Ed.* **2011,** *50* (23), 5392-5396.

65. Müllar, S.; Strohmeier, J.; Diederichsen, U., 8-Vinylguanine nucleo amino acid: a fluorescent PNA building block. *Org. Lett.* **2012,** *14* (6), 1382-1385.

66. Holzberger, B.; Strohmeier, J.; Siegmund, V.; Diederichsen, U.; Marx, A., Enzymatic synthesis of 8-vinyl- and 8-styryl-2'-deoxyguanosine modified DNA--novel fluorescent molecular probes. *Bioorg. Med. Chem. Lett.* **2012,** *22* (9), 3136-3139.

67. Ogasawara, S.; Saito, I.; Maeda, M., Synthesis and reversible photoisomerization of photoswitchable nucleoside, 8-styryl-2′-deoxyguanosine. *Tetrahedron Lett.* **2008,** *49* (15), 2479-2482.

68. Bußkamp, H.; Batroff, E.; Niederwieser, A.; Abdel-Rahman, O. S.; Winter, R. F.; Wittmann, V.; Marx, A., Efficient labelling of enzymatically synthesized vinyl-modified DNA by an inverse-electron-demand Diels–Alder reaction. *Chem. Commun.* **2014,** *50* (74), 10827-10829.

69. Seela, F.; Zulauf, M.; Sauer, M.; Deimel, M., 7-Substituted 7-deaza-2′-deoxyadenosines and 8-aza-7-deaza-2′-deoxyadenosines: fluorescence of DNA-base analogues induced by the 7-alkynyl side chain. *Helv. Chim. Acta* **2000,** *83* (5), 910-927.

70. Riedl, J.; Pohl, R.; Ernsting, N. P.; Orsag, P.; Fojta, M.; Hocek, M., Labelling of nucleosides and oligonucleotides by solvatochromic 4-aminophthalimide fluorophore for studying DNA-protein interactions. *Chem. Sci.* **2012,** *3* (9), 2797-2806.

71. Riedl, J.; Ménová, P.; Pohl, R.; Orság, P.; Fojta, M.; Hocek, M., GFP-like fluorophores as DNA labels for studying DNA-protein interactions. *J. Org. Chem.* **2012,** *77* (18), 8287-8293.

72. Ormo, M.; Cubitt, A. B.; Kallio, K.; Gross, L. A.; Tsien, R. Y.; Remington, S. J., Crystal structure of the Aequorea victoria green fluorescent protein. *Science* **1996,** *273* (5280), 1392-1395.

73. Reid, B. G.; Flynn, G. C., Chromophore formation in green fluorescent protein. *Biochemistry* **1997,** *36* (22), 6786-91.

74. Niwa, H.; Inouye, S.; Hirano, T.; Matsuno, T.; Kojima, S.; Kubota, M.; Ohashi, M.; Tsuji, F. I., Chemical nature of the light emitter of the Aequorea green fluorescent protein. *P. Natl. Acad. Sci.* **1996,** *93* (24), 13617-22.

75. Paige, J. S.; Wu, K. Y.; Jaffrey, S. R., RNA mimics of green fluorescent protein. *Science* **2011,** *333* (6042), 642-646.

76. Brown, J. A.; Suo, Z., Unlocking the sugar "steric gate" of DNA polymerases. *Biochemistry* **2011,** *50* (7), 1135-1142.

77. Berndl, S.; Herzig, N.; Kele, P.; Lachmann, D.; Li, X.; Wolfbeis, O. S.; Wagenknecht, H.-A., Comparison of a nucleosidic vs non-nucleosidic postsynthetic “click” modification of DNA with base-labile fluorescent probes. *Bioconjugate Chem.* **2009,** *20* (3), 558-564.

78. Wenge, U.; Ehrenschwender, T.; Wagenknecht, H.-A., Synthesis of 2′-O-propargyl nucleoside triphosphates for enzymatic oligonucleotide preparation and “click” modification of DNA with nile red as fluorescent porobe. *Bioconjugate Chem.* **2013,** *24* (3), 301-304.

79. Krishna, H.; Caruthers, M. H., Alkynyl phosphonate DNA: a versatile “click”able backbone for DNA-based biological applications. *J. Am. Chem. Soc.* **2012,** *134* (28), 11618-11631.

80. Paul, S.; Roy, S.; Monfregola, L.; Shang, S.; Shoemaker, R.; Caruthers, M. H., Oxidative substitution of boranephosphonate diesters as a route to post-synthetically modified DNA. *J. Am. Chem. Soc.* **2015,** *137* (9), 3253-3264.

81. Stubinitzky, C.; Cserép, G. B.; Bätzner, E.; Kele, P.; Wagenknecht, H.-A., 2′-Deoxyuridine conjugated with a reactive monobenzocyclooctyne as a DNA building block for copper-free click-type postsynthetic modification of DNA. *Chem. Commun.* **2014,** *50* (76), 11218-11221.

82. Arndt, S.; Wagenknecht, H.-A., "Photoclick" postsynthetic modification of DNA. *Angew. Chem. Int. Ed.* **2014,** *53* (52), 14580-14582.

83. Tuerk, C.; Gold, L., Systematic evolution of ligands by exponential enrichment: RNA ligands to bacteriophage T4 DNA polymerase. *Science* **1990,** *249* (4968), 505-10.

84. Ellington, A. D.; Szostak, J. W., In vitro selection of RNA molecules that bind specific ligands. *Nature* **1990,** *346* (6287), 818-22.

85. Bruno, J., A review of therapeutic aptamer conjugates with emphasis on new approaches. *Pharmaceuticals* **2013,** *6* (3), 340-357.

86. Germer, K.; Leonard, M.; Zhang, X., RNA aptamers and their therapeutic and diagnostic applications. *Int. J. Biochem. Mol. Biol.* **2013,** *4* (1), 27-40.

87. Hong, P.; Li, W.; Li, J., Applications of aptasensors in clinical diagnostics. *Sensors (Basel)* **2012,** *12* (2), 1181-1193.

88. Morris, K. N.; Jensen, K. B.; Julin, C. M.; Weil, M.; Gold, L., High affinity ligands from in vitro selection: Complex targets. *Proc Natl Acad Sci U S A* **1998,** *95* (6), 2902-2907.

89. Blank, M.; Weinschenk, T.; Priemer, M.; Schluesener, H., Systematic evolution of a DNA aptamer binding to rat brain tumor microvessels: selective targeting of endorhelial regulatory protein pigpen. *J. Biol. Chem.* **2001,** *276* (19), 16464-16468.

90. Wang, C.; Zhang, M.; Yang, G.; Zhang, D.; Ding, H.; Wang, H.; Fan, M.; Shen, B.; Shao, N., Single-stranded DNA aptamers that bind differentiated but not parental cells: subtractive systematic evolution of ligands by exponential enrichment. *J. Biotech.* **2003,** *102* (1), 15-22.

91. Shangguan, D.; Li, Y.; Tang, Z.; Cao, Z. C.; Chen, H. W.; Mallikaratchy, P.; Sefah, K.; Yang, C. J.; Tan, W., Aptamers evolved from live cells as effective molecular probes for cancer study. *Proc Natl Acad Sci U S A* **2006,** *103* (32), 11838-43.

92. Subramanian, N.; Sreemanthula, J. B.; Balaji, B.; Kanwar, J. R.; Biswas, J.; Krishnakumar, S., A strain-promoted alkyne–azide cycloaddition (SPAAC) reaction of a novel EpCAM aptamer–fluorescent conjugate for imaging of cancer cells. *Chem. Commun.* **2014,** *50*, 11810-11813.

93. Song, Y.; Zhu, Z.; An, Y.; Zhang, W.; Zhang, H.; Liu, D.; Yu, C.; Duan, W.; Yang, C. J., Selection of DNA aptamers against epithelial cell adhesion molecule for cancer cell imaging and circulating tumor cell capture. *Anal. Chem.* **2013,** *85* (8), 4141-4149.

94. Yoon, J.; Czarnik, A. W., Fluorescent Chemosensors of Carbohydrates. A Means of Chemically Communicating the Binding of Polyols in Water Based on Chelation-Enhanced Quenching. *J. Am. Chem. Soc.* **1992,** *114*, 5874-5875.

95. James, T. D.; Sandanayake, K. R. A. S.; Iguchi, R.; Shinkai, S., Novel saccharide-photoinduced electron transfer sensors based on the interaction of boronic acid and amine. *J. Am. Chem. Soc.* **1995,** *117* (35), 8982-8987.

96. Asher, S. A.; Alexeev, V. L.; Goponenko, A. V.; Sharma, A. C.; Lednev, I. K.; Wilcox, C. S.; Finegold, D. N., Photonic crystal carbohydrate sensors: low ionic strength sugar sensing. *J Am Chem Soc* **2003,** *125* (11), 3322-3329.

97. Jin, S.; Cheng, Y.; Reid, S.; Li, M.; Wang, B., Carbohydrate recognition by boronolectins, small molecules, and lectins. *Med. Res. Rev.* **2010,** *30* (2), 171-257.

98. Yan, J.; Fang, H.; Wang, B., Boronolectins and Fluorescent Boronolectins-An Examination of the Detailed Chemistry Issues Important for their Design. *Med. Res. Rev.* **2005,** *25*, 490-520.

99. Striegler, S., Selective carbohydrate recognition by synthetic receptors in aqueous solution. *Curr. Org. Chem.* **2003,** *7* (1), 81-102.

100. James, T. D.; Shinkai, S., Artificial Receptors as Chemosensors for Carbohydrates. *Top. Curr. Chem.* **2002,** *218*, 159-200.

101. Springsteen, G.; Wang, B., A detailed examination of boronic acid–diol complexation. *Tetrahedron* **2002,** *58* (26), 5291-5300.

102. Gamsey, S.; Miller, A.; Olmstead, M. M.; Beavers, C. M.; Hirayama, L. C.; Pradhan, S.; Wessling, R. A.; Singaram, B., Boronic acid-based bipyridinium salts as tunable receptors for monosaccharides and α-hydroxycarboxylates. *J. Am. Chem. Soc.* **2007,** *129* (5), 1278-1286.

103. Wang, Z.; Zhang, D.; Zhu, D., A new saccharide sensor based on a tetrathiafulvalene−anthracene dyad with a boronic acid group. *J. Org. Chem.* **2005,** *70* (14), 5729-5732.

104. Mohler, L. K.; Czarnik, A. W., .alpha.-Amino acid chelative complexation by an arylboronic acid. *J. Am. Chem. Soc.* **1993,** *115* (15), 7037-7038.

105. Aharoni, R.; Bronstheyn, M.; Jabbour, A.; Zaks, B.; Srebnik, M.; Steinberg, D., Oxazaborolidine derivatives inducing autoinducer-2 signal transduction in Vibrio harveyi. *Bioorg. Med. Chem.* **2008,** *16* (4), 1596-1604.

106. Jabbour, A.; Steinberg, D.; Dembitsky, V. M.; Moussaieff, A.; Zaks, B.; Srebnik, M., Synthesis and evaluation of oxazaborolidines for antibacterial activity against streptococcus mutans. *J. Med. Chem.* **2004,** *47* (10), 2409-2410.

107. Farr-Jones, S.; Smith, S. O.; Kettner, C. A.; Griffin, R. G.; Bachovchin, W. W., Crystal versus solution structure of enzymes: NMR spectroscopy of a peptide boronic acid-serine protease complex in the crystalline state. *Proc Natl Acad Sci U S A* **1989,** *86* (18), 6922-4.

108. Snow, R. J.; Bachovchin, W. W.; Barton, R. W.; Campbell, S. J.; Coutts, S. J.; Freeman, D. M.; Gutheil, W. G.; Kelly, T. A.; Kennedy, C. A., Studies on proline boronic acid dipeptide inhibitors of dipeptidyl peptidase IV: identification of a cyclic species containing a B-N bond. *J. Am. Chem. Soc.* **1994,** *116* (24), 10860-10869.

109. Dowlut, M.; Hall, D. G., An improved class of sugar-binding boronic acids, soluble and capable of complexing glycosides in neutral water. *J. Am. Chem. Soc.* **2006,** *128* (13), 4226-4227.

110. Badugu, R.; Lakowicz, J. R.; Geddes, C. D., Excitation and emission wavelength ratiometric cyanide-sensitive probes for physiological sensing. *Anal Biochem* **2004,** *327* (1), 82-90.

111. Badugu, R.; Lakowicz, J. R.; Geddes, C. D., Cyanide-sensitive fluorescent probes. *Dyes and Pigments* **2005,** *64* (1), 49-55.

112. R. Cooper, C.; Spencer, N.; D. James, T., Selective fluorescence detection of fluoride using boronic acids. *Chem. Commun.* **1998,** (13), 1365-1366.

113. DiCesare, N.; Lakowicz, J. R., New sensitive and selective fluorescent probes for fluoride using boronic acids. *Anal. Biochem.* **2002,** *301* (1), 111-116.

114. Yoon, J.; Czarnik, A. W., Fluorescent chemosensors of carbohydrates. A means of chemically communicating the binding of polyols in water based on chelation-enhanced quenching. *J. Am. Chem. Soc.* **1992,** *114* (14), 5874-5875.

115. Kondo, K.; Shiomi, Y.; Saisho, M.; Harada, T.; Shinkai, S., Specific Complexation of Disaccharides with Diphenyl-3,3'-diboronic Acid that Can Be Detected by Circular Dichroism. *Tetrahedron* **1992,** *48*, 8239-8252.

116. Eggert, H.; Frederiksen, J.; Morin, C.; Norrild, J. C., A new glucose-selective fluorescent bisboronic acid. first report of strong α-furanose complexation in aqueous solution at physiological pH. *J. Org. Chem.* **1999,** *64* (11), 3846-3852.

117. James, T. D.; Sandanayake, K. R. A. S.; Shinkai, S., Saccharide sensing with molecular receptors based on boronic acid. *Angew. Chem. Int. Ed.* **1996,** *35* (17), 1910-1922.

118. Wang, W.; Gao, S.; Wang, B., Building fluorescent sensors by template polymerization: the preparation of a fluorescent sensor for d-fructose. *Org. Lett.* **1999,** *1* (8), 1209-1212.

119. Gao, X.; Zhang, Y.; Wang, B., New boronic acid fluorescent reporter compounds. 2. a naphthalene-based on−off sensor functional at physiological pH. *Org. Lett.* **2003,** *5* (24), 4615-4618.

120. Fang, H.; Kaur, G.; Wang, B., Progress in boronic acid-based fluorescent glucose sensors. *J. Fluorescence* **2004,** *14* (5), 481-489.

121. Westmark, P. R.; Gardiner, S. J.; Smith, B. D., Selective monosaccharide transport through lipid bilayers using boronic acid carriers. *J. Am. Chem. Soc.* **1996,** *118* (45), 11093-11100.

122. Draffin, S. P.; Duggan, P. J.; Duggan, S. A. M., Highly fructose selective transport promoted by boronic acids based on a pentaerythritol core. *Org. Lett.* **2001,** *3* (6), 917-920.

123. Gardiner, S. J.; Smith, B. D.; Duggan, P. J.; Karpa, M. J.; Griffin, G. J., Selective fructose transport through supported liquid membranes containing diboronic acid or conjugated monoboronic acid-quaternary ammonium carriers. *Tetrahedron* **1999,** *55* (10), 2857-2864.

124. Karpa, M. J.; Duggan, P. J.; Griffin, G. J.; Freudigmann, S. J., Competitive transport of reducing sugars through a lipophilic membrane facilitated by aryl boron acids. *Tetrahedron* **1997,** *53* (10), 3669-3678.

125. Mohler, L. K.; Czarnik, A. W., Ribonucleoside membrane transport by a new class of synthetic carrier. *J. Am. Chem. Soc.* **1993,** *115* (7), 2998-2999.

126. Riggs, J. A.; Hossler, K. A.; Smith, B. D.; Karpa, M. J.; Griffin, G.; Duggan, P. J., Nucleotide carrier mixture with transport selectivity for ribonucleoside-5′-phosphates. *Tetrahedron Lett.* **1996,** *37* (35), 6303-6306.

127. Paugam, M.-F.; Bien, J. T.; Smith, B. D.; Chrisstoffels, L. A. J.; de Jong, F.; Reinhoudt, D. N., Facilitated catecholamine transport through bulk and polymer-supported liquid membranes. *J. Am. Chem. Soc.* **1996,** *118* (41), 9820-9825.

128. Liu, X.-C.; Hubbard, J. L.; Scouten, W. H., Synthesis and structural investigation of two potential boronate affinity chromatography ligands catechol [2-(diisopropylamino)carbonyl]phenylboronate and catechol [2-(diethylamino)carbonyl, 4-methyl]phenylboronate. *J. Organomet. Chem.* **1995,** *493* (1–2), 91-94.

129. Adamek, V.; Liu, X.-C.; Zhang, Y. A.; Adamkova, K.; Scouten, W. H., New aliphatic boronate ligands for affinity chromatography. *J. Chromatogr. A* **1992,** *625* (2), 91-99.

130. Westmark, P. R.; Valencia, L. S.; Smith, B. D., Influence of eluent anions in boronate affinity chromatography. *J. Chromatogr. A* **1994,** *664* (1), 123-128.

131. Springsteen, G.; Wang, B., Alizarin Red S. as a general optical reporter for studying the binding of boronic acids with carbohydrates. *Chem. Commun.* **2001**, 1608-1609.

132. Cheng, Y.; Ni, N.; Yang, W.; Wang, B., A new class of fluorescent boronic acids that have extraordinarily high affinities for diols in aqueous solution at physiological pH. *Chem. Eur. J.* **2010,** *16* (45), 13528-13538.

133. Akay, S.; Yang, W. Q.; Wang, J. F.; Lin, L.; Wang, B. H., Synthesis and evaluation of dual wavelength fluorescent benzo[b]thiophene boronic acid derivatives for sugar sensing. *Chemical Biology & Drug Design* **2007,** *70* (4), 279-289.

134. Han, F.; Chi, L. N.; Liang, X. F.; Ji, S. M.; Liu, S. S.; Zhou, F. K.; Wu, Y. B.; Han, K. L.; Zhao, J. Z.; James, T. D., 3,6-Disubstituted Carbazole-Based Bisboronic Acids with Unusual Fluorescence Transduction as Enantioselective Fluorescent Chemosensors for Tartaric Acid. *J. Org. Chem.* **2009,** *74* (3), 1333-1336.

135. Jin, S.; Wang, J. F.; Li, M. Y.; Wang, B. H., Synthesis, Evaluation, and Computational Studies of Naphthalimide-based Long-wavelength Fluorescent Boronic Acid Reporters. *Chem. Eur. J.* **2008,** *14* (9), 2795-2804.

136. Jin, S.; Zhu, C. Y.; Li, M. Y.; Wang, B. H., Identification of the First Fluorescent alpha-Amidoboronic Acids that Change Fluorescent Properties upon Sugar Binding. *Bioorg. Med. Chem. Lett.* **2009,** *19* (6), 1596-1599.

137. Wang, J. F.; Jin, S.; Akay, S.; Wang, B. H., Design and synthesis of long-wavelength fluorescent boronic acid reporter compounds. *European Journal of Organic Chemistry* **2007,** (13), 2091-2099.

138. Springsteen, G.; Wang, B., A detailed examination of boronic acid–diol complexation. *Tetrahedron* **2002,** *58*, 5291-5300.

139. Lin, N.; Yan, J.; Huang, Z.; Altier, C.; Li, M.; Carrasco, N.; Suyemoto, M.; Johnston, L.; Wang, S.; Wang, Q.; Fang, H.; Caton-Williams, J.; Wang, B., Design and synthesis of boronic-acid-labeled thymidine triphosphate for incorporation into DNA. *Nucleic Acids Res.* **2006,** *35* (4), 1222-1229.

140. Li, M.; Lin, N.; Huang, Z.; Du, L.; Altier, C.; Fang, H.; Wang, B., Selecting aptamers for a glycoprotein through the incorporation of the boronic acid moiety. *J. Am. Chem. Soc.* **2008,** *130* (38), 12636-12638.

141. Yang, X.; Dai, C.; Molina, A. D. C.; Wang, B., Boronic acid-modified DNA that changes fluorescent properties upon carbohydrate binding. *Chem. Commun.* **2010,** *46*, 1073-1075.

142. Dai, C.; Wang, L.; Sheng, J.; Peng, H.; Draganov, A.; Huang, Z.; Wang, B., The first chemical synthesis of boronic acid-modified DNA through a copper-free click reaction. *Chem. Commun.* **2011,** *47* (12), 3598-3600.

143. Cheng, Y.; Dai, C.; Peng, H.; Zheng, S.; Jin, S.; Wang, B., Design, synthesis, and polymerase catalyzed incorporation of Click modified boronic acid–TTP analogues. *Chem. Asian. J.* **2011,** *6* (10), 2747-2752.

144. Cheng, Y.; Peng, H.; Chen, W.; Ni, N.; Ke, B.; Dai, C.; Wang, B., Rapid and specific post-synthesis modification of DNA through a biocompatible condensation of 1,2-aminothiols with 2-cyanobenzothiazole. *Chem. Eur. J.* **2013,** *19* (12), 4036-4042.

145. Blackman, M.; Royzen, M.; Fox, J., Tetrazine ligation: fast bioconjugation based on inverse-electron-demand Diels-Alder reactivity. *J. Am. Chem. Soc.* **2008,** *130* (41), 13518-13519.

146. Taylor, M. T.; Blackman, M. L.; Dmitrenko, O.; Fox, J. M., Design and synthesis of highly reactive dienophiles for the tetrazine–*trans*-cyclooctene Ligation. *J. Am. Chem. Soc.* **2011,** *133*, 9646-9649.

147. Chen, W.; Wang, D.; Dai, C.; Hamelberg, D.; Wang, B., Clicking 1, 2, 4, 5-tetrazine and cyclooctynes with tunable reaction rates. *Chem. Commun.* **2012,** *48*, 1736-1738.

148. Kufe, D. W., Mucins in cancer: function, prognosis and therapy. *Nat. Rev. Cancer* **2009,** *9* (12), 874-885.

149. Maher, D. M.; Gupta, B. K.; Nagata, S.; Jaggi, M.; Chauhan, S. C., Mucin 13: structure, function, and potential roles in cancer pathogenesis. *Mol. Cancer Res.* **2011,** *9* (5), 531-7.

150. Chauhan, S. C.; Ebeling, M. C.; Maher, D. M.; Koch, M. D.; Watanabe, A.; Aburatani, H.; Lio, Y.; Jaggi, M., MUC13 mucin augments pancreatic tumorigenesis. *Mol. Cancer Ther.* **2012,** *11* (1), 24-33.

151. Royzen, M.; Yap, G. P.; Fox, J. M., A photochemical synthesis of functionalized trans-cyclooctenes driven by metal complexation. *J. Am. Chem. Soc.* **2008,** *130* (12), 3760-3761.

152. Marika, K.; Mia, H.; Pasi, V.; Harri, L. n., Synthesis of oligonucleotide glycoconjugates using sequential click and oximation ligations. *Bioconjugate Chem.* **2010,** *21* (4), 748-755.

153. Kuwahara, M.; Nagashima, J.-i.; Hasegawa, M.; Tamura, T.; Kitagata, R.; Hanawa, K.; Hososhima, S.-i.; Kasamatsu, T.; Ozaki, H.; Sawai, H., Systematic characterization of 2'-deoxynucleoside- 5'-triphosphate analogs as substrates for DNA polymerases by polymerase chain reaction and kinetic studies on enzymatic production of modified DNA. *Nucleic Acids Res.* **2005,** *34* (19), 5383-5394.

154. Henry, G. K., Electrophilic displacement reactions. III. kinetics of the reaction between hydrogen peroxide and benzeneboronic acid 1. *J. Am. Chem. Soc.* **1954,** *76*, 870-874.

155. Ji, K.; Lim, W. S.; Li, S. F. Y.; Bhakoo, K., … cell-SELEX method to generate a DNA aptamer to recognize inflamed human aortic endothelial cells as a potential in vivo molecular probe for atherosclerosis plaque …. *Anal. Bioanal. Chem.* **2013,** *405* (21), 6853-6861.

156. Ji, K.; de Carvalho, L. P.; Bi, X.; Seneviratnankn, A.; Bhakoo, K.; Chan, M.; Li, S. F. Y., Highly sensitive and quantitative human thrombospondin-1 detection by an M55 aptasensor and clinical validation in patients with atherosclerotic disease. *Biosens. Bioelectron.* **2014,** *55*, 405-411.

157. Kang, J.; Kim, M.; Chang, S.; Sim, S.; Jo, Y., CCAAT box is required for the induction of human thrombospondin 1 gene by trichostatin A. *J. Cell. Biochem.* **2008,** *104* (4), 1192-1203.

158. Wang, K.; Wang, D.; Ji, K.; Chen, W.; Zheng, Y.; Dai, C.; Wang, B., Post-synthesis DNA modifications using a trans-cyclooctene click handle. *Org. Biomol. Chem.* **2015,** *13* (3), 909-915.

159. Patel, D. J.; Suri, A. K.; Jiang, F.; Jiang, L.; Fan, P.; Kumar, R. A.; Nonin, S., Structure, recognition and adaptive binding in RNA aptamer complexes1. *J. Mol. Biol.* **1997,** *272* (5), 645-664.

160. Rodesch, M. J.; Ozers*, M. S.; Warren, C. L., Macromolecular Interactions: Aptamers. In *eLS*, John Wiley & Sons, Ltd: 2001.

161. Sefah, K.; Shangguan, D.; Xiong, X.; O'Donoghue, M. B.; Tan, W., Development of DNA aptamers using Cell-SELEX. *Nat. Protoc.* **2010,** *5* (6), 1169-1185.

162. Avci-Adali, M.; Paul, A.; Wilhelm, N.; Ziemer, G.; Wendel, H. P., Upgrading SELEX technology by using lambda exonuclease digestion for single-stranded DNA generation. *Molecules* **2009,** *15* (1), 1.

163. Gyllensten, U. B.; Erlich, H. A., Generation of single-stranded DNA by the polymerase chain reaction and its application to direct sequencing of the HLA-DQA locus. *Proc Natl Acad Sci U S A* **1988,** *85* (20), 7652-7656.

164. Paul, A.; Avci-Adali, M.; Ziemer, G.; Wendel, H. P., Streptavidin-coated magnetic beads for DNA strand separation implicate a multitude of problems during cell-SELEX. *Oligonucleotides* **2009,** *19* (3), 243-54.

165. Ji, K.; Lim, W.; Li, S.; Bhakoo, K., A two-step stimulus-response cell-SELEX method to generate a DNA aptamer to recognize inflamed human aortic endothelial cells as a potential in vivo molecular probe for atherosclerosis plaque detection. *Anal. Bioanal. Chem.* **2013,** *405* (21), 6853-6861.

166. Marimuthu, C.; Tang, T.-H.; Tominaga, J.; Tan, S.-C.; Gopinath, S. C. B., Single-stranded DNA (ssDNA) production in DNA aptamer generation. *Analyst* **2012,** *137* (6), 1307-1315.

167. Deer, E. L.; Gonzalez-Hernandez, J.; Coursen, J. D.; Shea, J. E.; Ngatia, J.; Scaife, C. L.; Firpo, M. A.; Mulvihill, S. J., Phenotype and genotype of pancreatic cancer cell lines. *Pancreas* **2010,** *39* (4), 425-35.

168. Sefah, K.; Bae, K. M.; Phillips, J. A.; Siemann, D. W.; Su, Z.; McClellan, S.; Vieweg, J.; Tan, W., Cell-based selection provides novel molecular probes for cancer stem cells. *Int. J. Cancer* **2013,** *132* (11), 2578-88.

169. Graham, J. C.; Zarbl, H., Use of cell-SELEX to generate DNA aptamers as molecular probes of HPV-associated cervical cancer cells. *PLoS One* **2012,** *7* (4), e36103.

170. Kang, D.; Wang, J.; Zhang, W.; Song, Y.; Li, X.; Zou, Y.; Zhu, M.; Zhu, Z.; Chen, F.; Yang, C. J., Selection of DNA aptamers against glioblastoma cells with high affinity and specificity. *PLoS One* **2012,** *7* (10), e42731.

171. Stellwagen, N. C.; Stellwagen, E., Effect of the matrix on DNA electrophoretic mobility. *J. Chromatogr. A* **2009,** *1216* (10), 1917-1929.

172. Lang, K.; Davis, L.; Wallace, S.; Mahesh, M.; Cox, D. J.; Blackman, M. L.; Fox, J. M.; Chin, J. W., Genetic encoding of bicyclononynes and trans-cyclooctenes for site-specific protein labeling in vitro and in live mammalian cells via rapid fluorogenic Diels–Alder reactions. *J. Am. Chem. Soc.* **2012,** *134* (25), 10317-10320.

173. Nuzzolo, M.; Grabulosa, A.; Slawin, A. M. Z.; Meeuwenoord, N.; Marel, G. A.; Kamer, P., Functionalization of mono- and oligonucleotides with phosphane ligands by amide bond formation. *European Journal of Organic Chemistry* **2010**, 3229-3236.

174. Wang, D.; Chen, W.; Zheng, Y.; Dai, C.; Wang, K.; Ke, B.; Wang, B., 3, 6-Substituted-1, 2, 4, 5-tetrazines: tuning reaction rates for staged labeling applications. *Org. Biomol. Chem.* **2014,** *12*, 3950-3955.

175. Beckmann, H. S. G.; Niederwieser, A.; Wiessler, M.; Wittmann, V., Preparation of carbohydrate arrays by using Diels-Alder reactions with inverse electron demand. *Chem. Eur. J* **2012,** *18* (21), 6548-6554.

176. Smirnov, D.; Dhall, A.; Sivanesam, K.; Sharar, R. J.; Chatterjee, C., Fluorescent probes reveal a minimal ligase recognition motif in the prokaryotic ubiquitin-like protein from mycobacterium tuberculosis. *J. Am. Chem. Soc.* **2013,** *135* (8), 2887-2890.

177. Moncada, S.; Palmer, R. M.; Higgs, E. A., Nitric oxide: physiology, pathophysiology, and pharmacology. *Pharmacol. Rev.* **1991,** *43* (2), 109-42.

178. Verma, A.; Hirsch, D. J.; Glatt, C. E.; Ronnett, G. V.; Snyder, S. H., Carbon monoxide: a putative neural messenger. *Science* **1993,** *259* (5093), 381-4.

179. Chen, X.; Jhee, K. H.; Kruger, W. D., Production of the neuromodulator H2S by cystathionine beta-synthase via the condensation of cysteine and homocysteine. *J Biol Chem* **2004,** *279* (50), 52082-52086.

180. Ishii, I.; Akahoshi, N.; Yu, X.; Kobayashi, Y.; Namekata, K.; Komaki, G.; Kimura, H., Murine cystathionine gamma-lyase: complete cDNA and genomic sequences, promoter activity, tissue distribution and developmental expression. *Biochemical Journal* **2004,** *381*, 113-123.

181. Kamoun, P.; Belardinelli, M.-C.; Chabli, A.; Lallouchi, K.; Chadefaux-Vekemans, B., Endogenous hydrogen sulfide overproduction in down syndrom. *Am. J. Med. Genet.* **2003,** *116A* (3), 310-311.

182. Chen, Y.; Yao, W.; Geng, B.; Ding, Y.; Lu, M.; Zhao, M.; Tang, C., Endogenous hydrogen sulfide in patients with COPD. *Chest* **2005,** *128*, 3205-3211.

183. Lefer, D. J., A new gaseous signaling molecule emerges: Cardioprotective role of hydrogen sulfide. *P. Natl. Acad. Sci. U. S. A.* **2007,** *104* (46), 17907-17908.

184. Kimura, H., Hydrogen sulfide as a neuromodulator. *Mol. Neurobiol.* **2002,** *26* (1), 13-19.

185. Zhang, L.; Sio, S. W. S.; Moochhala, S.; Bhatia, M., Role of Hydrogen Sulfide in Severe Burn Injury-Induced Inflammation in Mice. *Mol. Med.* **2010,** *16* (9-10), 417-424.

186. Li, L.; Bhatia, M.; Zhu, Y. Z.; Zhu, Y. C.; Ramnath, R. D.; Wang, Z.; Anuar, F. B. M.; Whiteman, M.; Salto-Tellez, M.; Moore, P. K., Hydrogen sulfide is a novel mediator of lipopolysaccharide-induced inflammation in the mouse. *FASEB J.* **2005,** *19* (6), 1196-1198.

187. Martelli, A.; Testai, L.; Breschi, M. C.; Blandizzi, C.; Virdis, A.; Teddei, S.; Calderone, V., Hydrogen sulfide: novel oppotunity for drug discovery. *Med. Res. Rev.* **2011**.

188. Vandiver, M. S.; Snyder, S. H., Hydrogen sulfide: a gasotransmitter of clinical relevance. *J. Mol. Med.* **2012,** *90* (3), 255-263.

189. Wei, L.; Dasgupta, P. K., Determination of sulfide and mercaptans in caustic scrubbing liquor. *Anal Chim Acta* **1989,** *226* (1), 165-170.

190. Doeller, J. E.; Isbell, T. S.; Benavides, G.; Koenitzer, J.; Patel, H.; Patel, R. P.; Lancaster, J. R.; Darley-Usmar, V. M.; Kraus, D. W., Polarographic measurement of hydrogen sulfide production and consumption by mammalian tissues. *Anal Biochem* **2005,** *341* (1), 40-51.

191. Schiavon, G.; Zotti, G.; Toniolo, R.; Bontempelli, G., Electrochemical detection of trace hydrogen-sulfide in gaseous samples by porous silver electrodes supported on ion-exchange membranes (solid polymer electrolytes). *Anal Biochem* **1995,** *67* (2), 318-323.

192. Ubuka, T.; Abe, T.; Kajikawa, R.; Morino, K., Determination of hydrogen sulfide and acid-labile sulfur in animal tissues by gas chromatography and ion chromatography. *J Chromatogr B Biomed Sci Appl* **2001,** *757* (1), 31-37.

193. Peng, H.; Chen, W.; Cheng, Y.; Hakuna, L.; Strongin, R.; Wang, B., Thiol reactive probes and chemosensors. *Sensors* **2012,** *12* (11), 15907.

194. Peng, H.; Chen, W.; Burroughs, S.; Wang, B., Fluorescent Probes for the Detection of Hydrogen Sulfide in Biological Systems. *Curr. Org. Chem.* **2013,** *17* (13), 641-653.

195. Xuan, W. M.; Sheng, C. Q.; Cao, Y. T.; He, W. H.; Wang, W., Fluorescent Probes for the Detection of Hydrogen Sulfide in Biological Systems. *Angew. Chem. Int. Ed.* **2012,** *51* (10), 2282-2284.

196. Peng, H.; Cheng, Y.; Dai, C.; Wang, B., A fluorescent probe for fast and quantitative detection of hydrogen sulfide in blood. *Angew. Chem. Int. Ed.* **2011,** *50* (41), 9672-9675.

197. Lippert, A. R.; New, E. J.; Chang, C. J., Reaction-based fluorescent probes for selective imaging of hydrogen sulfide in living cells. *J. Am. Chem. Soc.* **2011,** *133* (26), 10078-10080.

198. Liu, C.; Pan, J.; Li, S.; Zhao, Y.; Wu, L.; Berkman, C. E.; Whorton, A. R.; Xian, M., Capture and Visualization of Hydrogen Sulfide by a Fluorescent Probe. *Angew. Chem. Int. Ed.* **2011,** *50* (44), 10327-10329.

199. Qian, Y.; Karpus, J.; Kabil, O.; Zhu, H.-L.; Banerjee, R.; Zhao, J.; He, C., Selective fluorescent probes for live-cell monitoring of sulfide. *Nat. Commun.* **2011,** *2*, 495.

200. Liu, C.; Peng, B.; Li, S.; Park, C. M.; Whorton, A. R.; Xian, M., Reaction Based Fluorescent Probes for Hydrogen Sulfide. *Org. Lett.* **2012,** *14* (8), 2184-2187.

201. Qian, Y.; Zhang, L.; Ding, S.; Deng, X.; He, C.; Zhu, H.-L.; Zhao, J., A fluorescent probe for rapid detection of hydrogen sulfide in blood plasma and brain tissues in mice. *Chem. Sci.* **2012,** *3*, 2920-2923.

202. Xu, Z.; Xu, L.; Zhou, J.; Xu, Y. F.; Zhu, W. P.; Qian, X. H., A highly selective fluorescent probe for fast detection of hydrogen sulfide in aqueous solution and living cells. *Chem. Commun.* **2012,** *48* (88), 10871-10873.

203. Montoya, L. A.; Pluth, M. D., Selective turn-on fluorescent probes for imaging hydrogen sulfide in living cells. *Chem. Commun.* **2012,** *48* (39), 4767-4769.

204. Yu, F.; Li, P.; Song, P.; Wang, B.; Zhao, J.; Han, K., An ICT-based strategy to a colorimetric and ratiometric fluorescence probe for hydrogen sulfide in living cells. *Chem. Commun.* **2012,** *48*, 2852-2854.

205. Das, S. K.; Lim, C. S.; Yang, S. Y.; Han, J. H.; Cho, B. R., A small molecule two-photon probe for hydrogen sulfide in live tissues. *Chem. Commun.* **2012,** *48* (67), 8395-8397.

206. Chen, S.; Chen, Z.; Ren, W.; Ai, H., Reaction-Based Genetically Encoded Fluorescent Hydrogen Sulfide Sensors. *J. Am. Chem. Soc.* **2012,** *134* (23), 9589-9592.

207. Sasakura, K.; Hanaoka, K.; Shibuya, N.; Mikami, Y.; Kimura, Y.; Komatsu, T.; Ueno, T.; Terai, T.; Kimura, H.; Nagano, T., Development of a Highly Selective Fluorescence Probe for Hydrogen Sulfide. *J. Am. Chem. Soc.* **2011,** *133* (45), 18003-18005.

208. Choi, M. G.; Cha, S.; Lee, H.; Jeon, H. L.; Chang, S. K., Sulfide-selective chemosignaling by a Cu2+ complex of dipicolylamine appended fluorescein. *Chem. Commun.* **2009,** (47), 7390-7392.

209. Hou, F. P.; Huang, L.; Xi, P. X.; Cheng, J.; Zhao, X. F.; Xie, G. Q.; Shi, Y. J.; Cheng, F. J.; Yao, X. J.; Bai, D. C.; Zeng, Z. Z., A Retrievable and Highly Selective Fluorescent Probe for Monitoring Sulfide and Imaging in Living Cells. *Inorg. Chem.* **2012,** *51* (4), 2454-2460.

210. Lin, V.; Chang, C., Fluorescent probes for sensing and imaging biological hydrogen sulfide. *Curr Opin Chem Biol* **2012,** *16* (5-6), 595-601.

211. Pandey, S. K.; Kim, K. H.; Tang, K. T., A review of sensor-based methods for monitoring hydrogen sulfide. *TrAC, Trends Anal Chem* **2012,** *32*, 87-99.

212. Peng, H.; Chen, W.; Cheng, Y.; Hakuna, L.; Strongin, R.; Wang, B., Thiol reactive probes and chemosensors. *Sensors (Basel)* **2012,** *12* (11), 15907-15946.

213. Peng, H.; Chen, W.; Burroughs, S.; Wang, B., Recent advances in fluorescent probes for the detection of hydrogen sulfide. *Curr. Org. Chem.* **2013,** *17* (6), 641-653.

214. Liu, T.; Xu, Z.; Spring, D.; Cui, J., A lysosome-targetable fluorescent probe for imaging hydrogen sulfide in living cells. *Org Lett* **2013,** *15* (9), 2310-2313.

215. Chen, Y.; Zhu, C.; Yang, Z.; Chen, J.; He, Y.; Jiao, Y.; He, W.; Qiu, L.; Cen, J.; Guo, Z., A ratiometric fluorescent probe for rapid detection of hydrogen sulfide in mitochondria. *Angew Chem Int Ed* **2013,** *52* (6), 1688-1691.

216. Lutolf, M.; Tirelli, N.; Cerritelli, S.; Cavalli, L.; Hubbell, J., Systematic modulation of Michael-type reactivity of thiols through the use of charged amino acids. *Bioconjugate Chem* **2001,** *12* (6), 1051-1056.

217. Liu, J.; Sun, Y.-Q.; Zhang, J.; Yang, T.; Cao, J.; Zhang, L.; Guo, W., A ratiometric fluorescent probe for biological signaling molecule H2S: fast response and high selectivity. *Chem Eur J* **2013,** *19* (15), 4717-4722.

218. Wang, X.; Sun, J.; Zhang, W.; Ma, X.; Lv, J.; Tang, B., A near-infrared ratiometric fluorescent probe for rapid and highly sensitive imaging of endogenous hydrogen sulfide in living cells. *Chem Sci* **2013,** *4*, 2551-2556.

219. Wang, J.; Lin, W.; Li, W., Three-channel fluorescent sensing via organic white light-emitting dyes for detection of hydrogen sulfide in living cells. *Biomaterials* **2013,** *34*, 7429-7436.

220. Qian, Y.; Karpus, J.; Kabil, O.; Zhang, S.; Zhu, H.; Banerjee, R.; Zhao, J.; He, C., Selective fluorescent probes for live-cell monitoring of sulphide. *Nat. Commun.* **2011,** *2*, 495.

221. Yong, Q.; Ling, Z.; Shuting, D.; Xin, D.; Chuan, H.; Xi Emily, Z.; HaiLiang, Z.; Jing, Z., A fluorescent probe for rapid detection of hydrogen sulfide in blood plasma and brain tissues in mice. *Chem. Sci.* **2012,** *3*.

222. Lin, V.; Lippert, A.; Chang, C., Cell-trappable fluorescent probes for endogenous hydrogen sulfide signaling and imaging H2O2-dependent H2S production. *Proc Natl Acad Sci U. S. A.* **2013,** *110* (18), 7131-7135.

223. Bae, S. K.; Heo, C. H.; Choi, D. J.; Sen, D.; Joe, E. H.; Cho, B. R.; Kim, H. M., A ratiometric two-photon fluorescent probe reveals reduction in mitochondrial H2S production in parkinson's disease gene knockout astrocytes. *J Am Chem Soc* **2013,** *135* (26), 9915-9923.

224. Wang, B.; Li, P.; Yu, F.; Song, P.; Sun, X.; Yang, S.; Lou, Z.; Han, K., A reversible fluorescence probe based on Se-BODIPY for the redox cycle between HClO oxidative stress and H2S repair in living cells. *Chem Commun* **2013,** *49* (10), 1014-1016.

225. Wang, B.; Li, P.; Yu, F.; Chen, J.; Qu, Z.; Han, K., A near-infrared reversible and ratiometric fluorescent probe based on Se-BODIPY for the redox cycle mediated by hypobromous acid and hydrogen sulfide in living cells. *Chem Commun* **2013,** *49* (51), 5790-5792.

226. Xuan, W.; Pan, R.; Cao, Y.; Liu, K.; Wang, W., A fluorescent probe capable of detecting H2S at submicromolar concentrations in cells. *Chem Commun* **2012,** *48* (86), 10669-10671.

227. Chen, S.; Chen, Z.; Ren, W.; Ai, H., Reaction-based genetically encoded fluorescent hydrogen sulfide sensors. *J Am Chem Soc* **2012,** *134* (23), 9589-9592.

228. Li, Y.-H.; Chan, L.-M.; Tyer, L.; Moody, R. T.; Hirnel, C. M.; Hercules, D. M., Study of solvent effects on the fluorescence of 1-(dimethylamino)-5-naphthalenesulfonic acid and related compounds. *J. Am. Chem. Soc.* **1975,** *97* (11), 3118-3126.

229. Williams, A. T. R.; Winfield, S. A.; Miller, J. N., Relative fluorescence quantum yields using a computer-controlled luminescence spectrometer. *Analyst* **1983,** *108* (1290), 1067-1071.

230. Fava, A.; Iliceto, A.; Camera, E., Kinetics of the thiol/disulfide exchange. *J Am Chem Soc* **1956,** *70*, 833-838.

231. Go, Y. M.; Jones, D. P., Thiol/disulfide redox states in signaling and sensing. *Crit Rev Biochem Mol Biol* **2013,** *48* (2), 173-181.

232. Deneke, S. M., Thiol-based antioxidants. *Curr Top Cell Regul* **2000,** *36*, 151-180.

233. Murphy, M., Mitochondrial thiols in antioxidant protection and redox signaling: distinct roles for glutathionylation and other thiol modifications. *Antioxid Redox Signaling* **2012,** *16* (6), 476-495.

234. Chen, N.; Yang, F.; Capecci, L. M.; Gu, Z.; Schafer, A. I.; Durante, W.; Yang, X.; Wang, H., Regulation of homocysteine metabolism and methylation in human and mouse tissues. *FASEB J.* **2010,** *24* (8), 2804-2817.

235. Selhub, J., Homocysteine metabolism. *Annu. Rev. Nutr.* **1999,** *19*, 217-246.

236. Ueland, P. M., Homocysteine Species as Components of Plasma Redox Thiol Status. *Clin. Chem.* **1995,** *41* (3), 340-342.

237. Chambers, J. C.; Ueland, P. M.; Wright, M.; Dore, C. J.; Refsum, H.; Kooner, J. S., Investigation of relationship and protein-bound homocysteine between reduced, oxidized, and vascular endothelial function in healthy human subjects. *Circ. Res.* **2001,** *89* (2), 187-192.

238. Clarke, R.; Smith, A. D.; Jobst, K. A.; Refsum, H.; Sutton, L.; Ueland, P. M., Folate, vitamin B-12, and serum total homocysteine levels in confirmed Alzheimer disease. *Arch Neurol* **1998,** *55* (11), 1449-1455.

239. Falk, E.; Zhou, J.; Møller, J., Homocysteine and atherothrombosis. *Lipids* **2001,** *36*, 3-11.

240. Fung, T.; Rimm, E.; Spiegelman, D.; Rifai, N.; Tofler, G.; Willett, W.; Hu, F., Association between dietary patterns and plasma biomarkers of obesity and cardiovascular disease risk. *Am J Clin Nutr* **2001,** *73* (1), 61-67.

241. Miller, J. W.; Nadeau, M. R.; Smith, J.; Smith, D.; Selhub, J., Homocysteinemia - a consequence of disrupting S-adenosylmethionines regulation of homocysteine metabolism. *FASEB J.* **1992,** *6* (4), A1215-A1215.

242. Makino, A.; Nakanishi, T.; Sugiura-Ogasawara, M.; Ozaki, Y.; Suzumori, N.; Suzumori, K., No association of C677T methylenetetrahydrofolate reductase and an endothelial nitric oxide synthase polymorphism with recurrent pregnancy loss. *Am J Reprod Immunol* **2004,** *52* (1), 60-66.

243. Ebbing, M.; Bønaa, K.; Arnesen, E.; Ueland, P.; Nordrehaug, J.; Rasmussen, K.; Njølstad, I.; Nilsen, D.; Refsum, H.; Tverdal, A.; Vollset, S.; Schirmer, H.; Bleie, Ø.; Steigen, T.; Midttun, Ø.; Fredriksen, A.; Pedersen, E.; Nygård, O., Combined analyses and extended follow-up of two randomized controlled homocysteine-lowering B-vitamin trials. *J Intern Med* **2010,** *268* (4), 367-382.

244. Malinow, M. R.; Bostom, A. G.; Krauss, R. M., Homocyst(e)ine, diet, and cardiovascular diseases - A statement for healthcare professionals from the Nutrition Committee, American Heart Association. *Circulation* **1999,** *99* (1), 178-182.

245. Chen, X.; Zhou, Y.; Peng, X.; Yoon, J., Fluorescent and colorimetric probes for detection of thiols. *Chem Soc Rev* **2010,** *39* (6), 2120-2135.

246. Janáky, R.; Varga, V.; Hermann, A.; Saransaari, P.; Oja, S., Mechanisms of L-cysteine neurotoxicity. *Neurochem Res* **2000,** *25* (9-10), 1397-1405.

247. Martin, H. L.; Teismann, P., Glutathione-a review on its role and significance in Parkinson's disease. *Faseb Journal* **2009,** *23* (10), 3263-3272.

248. Jocelyn, P. C., The standard redox potential of cysteine-cystine from the thiol-disulphide exchange reaction with glutathione and lipoic acid *Eur J Biochem* **1967,** *2* (3), 327-331.

249. Sanadi, D. R.; Langley, M.; Searls, R. L., α-Ketoglutaric dehydrogenase: VI. reversible oxidation of dihydrothioctamide by diphosphopyridine nucleotide. *J Biol Chem* **1959,** *234*, 178-182.

250. Escobedo, J.; Rusin, O.; Wang, W.; Alptürk, O.; Kim, K.; Xu, X.; Strongin, R., Detection of Biological Thiols. In *Reviews in Fluorescence 2006*, Geddes, C.; Lakowicz, J., Eds. Springer US: 2006; Vol. 2006, pp 139-162.

251. Refsum, H.; Smith, A.; Ueland, P.; Nexo, E.; Clarke, R.; McPartlin, J.; Johnston, C.; Engbaek, F.; Schneede, J.; McPartlin, C.; Scott, J., Facts and recommendations about total homocysteine determinations: an expert opinion. *Clin Chem* **2004,** *50* (1), 3-32.

252. Burns, J. A.; Butler, J. C.; Moran, J.; Whitesides, G. M., Selective reduction of disulfides by tris(2-carboxyethyl)phosphine. *J Org Chem* **1991,** *56*, 2648-2650.

253. Mendel, F.; Cavins, J. F.; Wall, J. S., Relative nucleophilic reactivities of amino groups and mercaptide ions in addition reactions with α, β-unsaturated compounds. *J Am Chem Soc* **1965,** *87*.

254. Lai, Y.; Tseng, W., Gold nanoparticle extraction followed by o-phthaldialdehyde derivatization for fluorescence sensing of different forms of homocysteine in plasma. *Talanta* **2012,** *91*, 103-109.

255. Wang, W.; Escobedo, J.; Lawrence, C.; Strongin, R., Direct detection of homocysteine. *J Am Chem Soc* **2004,** *126* (11), 3400-3401.

256. Ueland, P. M.; Refsum, H.; Stabler, S. P.; Malinow, M. R.; Andersson, A.; Allen, R. H., Total Homocysteine in Plasma or Serum - Methods and Clinical-Applications. *Clin. Chem.* **1993,** *39* (9), 1764-1779.

257. Kusmierek, K.; Glowacki, R.; Bald, E., Analysis of urine for cysteine, cysteinylglycine, and homocysteine by high-performance liquid chromatography. *Anal. Bioanal. Chem.* **2006,** *385* (5), 855-860.

258. Chen, X.; Zhou, Y.; Peng, X. J.; Yoon, J., Fluorescent and colorimetric probes for detection of thiols. *Chem. Soc. Rev.* **2010,** *39* (6), 2120-2135.

259. Xiong, L.; Zhao, Q.; Chen, H.; Wu, Y.; Dong, Z.; Zhou, Z.; Li, F., Phosphorescence imaging of homocysteine and cysteine in living cells based on a cationic iridium(III) complex. *Inorg Chem* **2010,** *49* (14), 6402-6408.

260. Wang, W.; Rusin, O.; Xu, X.; Kim, K.; Escobedo, J.; Fakayode, S.; Fletcher, K.; Lowry, M.; Schowalter, C.; Lawrence, C.; Fronczek, F.; Warner, I.; Strongin, R., Detection of homocysteine and cysteine. *J Am Chem Soc* **2005,** *127* (45), 15949-15958.

261. Lu, C.; Zu, Y., Specific detection of cysteine and homocysteine: recognizing one-methylene difference using fluorosurfactant-capped gold nanoparticles. *Chem Commun* **2007,** (37), 3871-3873.

262. Chwatko, G.; Jakubowski, H., The determination of homocysteine-thiolactone in human plasma. *Anal Biochem* **2005,** *337* (2), 271-277.

263. Chen, H.; Zhao, Q.; Wu, Y.; Li, F.; Yang, H.; Yi, T.; Huang, C., Selective phosphorescence chemosensor for homocysteine based on an iridium(III) complex. *Inorg. Chem.* **2007,** *46* (26), 11075-11081.

264. Yang, X.; Guo, Y.; Strongin, R. M., Conjugate addition/cyclization sequence enables selective and simultaneous fluorescence detection of cysteine and homocysteine. *Angew. Chem. Int. Ed.* **2011,** *50* (4), 10690-10693.

265. Guo, Z.; Nam, S.; Park, S.; Yoon, J., A highly selective ratiometric near-infrared fluorescent cyanine sensor for cysteine with remarkable shift and its application in bioimaging. *Chem. Sci.* **2012,** *3*, 2760-2765.

266. Peng, H.; Chen, W.; Cheng, Y.; Hakuna, L.; Strongin, R.; Wang, B., Thiol Reactive Probes and Chemosensors. *Sensors* **2012,** *12* (11), 15907-15946.

267. Wang, K.; Peng, H.; Wang, B., Recent Advances in Thiol and Sulfide Reactive Probes. *J. Cell. Biochem.* **2014,** *115* (6), 1007-1022.

268. Strongin, R. M.; Wang, W. H.; Escobedo, J. O.; Lawrence, C. M., Direct detection of homocysteine. *J. Am. Chem. Soc.* **2004,** *126* (11), 3400-3401.

269. Rusin, O.; Wang, W. H.; Xu, X. Y.; Kim, K. K.; Escobedo, J. O.; Fakayode, S. O.; Fletcher, K. A.; Lowry, M.; Schowalter, C. M.; Lawrence, C. M.; Fronczek, F. R.; Warner, I. M.; Strongin, R. M., Detection of homocysteine and cysteine. *J. Am. Chem. Soc.* **2005,** *127* (45), 15949-15958.

270. Escobedo, J. O.; Wang, W. H.; Strongin, R. M., Use of a commercially available reagent for the selective detection of homocysteine in plasma. *Nat. Protoc.* **2006,** *1* (6), 2759-2762.

271. Hakuna, L.; Escobedo, J. O.; Lowry, M.; Barve, A.; McCallum, N.; Strongin, R. M., A photochemical method for determining plasma homocysteine with limited sample processing. *Chem. Commun.* **2014,** *50* (23), 3071-3073.

272. Lee, H. Y.; Choi, Y. P.; Kim, S.; Yoon, T.; Guo, Z.; Lee, S.; Swamy, K. M. K.; Kim, G.; Lee, J. Y.; Shin, I.; Yoon, J., Selective homocysteine turn-on fluorescent probes and their bioimaging applications. *Chem. Commun.* **2014,** *50*, 6967-6969.

273. Peng, H.; Cheng, Y.; Dai, C.; King, A. L.; Predmore, B. L.; Lefer, D. J.; Wang, B., A fluorescent probe for fast and quantitative detection of hydrogen sulfide in blood. *Angew. Chem. Int. Ed.* **2011,** *50* (41), 9672-9675.

274. Ellman, G. L., Tissue sulfhydryl groups. *Arch. Biochem. Biophys.* **1959,** *82* (1), 70-77.

275. Hogg, N., The effect of cyst(e)ine on the auto-oxidation of homocysteine. *Free Radical Bio.Med.* **1999,** *27* (1-2), 28-33.

276. Gabaldon, M., Oxidation of cysteine and homocysteine by bovine albumin. *Arch. Biochem. Biophys.* **2004,** *431* (2), 178-188.

277. O'Connor, N. A.; Sakata, S. T.; Zhu, H.; Shea, K. J., Chemically modified dansyl probes: A fluorescent diagnostic for ion and proton detection in solution and in polymers. *Org. Lett.* **2006,** *8* (8), 1581-1584.

278. Jones, D.; Carlson, J.; Samiec, P.; Sternberg, P.; Mody, V.; Reed, R.; Brown, L., Glutathione measurement in human plasma: evaluation of sample collection, storage and derivatization conditions for analysis of dansyl derivatives by HPLC. *Clin. Chim. Acta* **1998**.

279. Wang, K.; Peng, H.; Ni, N.; Dai, C.; Wang, B., 2,6-Dansyl azide as a fluorescent probe for hydrogen sulfide. *J. Fluoresc.* **2013,** *24* (1), 1-5.

280. Friedman, M.; Cavins, J. F.; Wall, J. S., Relative nucleophilic reactivities of amino groups and mercaptide ions in addition reactions with α,β-unsaturated compounds. *J. Am. Chem. Soc.* **1965,** *87* (16), 3672-3682.

281. Pitman, I. H.; Morris, I. J., Covalent Additions of Glutathione, Cysteine, Homocysteine, Cysteamine and Thioglycolic Acid to Quinazoline Cation. *Aust. J. Chem.* **1979,** *32* (7), 1567-1573.

282. Benesch, R. E.; Benesch, R., The Acid Strength of the -Sh Group in Cysteine and Related Compounds. *J. Am. Chem. Soc.* **1955,** *77* (22), 5877-5881.

283. Cao, X. W.; Lin, W. Y.; Yu, Q. X., A Ratiometric Fluorescent Probe for Thiols Based on a Tetrakis (4-hydroxyphenyl)porphyrin-Coumarin Scaffold. *J. Org. Chem.* **2011,** *76* (18), 7423-7430.

284. Scampicchio, M.; Lawrence, N. S.; Arecchi, A.; Mannino, S., Electrochemical reduction of Ellman's reagent: A novel selective detection protocol for thiol compounds. *Electroanalysis* **2007,** *19* (23), 2437-2443.

285. Iciek, M.; Chwatko, G.; Lorenc-Koci, E.; Bald, E.; Wlodek, L., Plasma levels of total, free and protein bound thiols as well as sulfane sulfur in different age groups of rats. *Acta Biochim. Pol.* **2004,** *51* (3), 815-824.

286. Cartwright, I. L.; Hutchinson, D. W.; Armstrong, V. W., The reaction between thiols and 8-azidoadenosine derivatives. *Nucleic Acids Res.* **1976,** *3* (9), 2331-2340.

287. Kerr, J. A., In *CRC Handbook of Chemistry and Physics 1999-2000 : A Ready-Reference Book of Chemical and Physical Data (CRC Handbook of Chemistry and Physics, D.R. Lide, (ed.)*, 81st edition ed.; CRC Press: Boca Raton, Florida, USA, 2000.

288. Bao, M.; Shimizu, M., N-Trifluoroacetyl arenesulfenamides, effective precursors for synthesis of unsymmetrical disulfides and sulfenamides. *Tetrahedron* **2003,** *59*, 9655-9659.

APPENDICES

Appendix A Spectra of compounds and DNA products in DNA modification

Appendix A.1 Spectra of Synthesized Compounds

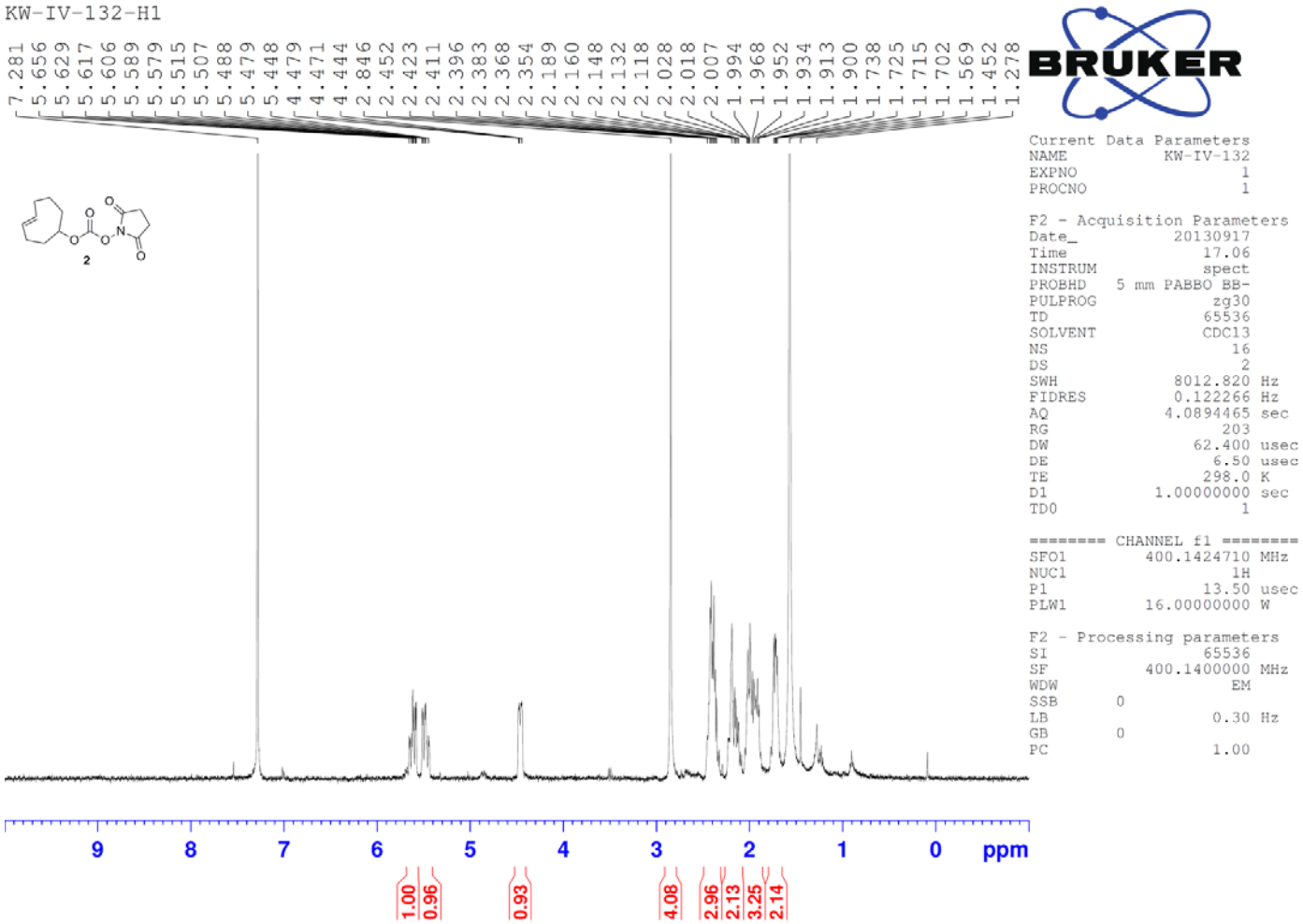

KW-IV-84-H1

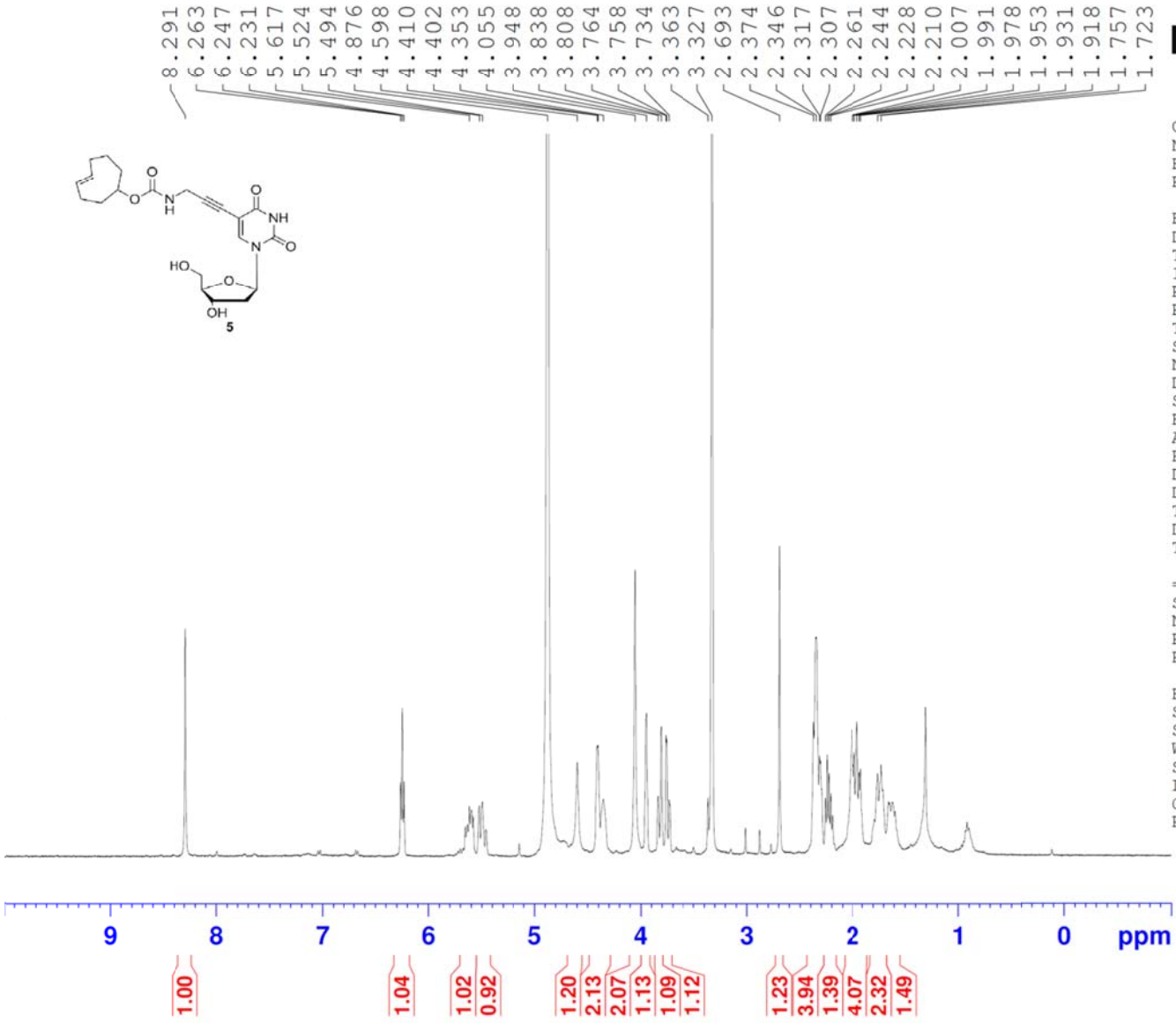

BRUKER

```
Current Data Parameters
NAME          KW-IV-84-a
EXPNO                  1
PROCNO                 1

F2 - Acquisition Parameters
Date_           20130605
Time               15.10
INSTRUM            spect
PROBHD   5 mm PABBO BB-
PULPROG             zg30
TD                 65536
SOLVENT             MeOD
NS                    16
DS                     2
SWH             8012.820 Hz
FIDRES          0.122266 Hz
AQ              4.0894465 sec
RG                   144
DW                62.400 usec
DE                 6.50 usec
TE                298.0 K
D1             1.00000000 sec
TD0                    1

======== CHANNEL f1 ========
SFO1         400.1424710 MHz
NUC1                   1H
P1                 13.50 usec
PLW1         16.00000000 W

F2 - Processing parameters
SI                 65536
SF           400.1400000 MHz
WDW                   EM
SSB       0
LB                 0.30 Hz
GB        0
PC                 1.00
```

KW-IV-84-c-APT

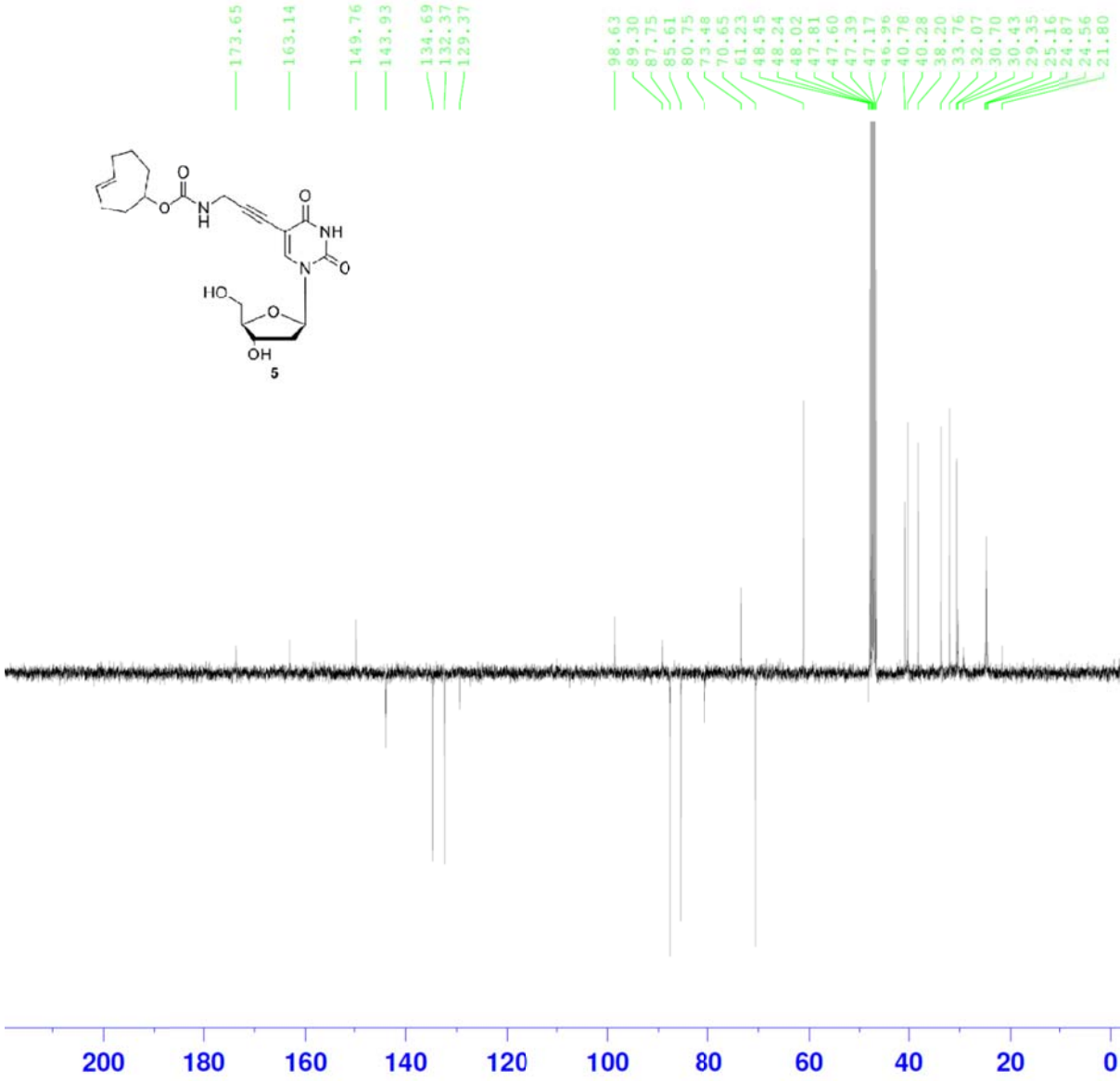

BRUKER

```
Current Data Parameters
NAME          KW-IV-84-c
EXPNO                  6
PROCNO                 1

F2 - Acquisition Parameters
Date_           20130609
Time               10.42
INSTRUM            spect
PROBHD   5 mm PABBO BB-
PULPROG             jmod
TD                 65536
SOLVENT             MeOD
NS                  2048
DS                     4
SWH          24038.461 Hz
FIDRES        0.366798 Hz
AQ            1.3631488 sec
RG                   203
DW              20.800 usec
DE               6.50 usec
TE              298.0 K
CNST2       145.0000000
CNST11        1.0000000
D1            2.00000000 sec
D20           0.00639655 sec
TD0                    1

======== CHANNEL f1 ========
SF01        100.6253446 MHz
NUC1               13C
P1                9.00 usec
P2               18.00 usec
PLW1        62.00000000 W

======== CHANNEL f2 ========
SF02        400.1416006 MHz
NUC2               1H
CPDPRG[2         waltz16
PCPD2             90.00 usec
PLW2        16.00000000 W
PLW12        0.36000001 W

F2 - Processing parameters
SI                 32768
SF          100.6152830 MHz
WDW                  EM
SSB       0
LB                1.00 Hz
GB        0
PC                1.40
```

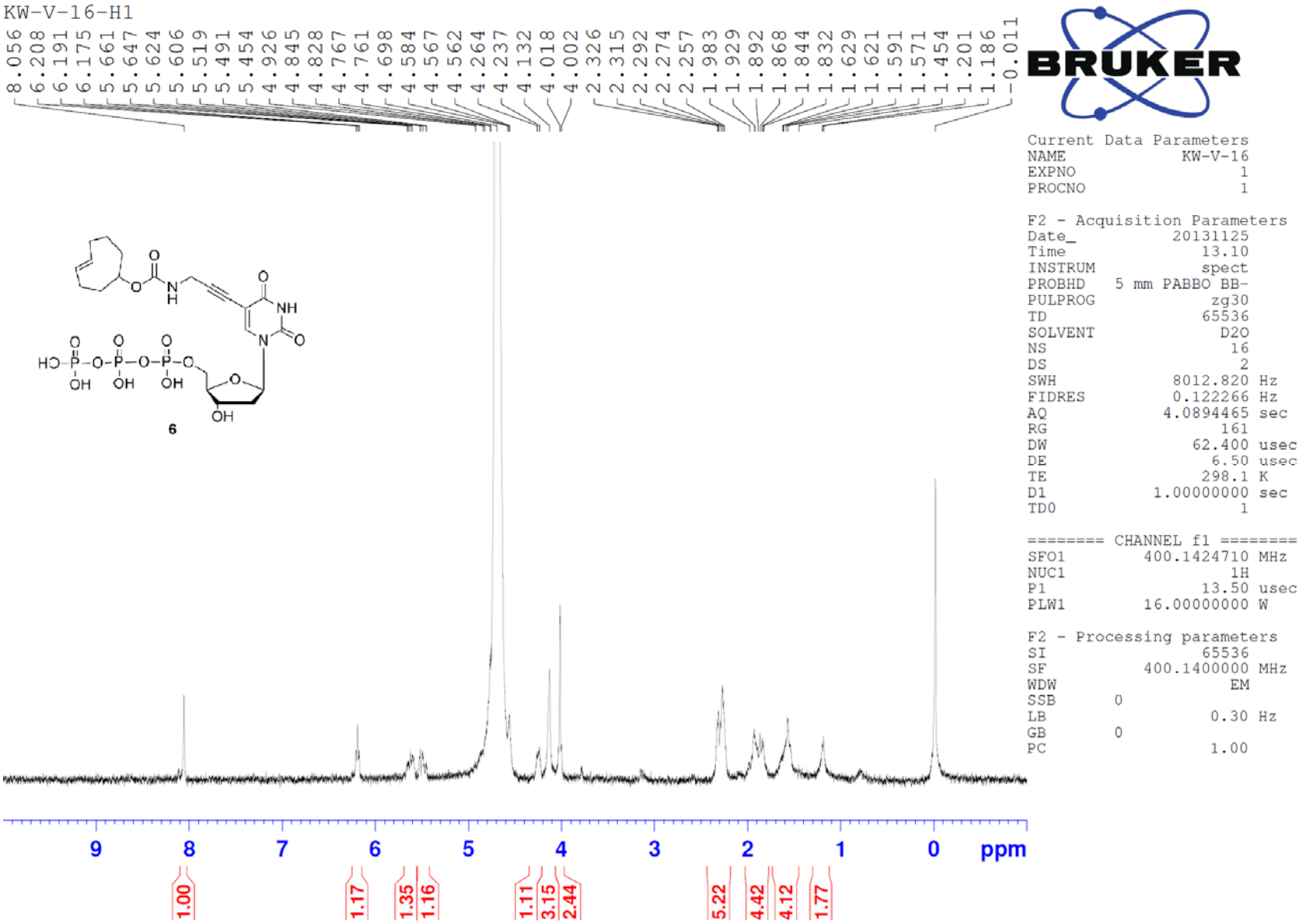

Current Data Parameters
NAME KW-V-16
EXPNO 1
PROCNO 1

F2 - Acquisition Parameters
Date_ 20131125
Time 13.10
INSTRUM spect
PROBHD 5 mm PABBO BB-
PULPROG zg30
TD 65536
SOLVENT D2O
NS 16
DS 2
SWH 8012.820 Hz
FIDRES 0.122266 Hz
AQ 4.0894465 sec
RG 161
DW 62.400 usec
DE 6.50 usec
TE 298.1 K
D1 1.00000000 sec
TD0 1

======== CHANNEL f1 ========
SFO1 400.1424710 MHz
NUC1 1H
P1 13.50 usec
PLW1 16.00000000 W

F2 - Processing parameters
SI 65536
SF 400.1400000 MHz
WDW EM
SSB 0
LB 0.30 Hz
GB 0
PC 1.00

KW-V-5-C13

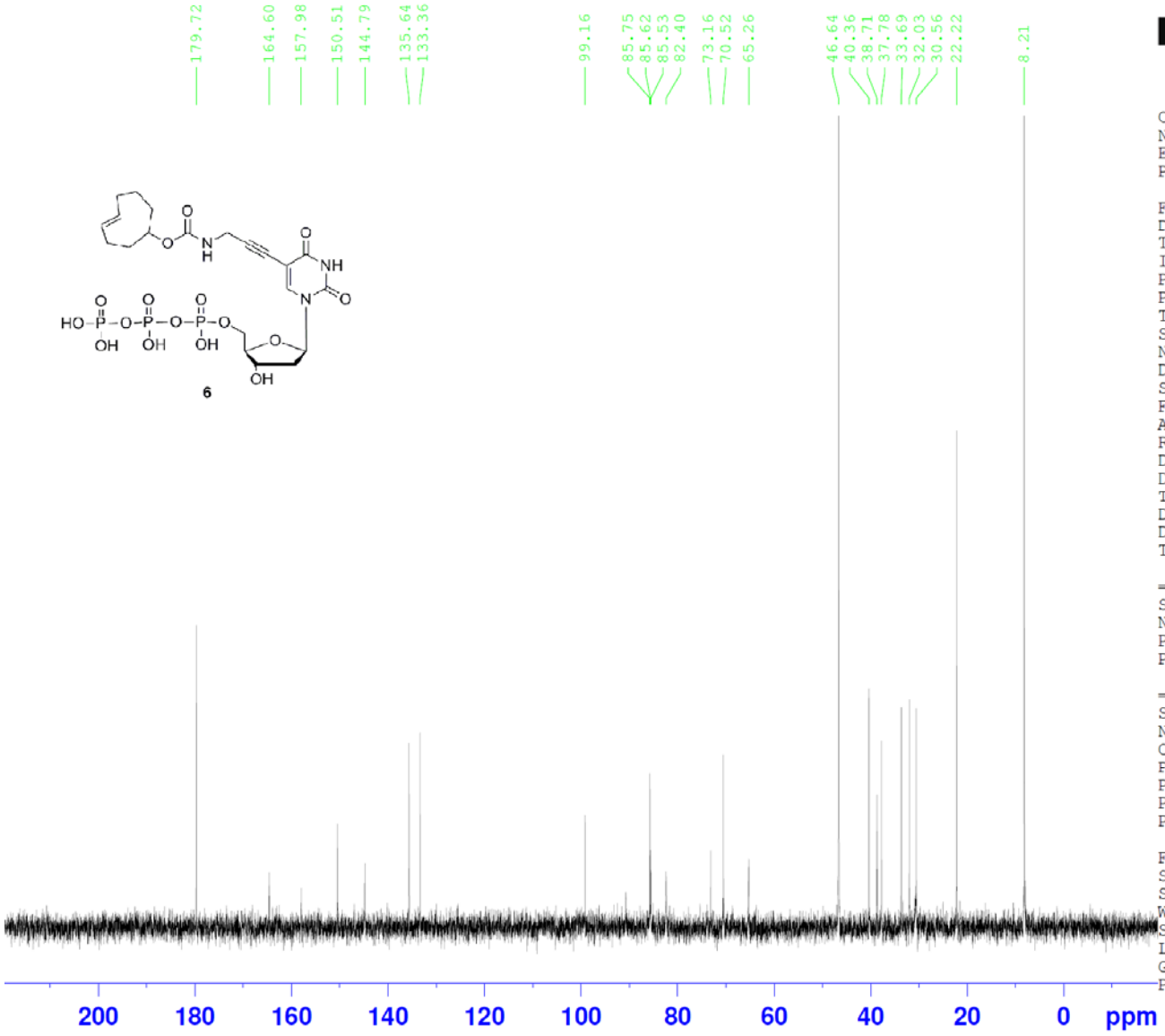

BRUKER

```
Current Data Parameters
NAME            KW-V-5-b
EXPNO                  2
PROCNO                 1

F2 - Acquisition Parameters
Date_           20131119
Time              21.15
INSTRUM           spect
PROBHD   5 mm PABBO BB-
PULPROG         zgpg30
TD                65536
SOLVENT             D2O
NS                10240
DS                    4
SWH           24038.461 Hz
FIDRES         0.366798 Hz
AQ             1.3631488 sec
RG                  203
DW               20.800 usec
DE                6.50 usec
TE                298.4 K
D1            2.00000000 sec
D11           0.03000000 sec
TD0                   1

======== CHANNEL f1 ========
SFO1         100.6253441 MHz
NUC1                13C
P1                9.00 usec
PLW1         62.00000000 W

======== CHANNEL f2 ========
SFO2         400.1416006 MHz
NUC2                1H
CPDPRG[2         waltz16
PCPD2            90.00 usec
PLW2         16.00000000 W
PLW12         0.36000001 W
PLW13         0.29159999 W

F2 - Processing parameters
SI                 32768
SF           100.6152830 MHz
WDW                  EM
SSB      0
LB                1.00 Hz
GB       0
PC                1.40
```

KW-V-5-P31-with dilute standard

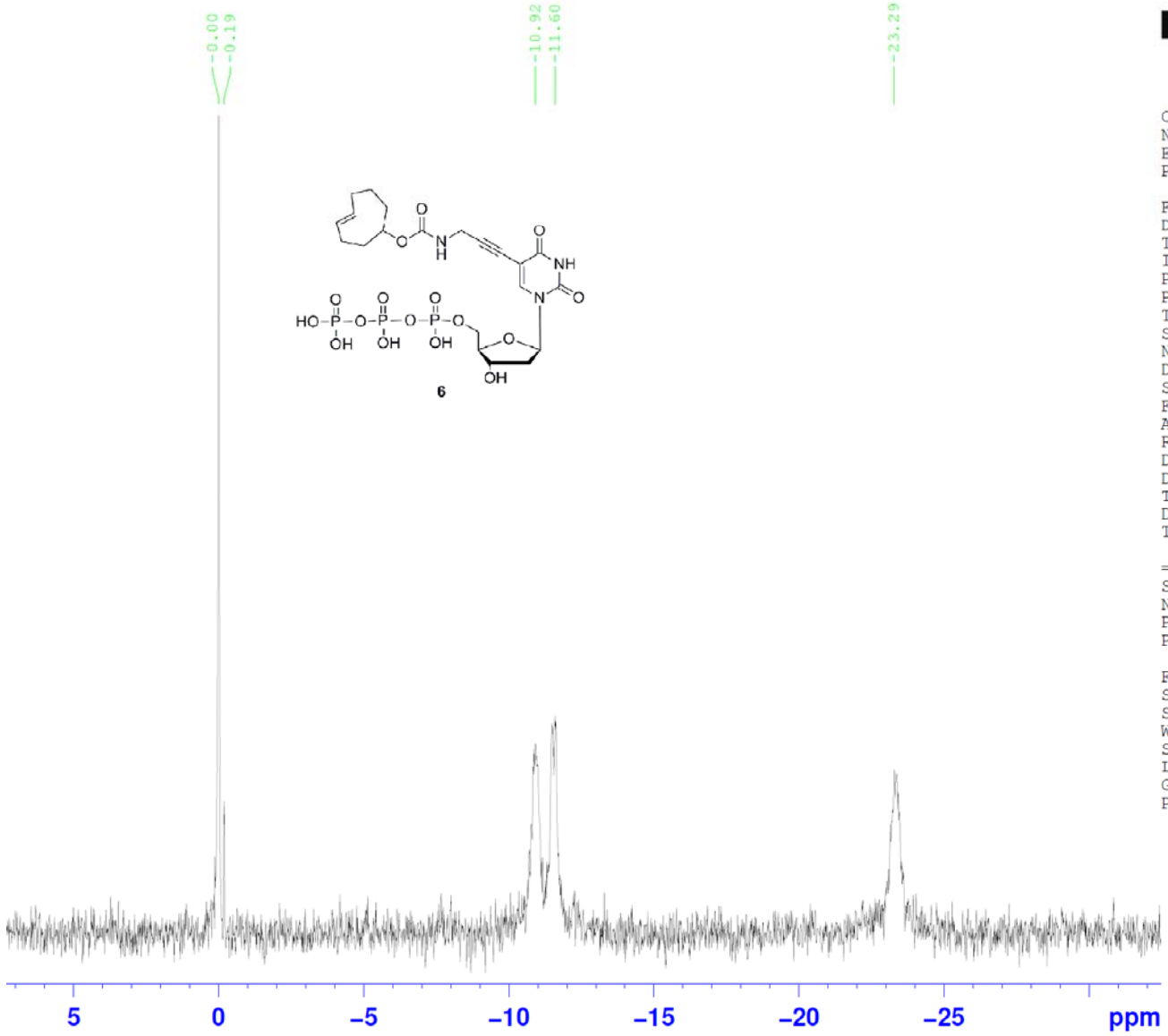

6

```
Current Data Parameters
NAME                  KW-V-5
EXPNO                      7
PROCNO                     1

F2 - Acquisition Parameters
Date_              20131104
Time                  13.56
INSTRUM               spect
PROBHD    5 mm PABBO BB-
PULPROG                zg30
TD                    65536
SOLVENT                 D2O
NS                         64
DS                          4
SWH              64102.563 Hz
FIDRES            0.978127 Hz
AQ               0.5111808 sec
RG                       203
DW                   7.800 usec
DE                   6.50 usec
TE                   298.1 K
D1              2.00000000 sec
TD0                        1

======== CHANNEL f1 ========
SFO1           161.9715421 MHz
NUC1                   31P
P1                   14.00 usec
PLW1           12.50000000 W

F2 - Processing parameters
SI                     32768
SF             161.9796458 MHz
WDW                       EM
SSB         0
LB                    1.00 Hz
GB          0
PC                    1.40
```

BW-BBA-1-H1

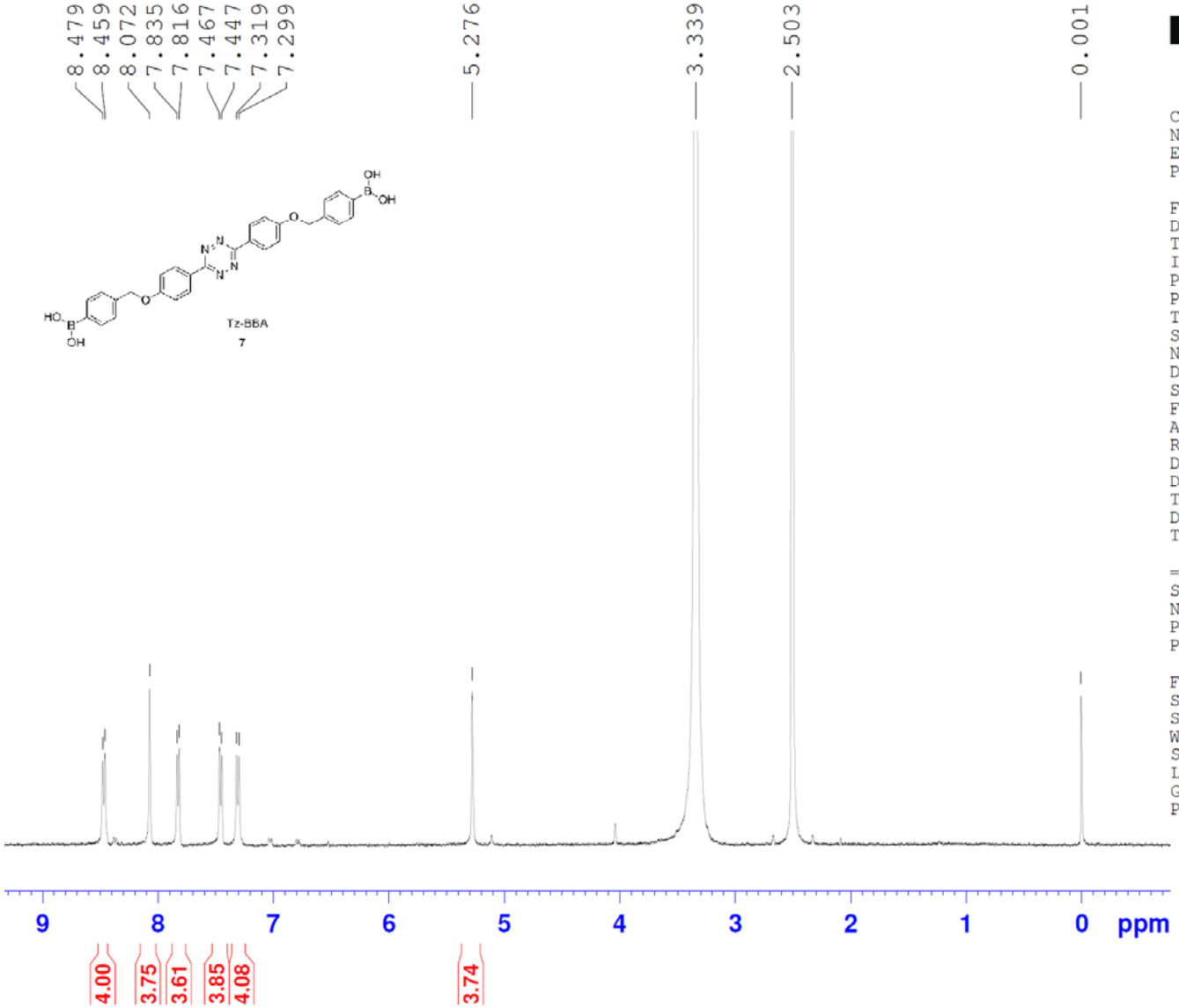

Current Data Parameters

NAME	BW-BBA-1
EXPNO	1
PROCNO	1

F2 - Acquisition Parameters

Date_	20130221
Time	19.20
INSTRUM	spect
PROBHD	5 mm PABBO BB-
PULPROG	zg30
TD	65536
SOLVENT	DMSO
NS	16
DS	2
SWH	8012.820 Hz
FIDRES	0.122266 Hz
AQ	4.0894465 sec
RG	203
DW	62.400 usec
DE	6.50 usec
TE	298.0 K
D1	1.00000000 sec
TD0	1

======== CHANNEL f1 ========

SFO1	400.1424710 MHz
NUC1	1H
P1	13.50 usec
PLW1	16.00000000 W

F2 - Processing parameters

SI	65536
SF	400.1400000 MHz
WDW	EM
SSB	0
LB	0.30 Hz
GB	0
PC	1.00

DZ-V-119-1H

10.421 9.214 9.201 8.963 8.678 8.657 8.470 8.297 8.214 8.194 7.857 7.845 7.833 7.803 7.784 7.189 7.168 6.684 6.617 6.595 6.564 6.543 3.774 3.506 2.500 -0.005

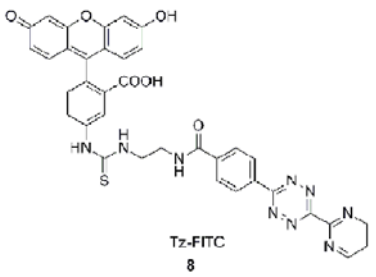

Tz-FITC
8

BRUKER

```
Current Data Parameters
NAME            DZ-V-119
EXPNO                  1
PROCNO                 1

F2 - Acquisition Parameters
Date_           20130907
Time               18.52
INSTRUM            spect
PROBHD   5 mm PABBO BB-
PULPROG             zg30
TD                 65536
SOLVENT             DMSO
NS                    16
DS                     2
SWH             8012.820 Hz
FIDRES          0.122266 Hz
AQ              4.0894465 sec
RG                   203
DW                62.400 usec
DE                 6.50 usec
TE                296.3 K
D1             1.00000000 sec
TD0                    1

======== CHANNEL f1 ========
SFO1          400.1424710 MHz
NUC1                  1H
P1                 13.50 usec
PLW1          16.00000000 W

F2 - Processing parameters
SI                 65536
SF            400.1400013 MHz
WDW                   EM
SSB       0
LB                 0.30 Hz
GB        0
PC                 1.00
```

Appendix A.2 MALDI-TOF Spectra of DNA Products

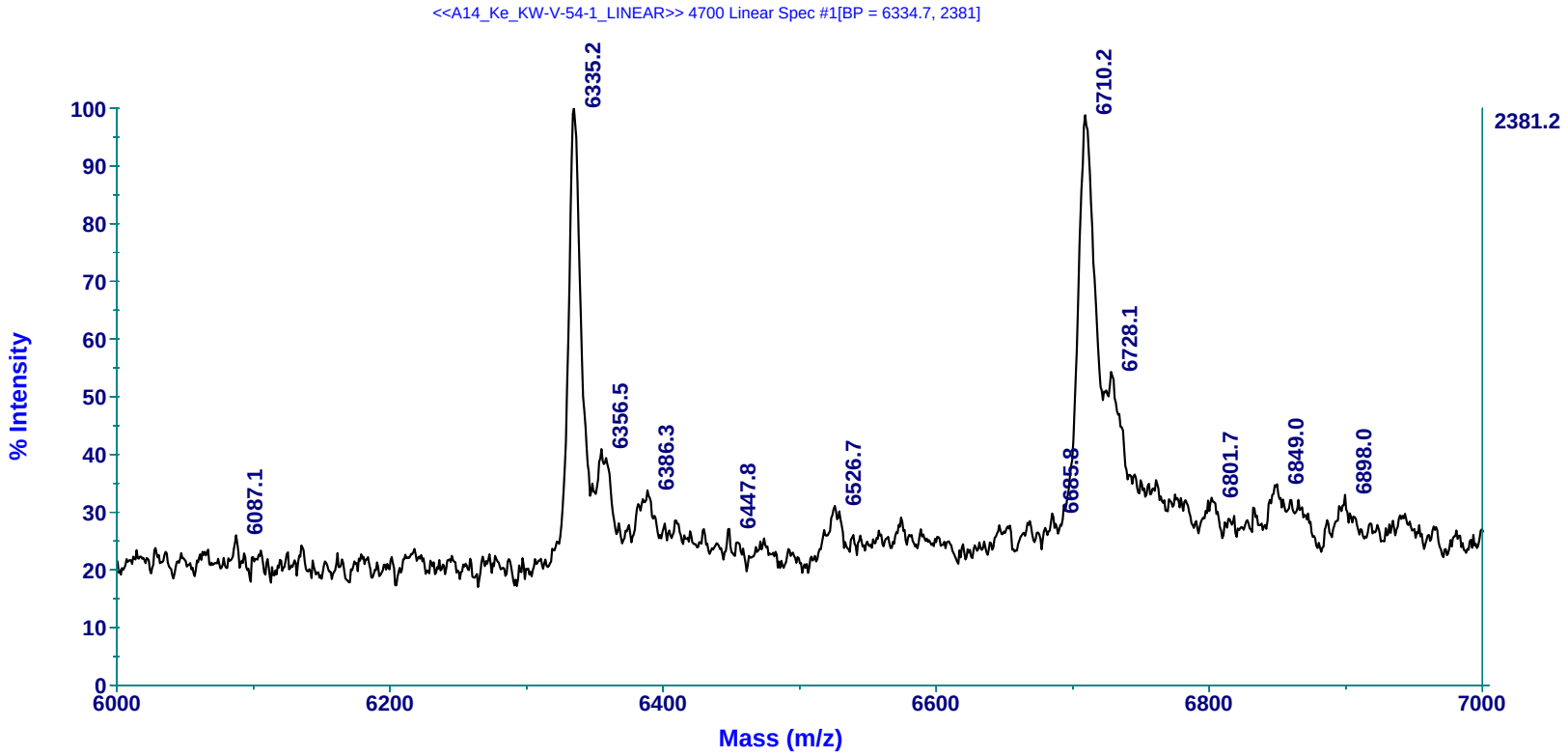

MALDI-TOF spectrum of TCO-DNA_{21} (Template-1)

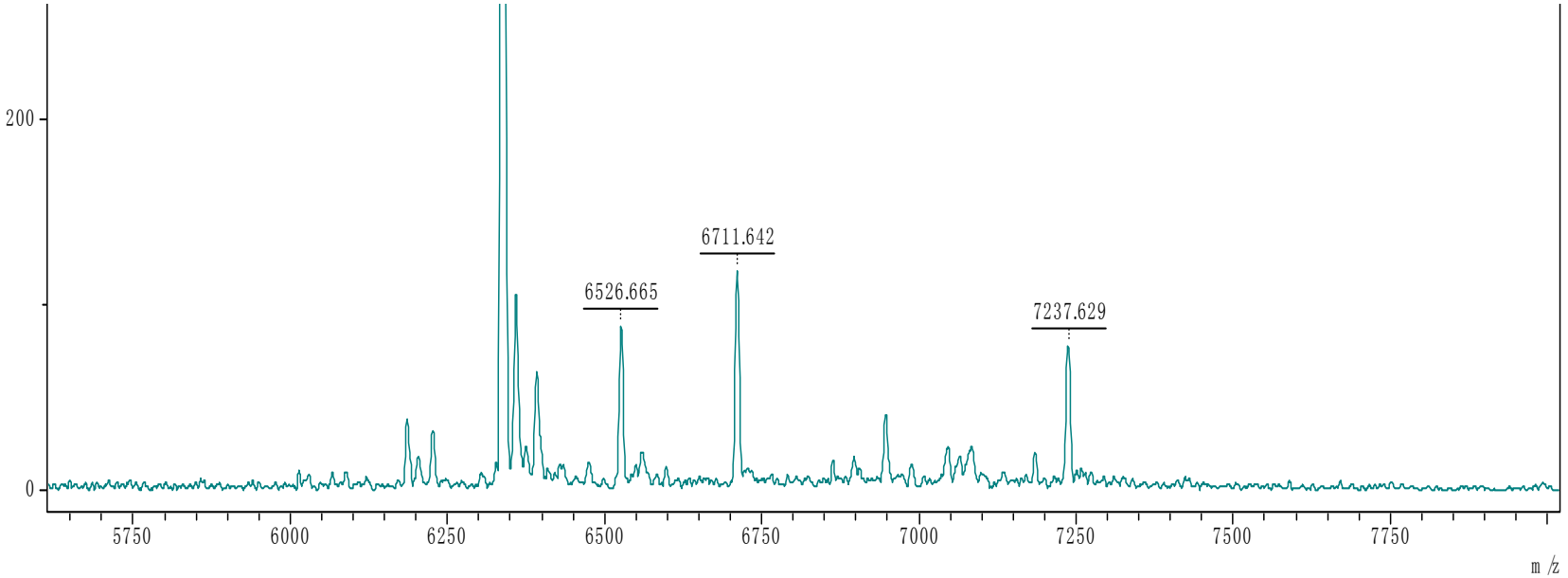

MALDI-TOF spectrum of TCO-DNA_{21} (Template-1) after reacting with Tz-BBA

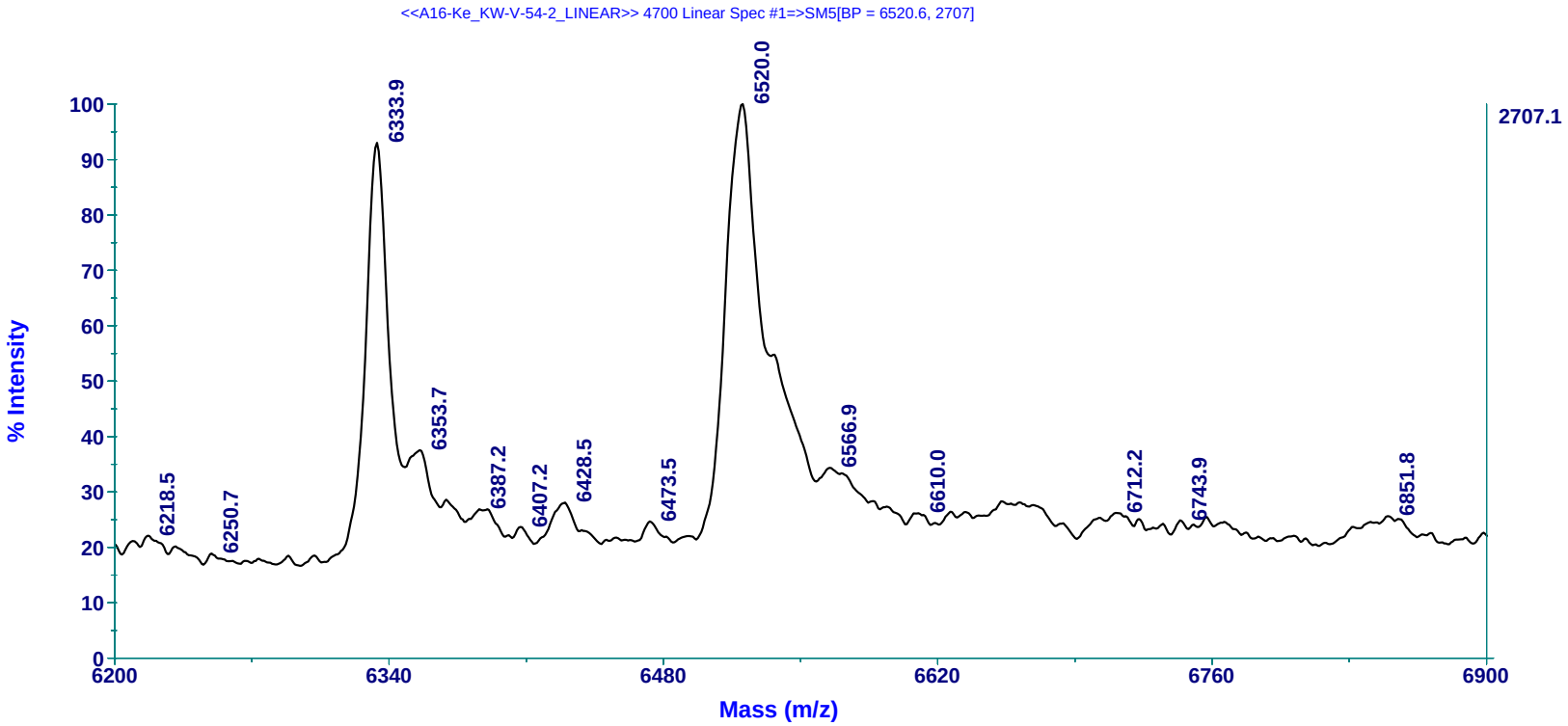

MALDI-TOF spectrum of dNTP-DNA_{21} (Template-1) after reacting with Tz-BBA

Appendix B Spectra of compounds in hydrogen sulfide probe

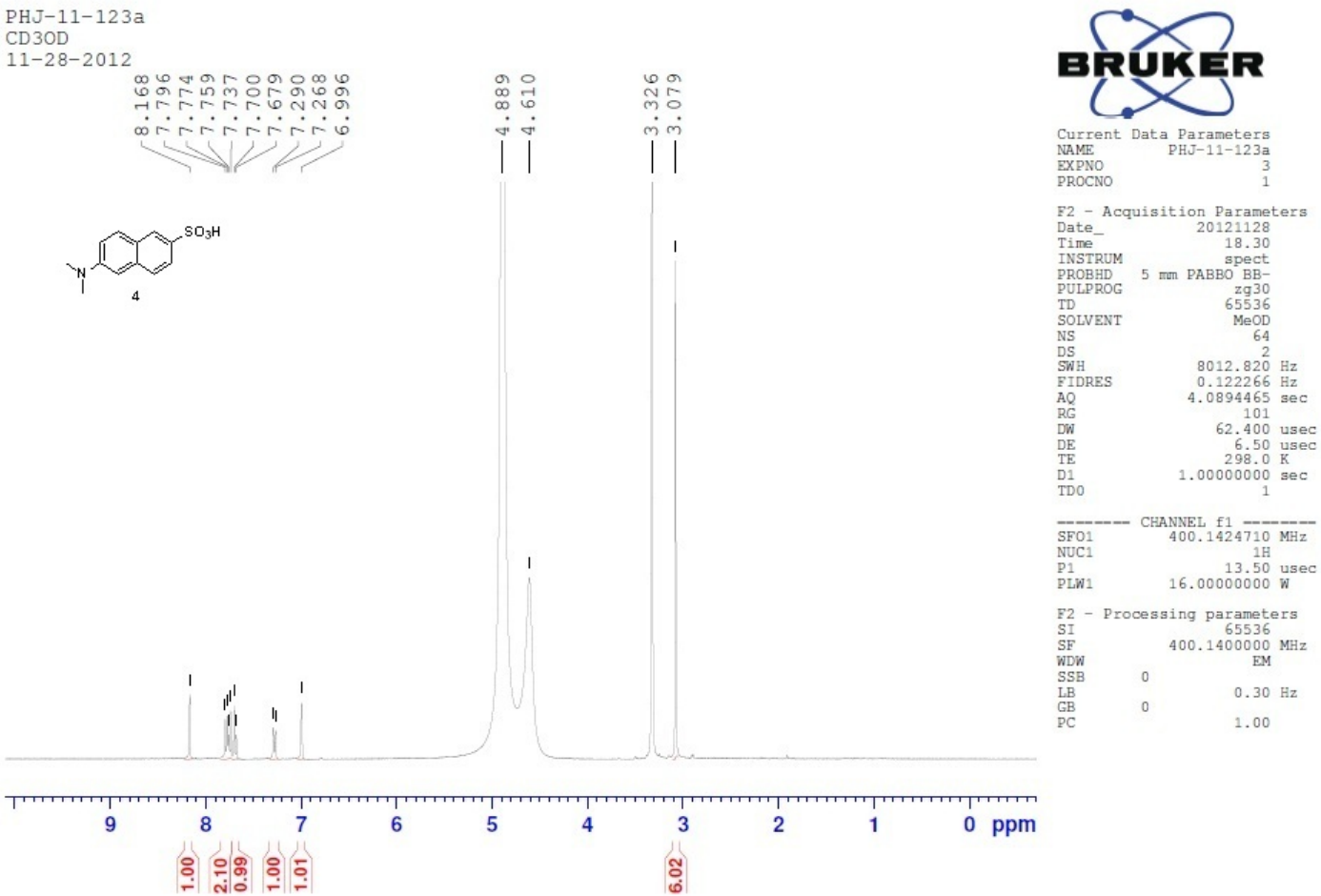

BRUKER

```
Current Data Parameters
NAME          PHJ-11-123a
EXPNO                   3
PROCNO                  1

F2 - Acquisition Parameters
Date_            20121128
Time                18.30
INSTRUM             spect
PROBHD   5 mm PABBO BB-
PULPROG              zg30
TD                  65536
SOLVENT              MeOD
NS                     64
DS                      2
SWH              8012.820 Hz
FIDRES           0.122266 Hz
AQ               4.0894465 sec
RG                    101
DW                 62.400 usec
DE                  6.50 usec
TE                 298.0 K
D1            1.00000000 sec
TD0                     1

======== CHANNEL f1 ========
SFO1         400.1424710 MHz
NUC1                   1H
P1                 13.50 usec
PLW1         16.00000000 W

F2 - Processing parameters
SI                  65536
SF           400.1400000 MHz
WDW                    EM
SSB       0
LB                  0.30 Hz
GB        0
PC                  1.00
```

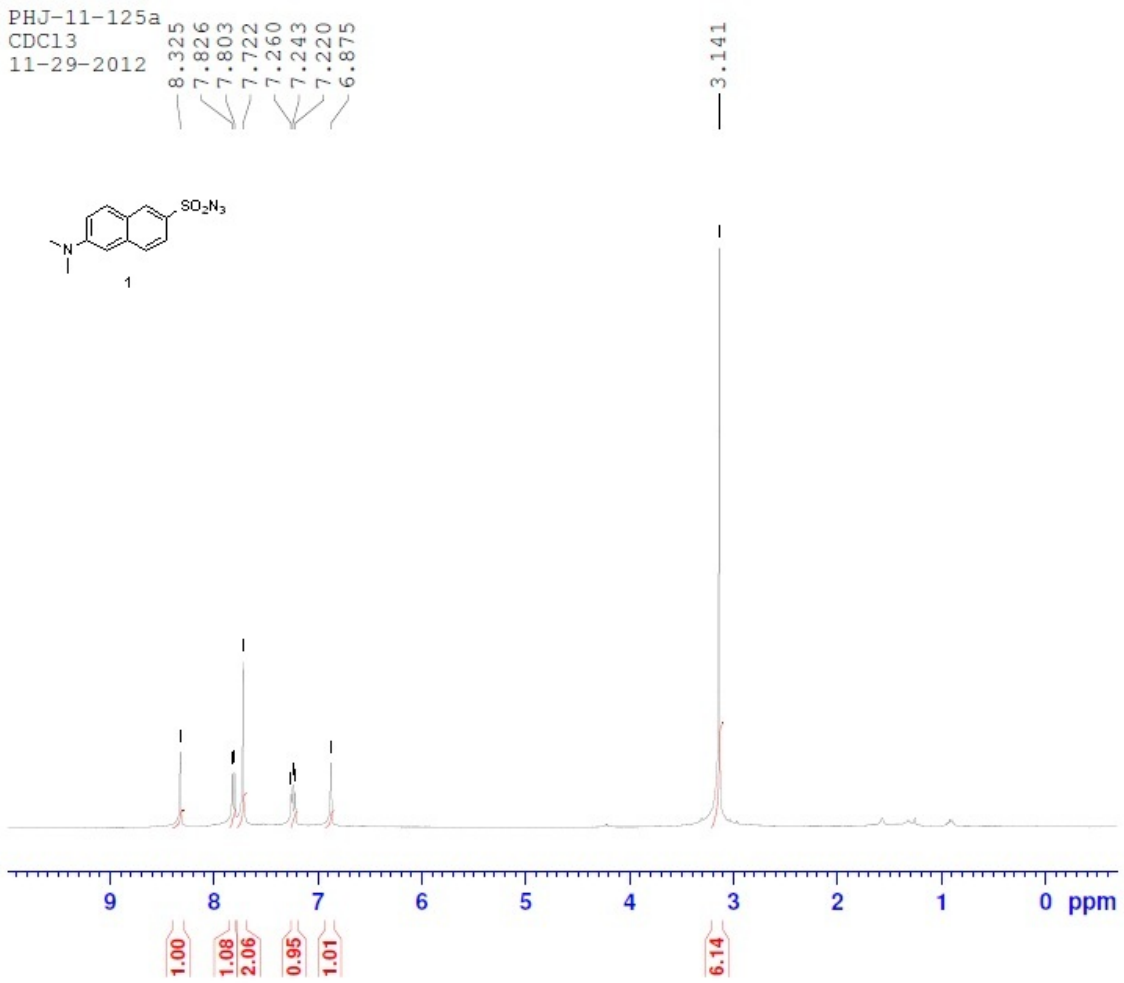

BRUKER

Current Data Parameters
NAME PHJ-11-125a
EXPNO 4
PROCNO 1

F2 - Acquisition Parameters
Date_ 20121130
Time 18.09
INSTRUM spect
PROBHD 5 mm PABBO BB-
PULPROG zg30
TD 65536
SOLVENT CDC13
NS 16
DS 2
SWH 8012.820 Hz
FIDRES 0.122266 Hz
AQ 4.0894465 sec
RG 144
DW 62.400 usec
DE 6.50 usec
TE 298.0 K
D1 1.00000000 sec
TD0 1

-------- CHANNEL f1 --------
SFO1 400.1424710 MHz
NUC1 1H
P1 13.50 usec
PLW1 16.00000000 W

F2 - Processing parameters
SI 65536
SF 400.1400073 MHz
WDW EM
SSB 0
LB 0.30 Hz
GB 0
PC 1.00

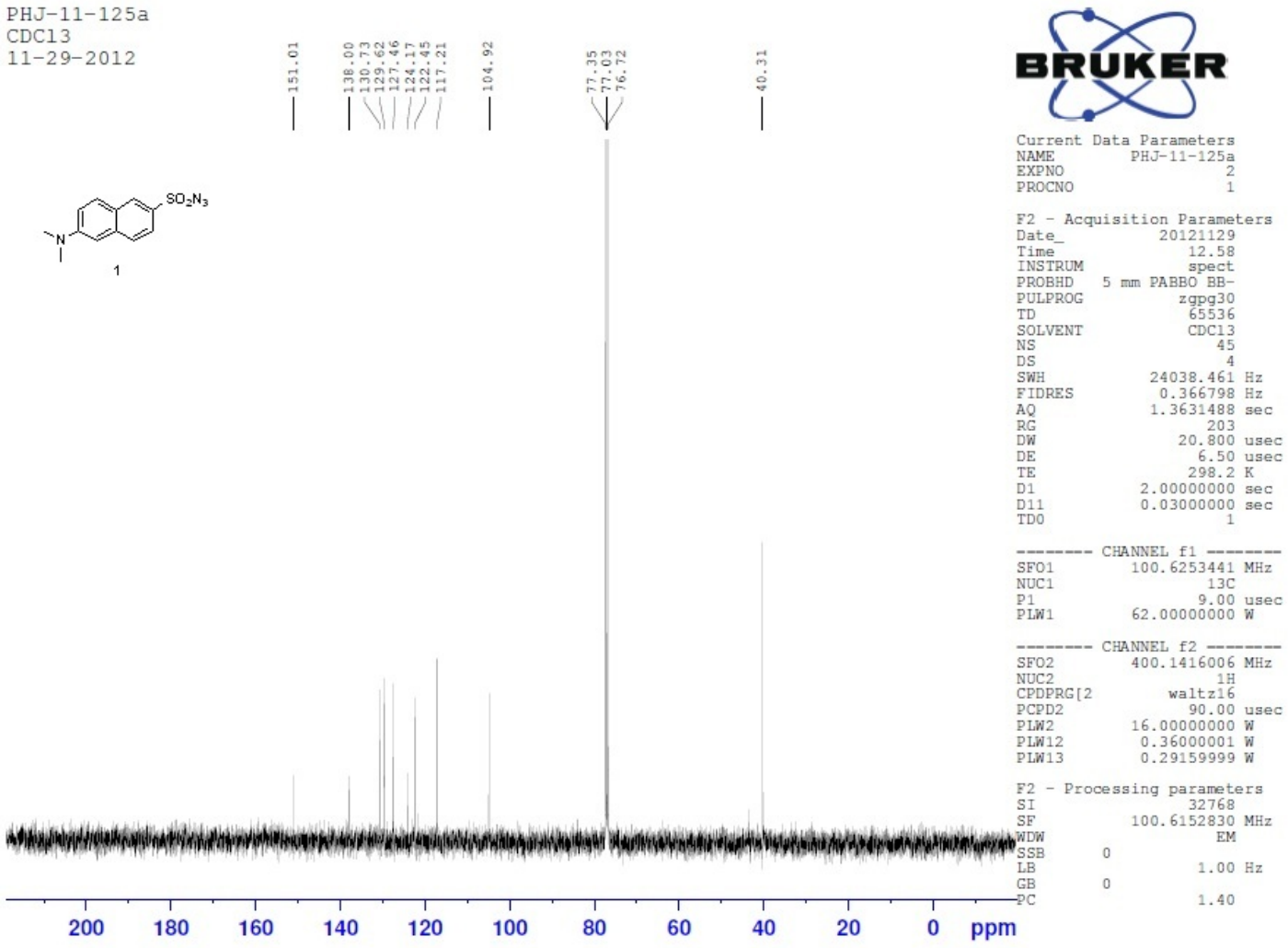

BRUKER

Current Data Parameters
NAME PHJ-11-125a
EXPNO 2
PROCNO 1

F2 - Acquisition Parameters
Date_ 20121129
Time 12.58
INSTRUM spect
PROBHD 5 mm PABBO BB-
PULPROG zgpg30
TD 65536
SOLVENT CDCl3
NS 45
DS 4
SWH 24038.461 Hz
FIDRES 0.366798 Hz
AQ 1.3631488 sec
RG 203
DW 20.800 usec
DE 6.50 usec
TE 298.2 K
D1 2.00000000 sec
D11 0.03000000 sec
TD0 1

-------- CHANNEL f1 --------
SFO1 100.6253441 MHz
NUC1 13C
P1 9.00 usec
PLW1 62.00000000 W

-------- CHANNEL f2 --------
SFO2 400.1416006 MHz
NUC2 1H
CPDPRG[2 waltz16
PCPD2 90.00 usec
PLW2 16.00000000 W
PLW12 0.36000001 W
PLW13 0.29159999 W

F2 - Processing parameters
SI 32768
SF 100.6152830 MHz
WDW EM
SSB 0
LB 1.00 Hz
GB 0
PC 1.40

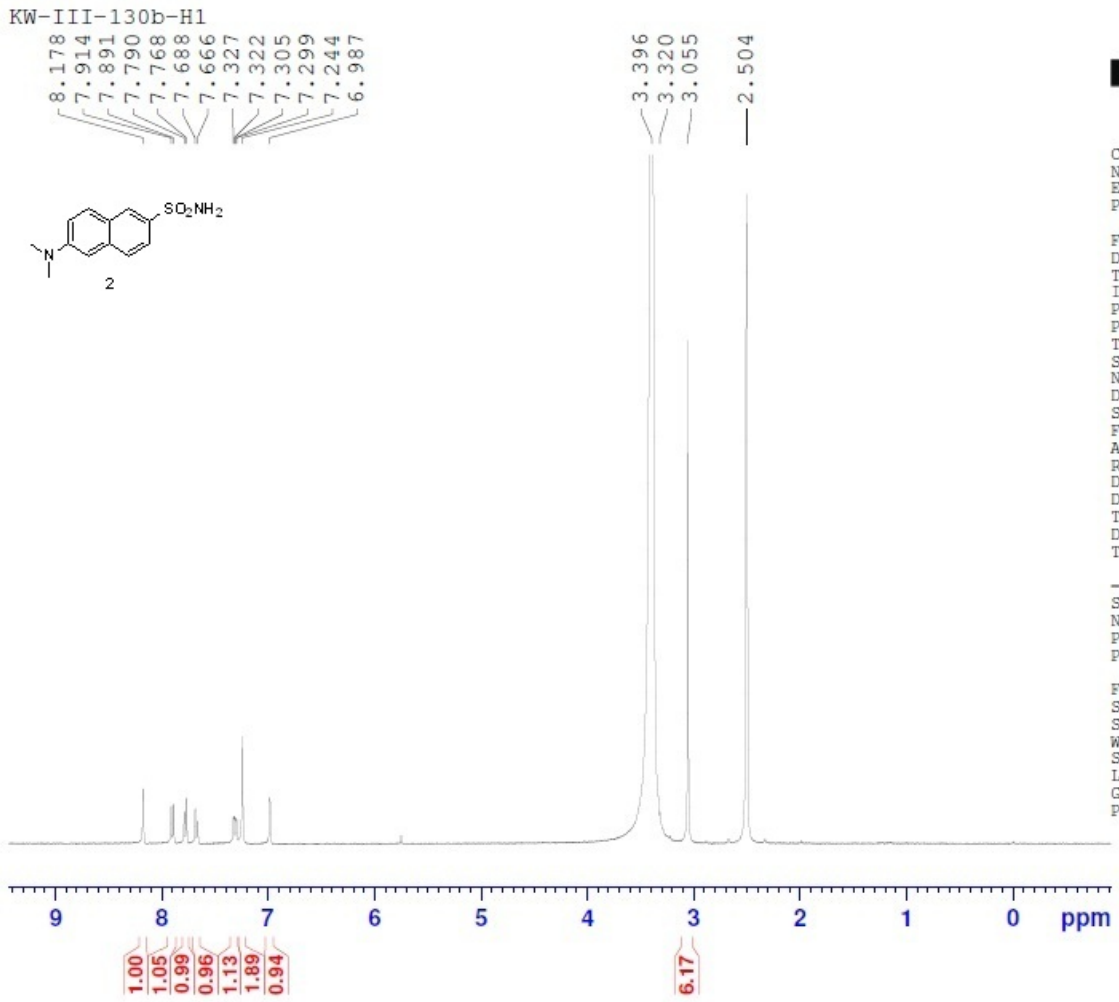

Current Data Parameters
NAME KW-III-130b
EXPNO 1
PROCNO 1

F2 - Acquisition Parameters
Date_ 20130116
Time 15.45
INSTRUM spect
PROBHD 5 mm PABBO BB-
PULPROG zg30
TD 65536
SOLVENT DMSO
NS 16
DS 2
SWH 8012.820 Hz
FIDRES 0.122266 Hz
AQ 4.0894465 sec
RG 114
DW 62.400 usec
DE 6.50 usec
TE 295.0 K
D1 1.00000000 sec
TD0 1

-------- CHANNEL f1 --------
SFO1 400.1424710 MHz
NUC1 1H
P1 13.50 usec
PLW1 16.00000000 W

F2 - Processing parameters
SI 65536
SF 400.1400000 MHz
WDW EM
SSB 0
LB 0.30 Hz
GB 0
PC 1.00

KW-III-130b-C13

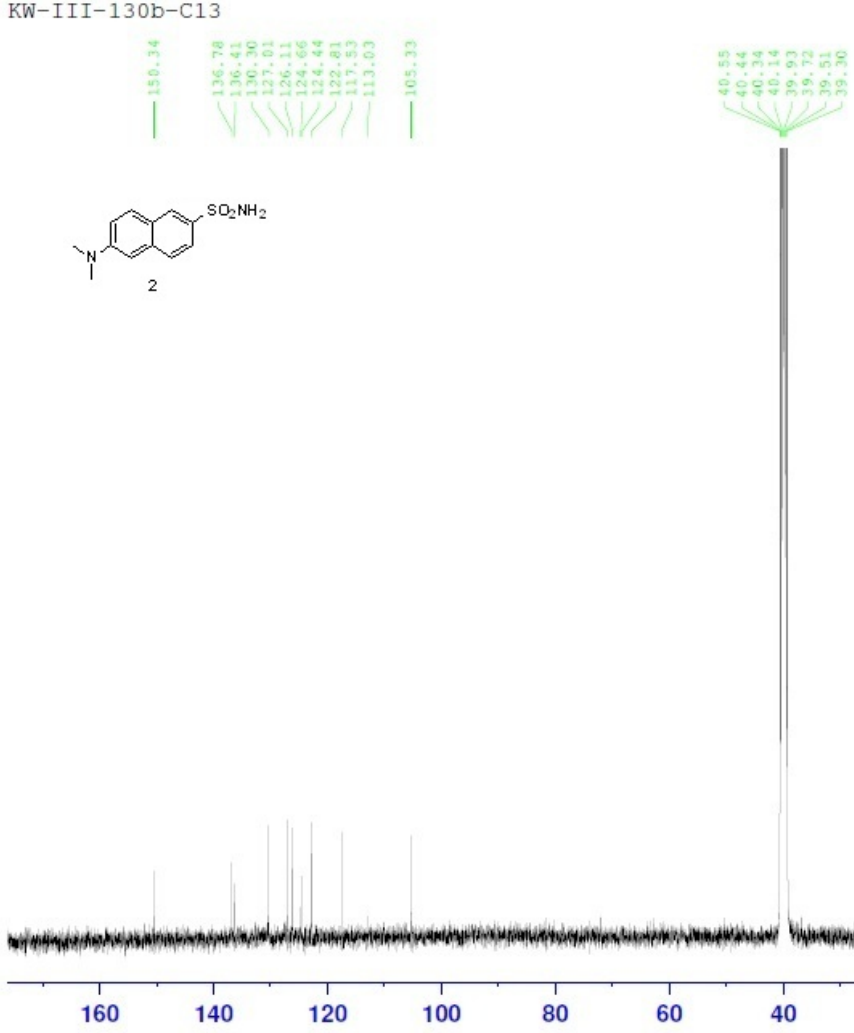

BRUKER

```
Current Data Parameters
NAME         KW-III-130b
EXPNO                  2
PROCNO                 1

F2 - Acquisition Parameters
Date_           20130124
Time              21.09
INSTRUM           spect
PROBHD   5 mm PABBO BB-
PULPROG         zgpg30
TD                65536
SOLVENT             DMSO
NS                10240
DS                    4
SWH           24038.461 Hz
FIDRES         0.366798 Hz
AQ             1.3631488 sec
RG                  128
DW               20.800 usec
DE                6.50 usec
TE                295.1 K
D1            2.00000000 sec
D11           0.03000000 sec
TD0                   1

-------- CHANNEL f1 --------
SFO1         100.6253441 MHz
NUC1                13C
P1                 9.00 usec
PLW1         62.00000000 W

-------- CHANNEL f2 --------
SFO2         400.1416006 MHz
NUC2                1H
CPDPRG[2         waltz16
PCPD2             90.00 usec
PLW2         16.00000000 W
PLW12         0.36000001 W
PLW13         0.29159999 W

F2 - Processing parameters
SI                 32768
SF           100.6152830 MHz
WDW                   EM
SSB       0
LB                 1.00 Hz
GB        0
PC                 1.40
```

Appendix C Spectra of compounds in homocysteine probe

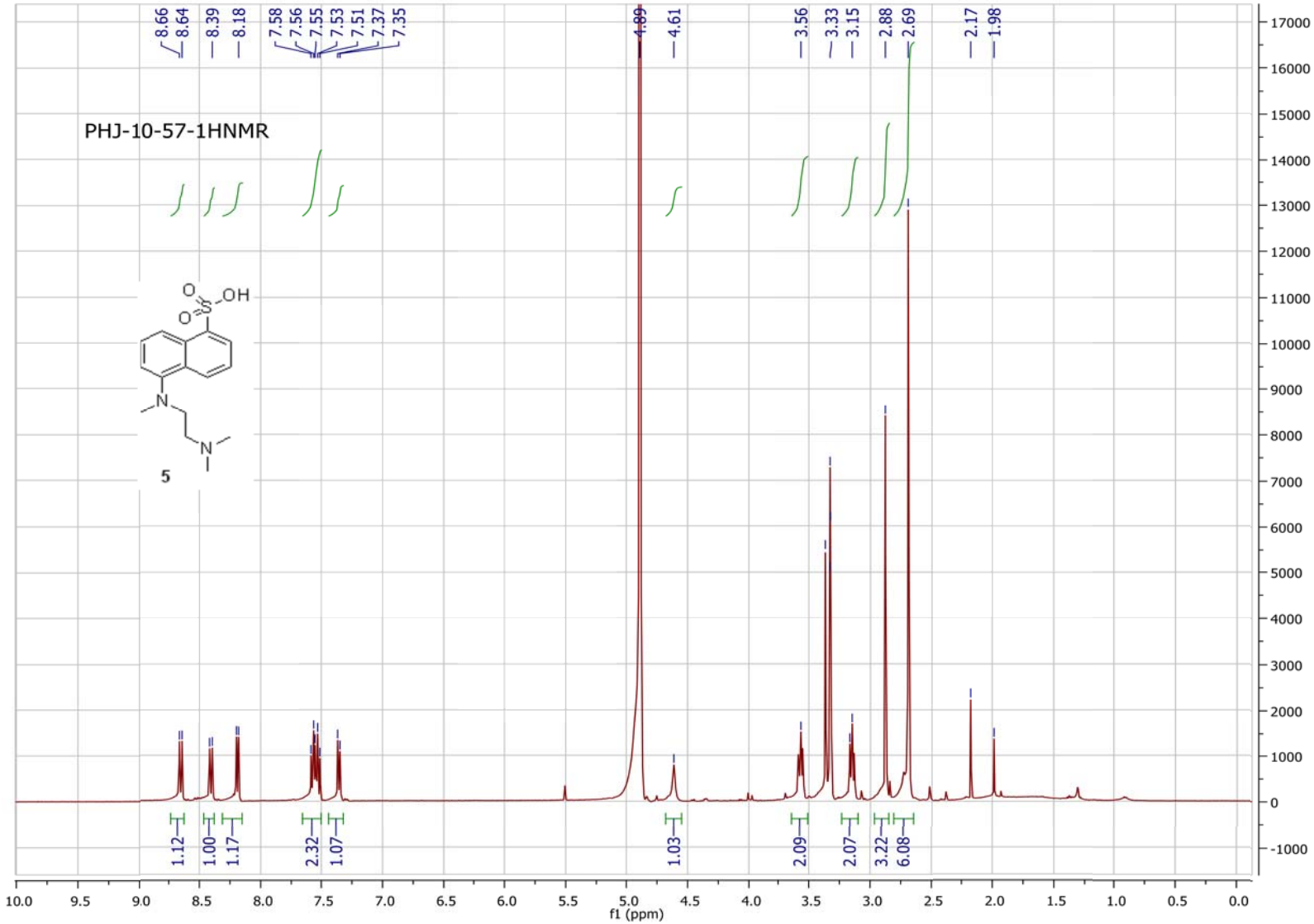

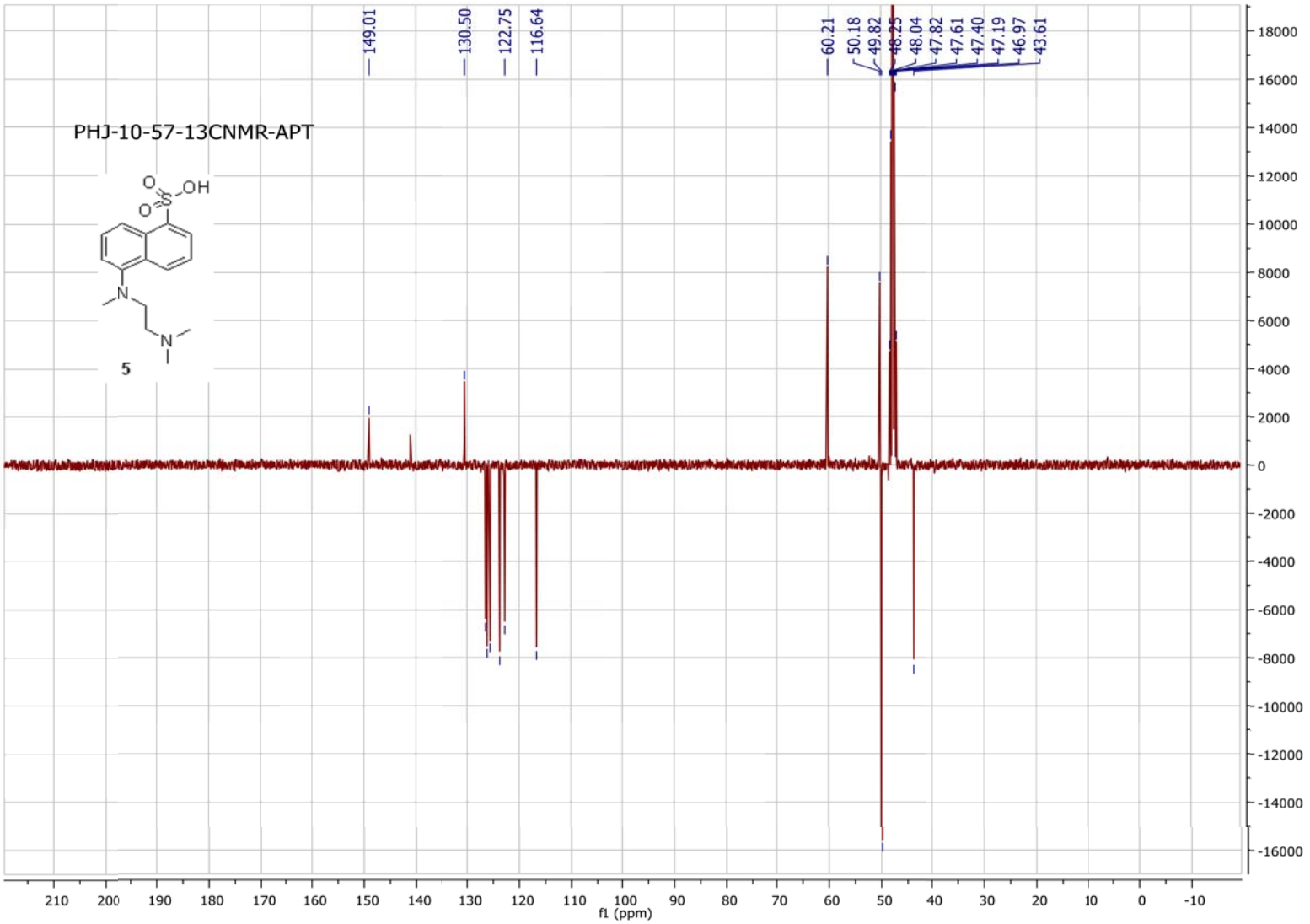
PHJ-10-57-13CNMR-APT
5
149.01
130.50
122.75
116.64
60.21
50.18
49.82
48.25
48.04
47.82
47.61
47.40
47.19
46.97
43.61
f1 (ppm)

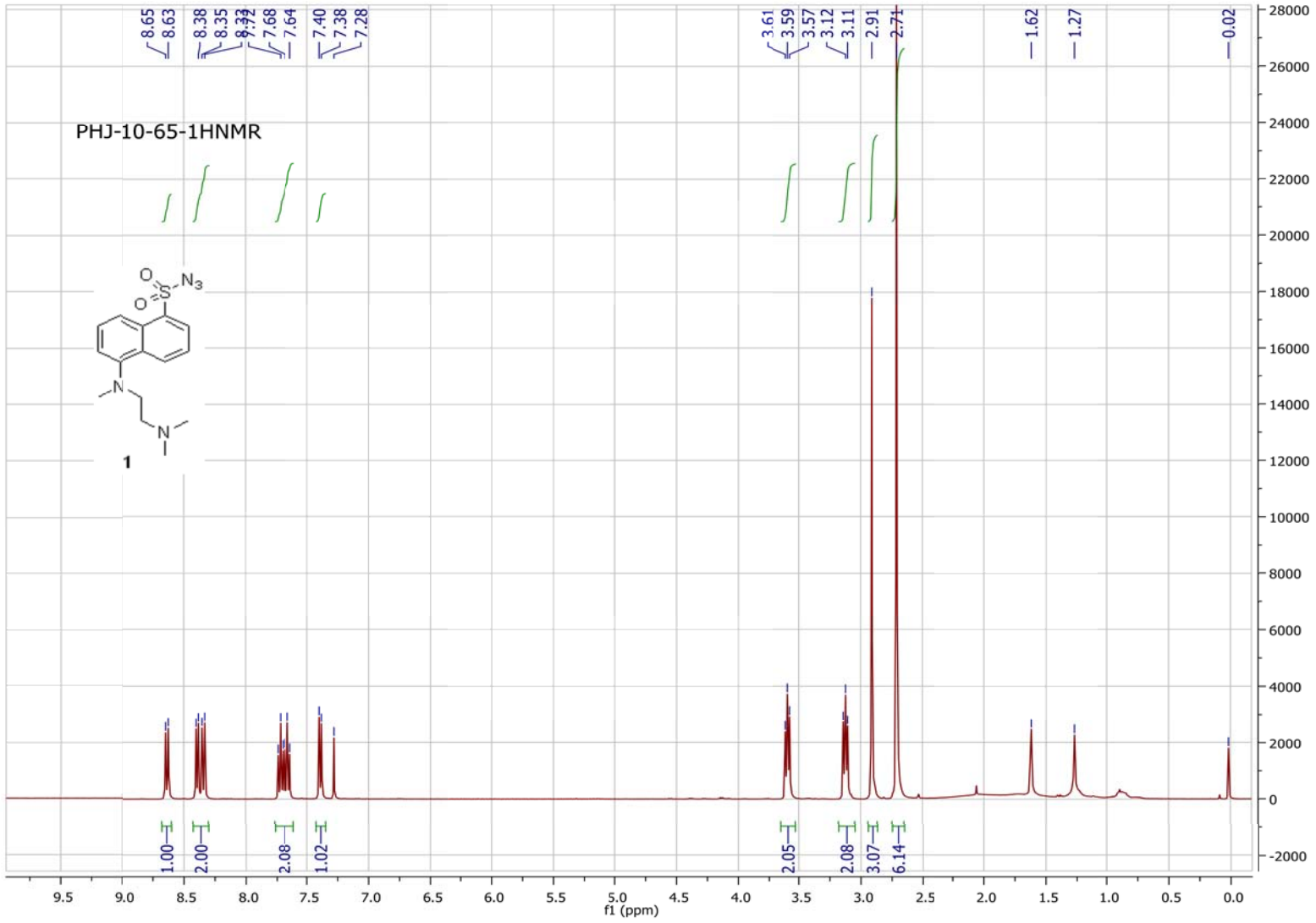
PHJ-10-65-1HNMR
8.65
8.63
8.38
8.35
7.68
7.64
7.40
7.38
7.28
3.61
3.59
3.57
3.12
3.11
2.91
2.71
1.62
1.27
0.02
1.00
2.00
2.08
1.02
2.05
2.08
3.07
6.14
f1 (ppm)

1

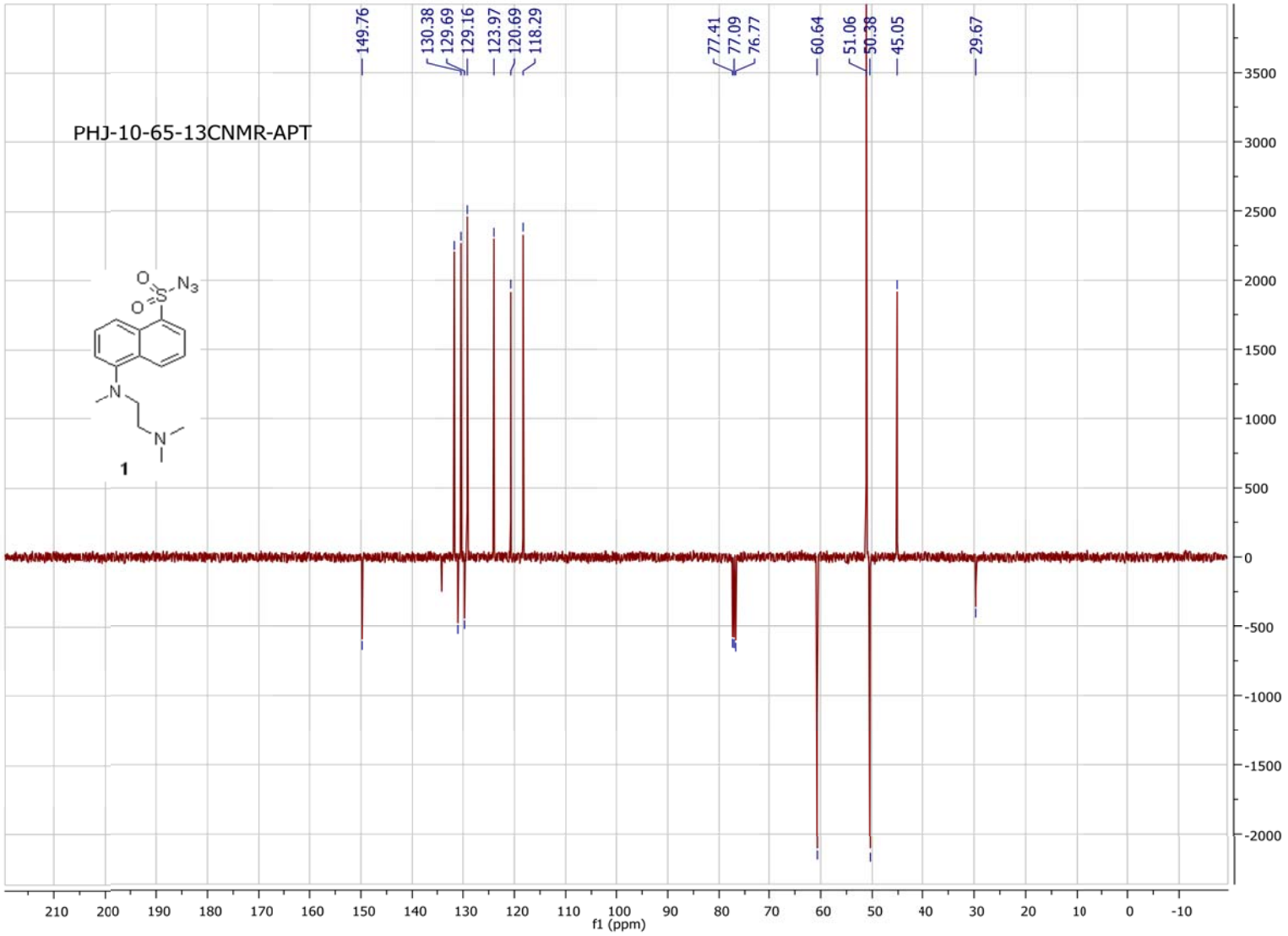
PHJ-10-65-13CNMR-APT
149.76
130.38
129.69
129.16
123.97
120.69
118.29
77.41
77.09
76.77
60.64
51.06
50.38
45.05
29.67
1
f1 (ppm)

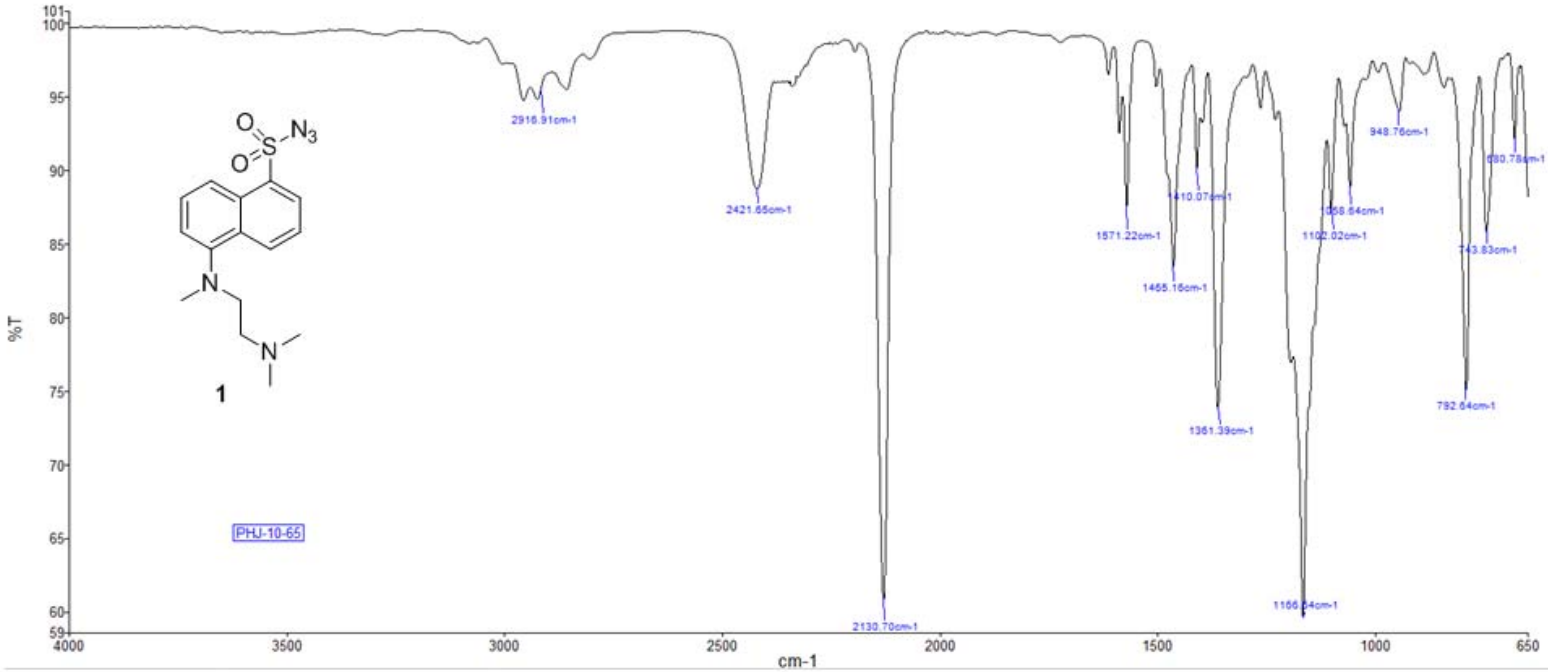
%T
cm-1
2916.91cm-1
2421.65cm-1
2139.70cm-1
1571.22cm-1
1465.15cm-1
1410.07cm-1
1361.39cm-1
1166.64cm-1
1102.02cm-1
1058.64cm-1
948.76cm-1
792.64cm-1
743.83cm-1
680.78cm-1
PHJ-10-65
1